UNIVERSITAT JAUME·I
ESCOLA DE TECNOLOGIA I CIÈNCIES EXPERIMENTALS
DEPARTAMENT D'ENGINYERIA MECÀNICA I CONSTRUCCIÓ
DEPARTAMENT DE SISTEMES INDUSTRIALS I DISSENY

# Evaluation and improvement of road vehicle pollutant emission factors based on instantaneous emissions data processing

TESI DOCTORAL
Juny 2014

*Autor:*

Vicente FRANCO GARCÍA

*Directors:*

Dra. María Rosario VIDAL NADAL
Dr. Daniel GARRAÍN CORDERO
Dra. Panagiota DILARA


Escola de Tecnologia i Ciències Experimentals
Departament d'Enginyeria Mecànica i Construcció
Departament de Sistemes Industrials i Disseny

# Evaluation and improvement of road vehicle pollutant emission factors based on instantaneous emissions data processing

*Tesi Doctoral*

*Autor:*

Vicente Franco García

*Directors:*

Dra. María Rosario Vidal Nadal
Dr. Daniel Garraín Cordero
Dra. Panagiota Dilara

2014

*

Ispra (Itàlia)—Castelló de la Plana


School of Technology and Experimental Sciences

Department of Mechanical Engineering and Construction
Department of Industrial Systems Engineering and Design

# Evaluation and improvement of road vehicle pollutant emission factors based on instantaneous emissions data processing

*a dissertation submitted in partial fulfilment of the requirements for the degree of Doctor of Philosophy*

*Author:*

Vicente Franco García

*Supervisors:*

Dr María Rosario Vidal Nadal
Dr Daniel Garraín Cordero
Dr Panagiota Dilara

2014

*

Ispra (Italy)—Castelló de la Plana (Spain)

A mon pare, que tot ho arregla
*To my dad, who can fix anything*

# Resum

Els instruments actuals permeten mesurar les emissions dels vehicles amb elevada resolució temporal. Les instal·lacions de dinamòmetres de xassís i motor, i també els sistemes portàtils de mesura d'emissions (*portable emission measurement systems*, PEMS), són capaços d'enregistrar senyals de concentracions de contaminants i cabdals de gas amb resolucions d'1 Hz, i alguns analitzadors arriben fins i tot als 10 Hz.

Aquestes dades d'emissions es poden emprar per a produir factors d'emissió instantanis, que són relacions funcionals empíriques entre l'estat operatiu instantani del vehicle (normalment definit pel règim de gir i el parell motor, en el qual cas es parla de *mapes d'emissió*) i el seu perfil d'emissions a l'eixida del catalitzador. Els mapes d'emissió es poden utilitzar en *entorns de simulació* per a predir les masses d'emissions de contaminants sota qualsevol cicle d'ús, tot reduint la despesa en experiments, però també la quantitat de dades realment mesurades. Per tant, és essencial que aquests mapes es construïsquen a partir de dades exactes.

L'elevada resolució temporal dels senyals mesurats no implica una major exactitud. Un prerequisit per a la producció de factors d'emissió de qualitat és la correcta atribució temporal de les masses de contaminants mesurades als estats del vehicle o del motor que s'han enregistrat. Açò planteja un repte tècnic perquè les instal·lacions de mesura d'emissions de vehicles no han sigut dissenyades per a facilitar el modelat instantani de les emissions. Primerament, trobem que les concentracions dels contaminants, els cabdals de gas i les dades del motor (és a dir, els 'ingredients' dels mapes d'emissió) provenen d'instruments diferents que sovint no disposen d'un

Aquest resum s'inclou de conformitat amb l'article 24 de la normativa dels estudis de doctorat de la Universitat Jaume I regulats pel Reial Decret 99/2011.

senyal de temps comú. A més a més, degut a restriccions en la configuració física dels sistemes de mesura, les concentracions de contaminants i el cabdal de gasos d'escapament es mesuren a alguns metres de distància del punt d'emissió (l'eixida del catalitzador), de forma que aquests senyals mesurats es veuen afectats per retards en el transport i per fenòmens de mescla que varien de forma no linial amb el cabdal. Per fi, els analitzadors químics tenen una característica de resposta dinàmica que retarda i distorsiona més encara els senyals. Totes aquestes distorsions es tradueixen en un sol efecte observable: els senyals mesurats són versions dinàmicament retardades, suavitzades i aplanades (és a dir, amb pics menys pronunciats) dels senyals 'vertaders' que s'observarien a l'eixida del catalitzador.

L'*objecte* d'aquesta tesi és millorar la qualitat de la mesura i el modelat instantani de les emissions dels vehicles mitjançant l'aplicació de tècniques de post-processament de dades. Els *objectius de recerca* que se'n deriven són els següents:

1. Avaluar els efectes que distorsionen i afecten l'exactitud dels senyals instantanis d'emissions emprats en el modelat de les emissions dels vehicles, i desenvolupar un marc metodològic per a la compensació dels senyals.

2. Desenvolupar una metodologia completa per a la compensació dels senyals, i disseminar-la entre les parts interessades del grup ERMES (*European Research on Mobile Emission Sources*), que aglutina els laboratoris i altres entitats de recerca europeus dedicats a la mesura i modelat de les emissions dels vehicles.

Les distorsions que afecten l'exactitud dels senyals instantanis es poden compensar amb una combinació de *modelat físic* i *post-processament de dades*. La principal aportació original d'aquesta tesi és una nova metodologia—que s'hi descriu completament—per a compensar els senyals instantanis d'emissions. Mentre que les metodologies anteriors es basaven en tècniques de modelat de teoria de sistemes que requereixen una caracterització experimental exhaustiva (per sub-sistema) de les distorsions imposades per l'equip de mesura, el mètode alternatiu utilitza el $CO_2$ com a traçador per tal de caracteritzar el sistema de forma agregada.

Les *conclusions* principals d'aquesta tesi són les següents:

1. La compensació dels senyals instantanis és necessària per a la producció de factors d'emissió amb elevada resolució temporal. Qualsevol esquema de compensació de senyals instantanis es fonamentarà en una combinació de modelat físic dels sistemes de mesura i post-processament de dades.

2. El mètode del traçador de $CO_2$—del qual s'hi aporta una descripció detallada i una validació experimental en aquesta tesi—és una metodologia completa i flexible que permet compensar els senyals produïts pels sistemes de mesura habitualment emprats en el modelat instantani de les emissions dels vehicles (dinamòmetres de xassís o de motor i PEMS) de forma semiautomàtica, tot facilitant la creació de mapes instantanis d'emissions i reduint la càrrega experimental en comparació amb les metodologies anteriors.

**Mots clau:** *emissions dels vehicles, model d'emissió, factor d'emissió, mapa d'emissions, $CO_2$, consum de carburant, contaminants regulats, senyals instantanis, exactitud, aliniament temporal, post-processament de senyals, dinamòmetre de xassís, dinamòmetre de motor, PEMS, harmonització, grup ERMES, Comissió Europea, traçador de $CO_2$.*

# Abstract

Current instrumentation can measure vehicle emissions with high temporal resolution. Chassis and engine dynamometer test facilities, and also portable emissions measurement systems (PEMS), can record instantaneous pollutant concentration and exhaust flow data streams at 1 Hz, and some setups now provide 10 Hz resolutions.

Vehicle emission modellers can use instantaneous emissions data to produce instantaneous emission factors, which are empirical functional relations between the instantaneous driving state of a vehicle (normally characterised by engine speed and torque, in which case they are called *engine emission maps*) and its emission behaviour at the catalyst-out point. Engine emission maps can then be applied in vehicle or engine *simulation environments* to predict the mass emissions of pollutants of a vehicle for any given duty cycle—thus reducing the need for costly measurements, but also the amount of measured data—. It is therefore crucial that these engine emission maps be derived from accurate data.

The increased resolution of emissions signals does not equate with increased accuracy. A prerequisite for the derivation of accurate emission factors from instantaneous vehicle emissions data is a fine allocation of measured mass emissions to recorded engine or vehicle states. This poses a technical challenge, because vehicle emission test facilities are not designed to support instantaneous emissions modelling, and they introduce number of *distorting effects* that compromise the instantaneous accuracy of the measured signals. First of all, pollutant concentrations, flow rates and engine data (*i.e.*, the 'building blocks' of engine emission maps) come from different instruments often lacking a clear common time reference signal for a proper alignment. Also, due to measurement setup constraints, pollutant concentrations and exhaust gas flow rates will often be measured several metres away from the catalyst-out point,

and so the measured concentration signals are affected by transport delays and gas mixing phenomena, which vary non-linearly with flow. Finally, exhaust gas analysers have a dynamic response characteristic that further delays and distorts the measured concentration signals. All of the aforementioned distortions have one observable effect: measured signals that are dynamically delayed, smoothed and flattened (*i.e.*, having less sharp peaks) versions of the 'true' emissions that would be observed at the catalyst-out point.

These distorting effects can be compensated through a combination of *physical modelling* and *data post-processing*. The main original contribution of this dissertation is a novel methodology for the compensation of instantaneous emission signals, which is fully described herein. Whereas previous methodologies relied upon systems theory modelling—including a comprehensive experimental characterisation—to model the sub-systems of the measurement setup, the alternative approach uses $CO_2$ as a tracer of the distortions brought about by the measurement setup, which is modelled as a 'lump' system.

**Keywords:** *vehicle emissions, emission model, emission factor, engine emission map, $CO_2$, fuel consumption, regulated pollutants, instantaneous signals, accuracy, time alignment, signal post-processing, chassis dynamometer, engine dynamometer, PEMS, harmonisation, ERMES group, European Commission, $CO_2$ tracer*.

# Acknowledgements

Berlin, May 2014

My 'thesis years' will likely go down in history as the worst of a global financial crisis, and yet I will remember them as a time of steady personal growth and transformation. I owe a large debt of gratitude to many people (incidentally quite a few Greeks and nationals of other debt-laden countries) that helped me along the way: Rosario Vidal and Daniel Garraín—besides being the reason I started doing research in the first place—for supervising me over the long distance; Penny Dilara for giving me the opportunity to join the Joint Research Centre of the European Commission and allowing me to pursue my own research interests even when the prospects of success were uncertain; Georgios Fontaras for giving my research a real purpose and helping me navigate my periods of obfuscation; Savas Geivanidis and Martin Weilenmann for being an inspiration and generously sharing their expertise; Stefan Hausberger and Leonidas Ntziachristos for performing the external review of the dissertation manuscript; Urbano Manfredi, Franz Mühlberger and the rest of the VELA laboratories staff for their help during the experimental campaign, and Konstantinos Agnanostopoulos for his commitment to improving the algorithm of the $CO_2$ tracer methodology.

The funding of the European Commission during my three years in Ispra as a doctoral research grantholder is gratefully acknowledged, as is the funding and loving support of my extended family during the preceding twenty-seven years. In no particular order, a word of appreciation also goes to my beloved friends and colleagues Nana Amoateng, *onorevole* Mirko (Vittorio) Busto, David Pamies, Lorena Hojas, Julio González Romero, Pepa Pérez Barral, Guadalupe Sepulcre, Pascual Dionís, Irene Pinedo, Lara Vilar, Georgina Harris-López, Marina Kousoulidou, Cinzia Pastorello, Fabio Dalan, Biagio Ciuffo, Alessandro Marotta, Laura Lonza, Yoannis Drossinos, Covadonga Astorga, Pierre Bonnel, Denise Pernigotti, Lorenzino Vaccari, Teresita Freddi, Fulvio Ardente, Andrea Marsano, Vera Thiemig, Martha Dunbar, Alison Pridmore, Ben Murphy, Andrew Singleton, Alexandros Nikolian, Nafsika Stavridou, Tiberiu Antofie, Simone Russo, Hugo Carrão, Silvia Cirillo, Giovanna Indrio, Martin Weiss, Monica Ţuţuianu, Elena Monea, Zuzana Koritschanová, Carme Calduch, Javier Sanfélix, David Cebrián, Enrique Moliner, Marta Royo, Carlos Muñoz, Peter Mock and many others for making these years thoroughly enjoyable and productive.

From the bottom of my heart,
Many thanks / Muchas gracias / Moltes gràcies / Grazie tante / ευχαριστώ πολύ

# Contents

# List of figures

# List of tables

# Acronyms and abbreviations

**ADVISOR**: Advanced Vehicle Simulator (vehicle simulation software).
**AM**: Alignment Margin.
**ARTEMIS**: Assessment and Reliability of Transport Emission Models and Inventory Systems (EU-funded research project).
**BIBO**: Bounded Input - Bounded Output.
**CADC**: Common ARTEMIS Driving Cycle.
**CFV**: Critical Flow Venturi.
**CI-MS**: Chemical Ionisation Mass Spectrometry.
**CLD**: Chemiluminiscent Detector.
**CMEM**: Comprehensive Modal Emissions Model.
**CNG**: Compressed Natural Gas.
**CO**: Carbon monoxide.
**COPERT**: Computer Programme to calculate Emissions from Road Transport.
**CRT**: Continuously Regenerating Trap (particle filter).
**CVS**: Continuous Volume Sampling.
**DACH-NL-S**: Germany, Austria, Switzerland, the Netherlands and Sweden (group of countries that use HBEFA).
**DG**: Directorate-General (administrative branch of the European Commission).
**DOC**: Diesel Oxidation Catalyst.
**DPF**: Diesel Particulate Filter.
**Dyno**: [chassis or engine] dynamometer.
**EC**: European Commission.
**ECU**: Electronic Control Unit.
**EEA**: European Environment Agency.
**EF**: Emission Factor.
**EMPA**: *Eidgenössische Materialprüfungs und ForschungsAnstalt* (Swiss Federal Laboratories for Materials Testing and Research).
**ERMES**: European Research on Mobile Emission Sources.
**ESC**: European Stationary Cycle.
esto: emission signals synchronisation tool.
**ETC**: European Transient Cycle.
**EV**: Electric Vehicle.
**FC**: Fuel Consumption.
**FTIR**: Fourier Transform Infrared spectroscopy (chemical analysis technique).
**FTP**: Federal Test Procedure (USA standard driving cycle).
**GPS**: Global Positioning System.
**GRPE**: Global Regulation working party on Pollution and Energy.
**HBEFA**: *Handbuch für Emissions-faktoren des Strassen-verkehrs* (Handbook of emission factors from road transport).
**HC**: Hydrocarbons.
**HDV**: Heavy-Duty Vehicle.
**HEV**: Hybrid Electric Vehicle.
**HFID**: Heat Flame Ionisation Detector.
**HILS**: Hardware-In-the-Loop Simulation.

**ICCT**: International Council on Clean Transportation.
**IET**: Institute for Energy and Transport (part of Directorate-General Joint Research Centre).
**IPCC**: Intergovernmental Panel on Climate Change.
**JRC**: Joint Research Centre (Directorate-General of the European Commission).
**LAT**: Laboratory of Applied Thermodynamics (Aristotle University of Thessaloniki, Greece).
**LCV**: Light Commercial Vehicle.
**LDV**: Light-Duty Vehicle.
**LPG**: Liquefied Petroleum Gas.
**LTI**: Linear, Time-Invariant (system).
**MEL**: Mobile Emissions Laboratory (of the Center for Environmental Research & Technology of the University of California Riverside).
**MOVES**: Motor Vehicle Emission Simulator (USEPA emission model).
**MSE**: Mean Squared Error.
**NDIR**: Non-dispersive Infrared (gas concentration measurement principle).
**NDUV**: Non-dispersive Ultraviolet (gas concentration measurement principle).
**NEDC**: New European Driving Cycle.
**NMVOC**: Non-Methane Volatile Organic Compounds.
**$NO_x$**: Nitrogen oxides (NO and $NO_2$).
**NTE**: Not-to-exceed (emission limits associated with delimited engine operating areas).
**OBD**: On-board Diagnostics unit.
**PC**: Passenger Car.
**PEMS**: Portable Emissions Measurement System.
**PHEM**: Passenger car and Heavy duty vehicle Emission Model.
**PHEV**: Plug-in Hybrid Electric Vehicle.
**PM**: Particulate Matter.
**$PM_{2.5}$**: Particulate matter having a diameter below 2.5 micrometres.
***Re***: Reynolds number.
**RPM**: Revolutions per minute (unit of engine rotating speed).
**SAD**: Sum of Absolute Deviations.
**SCR**: Selective Catalytic Reduction.
**SFTP**: Supplemental Federal Test Procedure (USA standard driving cycle).
**SSR**: Sum of Squared Residuals.
**STU**: Sustainable Transport Unit (administrative subdivision of the Institute for Energy and Transport).
**SULEV**: Super Ultra Low Emission Vehicle.
**THC**: Total Hydrocarbons.
**TUG**: Technical University of Graz (Austria).
**UNECE**: United Nations Economic Commission for Europe.
**USEPA**: United States Environmental Protection Agency.
**VELA**: Vehicle Emissions Laboratories of JRC in Ispra.
**VSP**: Vehicle-specific Power.
**WHSC**: World Harmonised Stationary Cycle.
**WHTC**: World Harmonised Transient Cycle.
**WLTC**: Worldwide harmonised Light-duty driving Test Cycle.
**WLTP**: Worldwide harmonised Light-duty driving Test Procedures.

# Chapter 1

# Introduction

Pollutant emissions from road transport need to be accurately estimated to ensure that air quality plans are appropriately designed and implemented. This is no easy task, because road vehicles are operated under a wide range of conditions and their emissions exhibit a highly transient behaviour. Moreover, their emission profiles have a strong dependency on vehicle class, on operating and environmental conditions, and on the characteristics of the fuels used. Last but not least, road vehicle emission regulations are frequently updated, which drives constant technological changes in powertrains, fuels and after-treatment devices.

*Emission models* are used to perform the calculations needed to estimate emissions from road transport at large geographic scales (*e.g.*, for the compilation of national emission inventories). These range from models which only require mean travelling speeds to estimate emissions (*e.g.*, COPERT) and models that require a description of the traffic situation—*i.e.*, qualitative assessments of driving conditions—to predict emissions (*e.g.*, HBEFA) to models that require second-by-second engine or vehicle state data (*e.g.*, PHEM, MOVES) to derive emission information for the complete driving profile. Whatever the case, modelling road vehicle emissions requires intensive testing to produce *emission factors* that cover all the relevant driving situations. On the other hand, vehicle emissions tests are costly experiments, and not every single vehicle model is tested for modelling purposes. This makes time-resolved, accurate emissions data a very valuable resource for vehicle emission modellers.

## 1.1 Goal and scope

This academic dissertation aims to improve the quality of *instantaneous* road vehicle emissions measurement and modelling through the application of *data post-processing* techniques.

This document provides a description of the distorting effects that compromise the accuracy of instantaneous emissions signals reported by conventional emission measurement equipment, and a theoretical framework for their compensation. The distorting effects covered include the time misalignments among signals output by different instruments, the mixing of exhaust gas within the exhaust system of vehicles and within 'pipe' elements of the measurement setup, the variable transport times of exhaust gas associated with non-steady exhaust flow rates and the dynamic response characteristics of gas analysers.

The most successful existing methods for the compensation of instantaneous vehicle emission signals rely upon *systems theory* concepts. These methods individually model the constituting elements—or sub-systems—of the measurement chain (*e.g.*, raw gas line, diluted gas line, chemical analysers) through 'unit step' characterisation experiments. These methods, which require access to an ultra-fast analyser and additional apparatus to produce the step inputs, will be reviewed and explained in simple terms so that no expert knowledge is required.

The main original contribution of the research work presented herein is the proposal of a *new, comprehensive method for the compensation of instantaneous road vehicle emission signals through data post-processing*. The method can be applied to emission signals obtained from vehicle emissions testing on chassis and engine dynamometer facilities, or with portable emissions measurement systems (PEMS), therefore covering the three main setups used in vehicle emissions measurement for modelling purposes.

The new method uses $CO_2$ as a tracer of the distortions suffered by mass emission signals, and models the complete measurement setup as a 'lump' system. In principle, the method could be made to operate with other gaseous pollutants (*e.g.*, $NO_x$), but the advantages of using $CO_2$ (which will become apparent in chapter 5, where the method is described in detail) are too many to warrant the choice of any other tracer gas. Thus the method is (rather unimaginatively) called *the $CO_2$ tracer method*. In comparison to previous methodologies, the new method sacrifices some

insight regarding the behaviour of emission signals within each sub-system of the measurement setup in exchange for much lower experimental work and reduced maintenance and technological requirements. It also brings improvements in terms of flexibility, since it can be adapted to the specific measurement setups of the individual vehicle emission laboratories with only minor effort.

## 1.2 Justification

The ERMES (European Research on Mobile Emission Sources; see section 2.1.1 on page 12 for a description of its activities) is a European network of researchers, regulators and other stakeholders in vehicle emissions modelling. ERMES is coordinated by Directorate-General Joint Research Centre (JRC) of the European Commission (EC).[1] The development priorities of the two leading vehicle emission models in Europe (COPERT and HBEFA) are set during the ERMES annual plenary meetings. To that avail, the executive board of ERMES proposes a list of research issues to all stakeholders, and following an open discussion these are assigned a priority level (high, medium or low). The work programmes of participating research bodies—as well as the measurement programmes of participating laboratories—are then adjusted according to these priority levels, and a pool of measured data is made available to participating vehicle emission modellers as a result (figure 1.1).

Amongst the high-priority research issues included in the ERMES work programme for the year 2012 was the '*development of tools for data collection and for correction of instantaneous test results*'. This resulted in an allocation of research efforts and funds from the Sustainable Transport Unit (STU) of the Institute for Energy and Transport (IET, a part of JRC) to the development of a new instantaneous signal compensation method that could be disseminated within the ERMES network of laboratories.

[1] The author of this dissertation had the pleasure of serving as scientific secretary of the ERMES group between the years 2010 and 2012 before passing his duties onto the much more efficient (and dear friend and colleague) Mr Fabio Dalan.

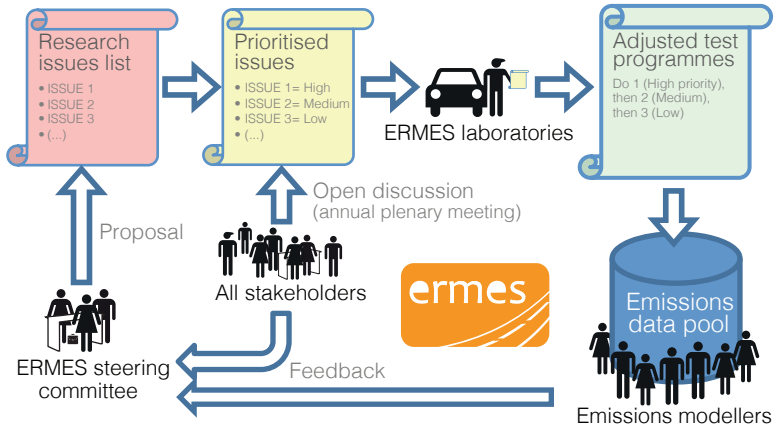


**Figure 1.1:** Prioritisation of emissions modelling research issues within ERMES

The research work presented herein—and specifically the newly-proposed method for the compensation of instantaneous emission signals—is thus a result of the commitment of DG-JRC to the harmonisation of data collection and reporting procedures within ERMES. This work was carried out to support the quality of the emission models used for the estimation of emissions from road transport in Europe, and to that avail it is made available to all the laboratories that provide instantaneous emissions data to the ERMES vehicle emissions database.

## 1.3 Hypotheses

The hypotheses that guided our research are formulated as follows:

1. Vehicle emission models have traditionally been backed by measured emissions data with low time resolution (*i.e.*, aggregated over several minutes; over test cycles or sub-cycles, trips or sub-trips). Recent modelling approaches try to predict the *instantaneous emissions* of road vehicles.

   (a) Current-technology road vehicles often concentrate their emissions during so-called *emission events* (*i.e.*, highly transient emission peaks of short duration).

   (b) Conventional vehicle emissions measurement instrumentation is able to report emissions data at fine time resolutions (of 1 to 10 Hz).

2. Instantaneous vehicle emission signals reported by conventional vehicle emissions measurement instrumentation are affected by a number of *distorting effects* that compromise their accuracy.

   (a) These distorting effects have little impact upon aggregated vehicle emission test results (*i.e.*, reported pollutant mass emissions over time periods larger than a few seconds), and so they have been largely overlooked by emission modellers.

   (b) These distorting effects can have a large impact upon the accuracy of instantaneous vehicle emission test results (*i.e.*, pollutant mass emissions over time periods smaller than a few seconds), and also upon the reliability of emission factors and models developed from them (*e.g.*, *engine emission maps*).

3. The aforementioned distorting effects can be compensated through a combination of *physical modelling* and *data post-processing*, thereby improving the accuracy of the signals and the reliability of emission factors developed from them.

   (a) Signal compensation approaches that rely upon *physical modelling* perform well, but the compilation of a complete physical model of a vehicle emissions measurement setup is a difficult task that requires expert knowledge and *ad hoc* characterisation experiments.

   (b) Signal compensation approaches that rely upon *data post-processing* require fewer experiments and resources for their implementation, but they are less sophisticated and provide less information about the ways in which instantaneous emission signals become distorted throughout the measurement setup.

   (c) A new methodology for the compensation of instantaneous emission signals could be developed by combining new, advanced data post-processing methods with existing knowledge from previous physical modelling efforts.

## 1.4 Objectives

The stated goal of the research work presented in this document is 'to improve the quality of instantaneous road vehicle emissions measurement and modelling through the application of data post-processing'. The specific *research objectives* that will be addressed in relation to the aforementioned goal are structured as follows:

1. To assess the distorting effects that compromise the accuracy of instantaneous vehicle emissions signals used for vehicle emissions modelling, and to develop a *methodological framework* for the compensation of instantaneous emission signals. It is assumed that this could be accomplished by achieving the following secondary objectives:

   (a) To identify and describe all the relevant distorting effects and the signals affected.

   (b) To assess the impact of the identified distorting effects upon the accuracy of instantaneous emissions signals reported by conventional emission measurement equipment and upon emission factors derived from non-compensated signals.

   (c) To make a classification of these effects with regard to vehicle emissions measurement and modelling, presenting them in a clear manner and providing simple, 'best-practice' data compensation strategies.

2. To develop a comprehensive, flexible methodology for the compensation of the distorting effects, and disseminate it among the stakeholders of the ERMES group. It is assumed that this could be accomplished by achieving the following secondary objectives:

   (a) To study the existing instantaneous emission signal compensation methodologies, identifying potential shortcomings and reasons why 'expert' compensation methodologies are not standard practice among vehicle emission laboratories.

   (b) To formulate and validate a new signal compensation methodology that relies heavily on data post-processing. Said methodology should be flexible and easy to apply, and yet have performance levels comparable to those of advanced compensation strategies based on physical modelling.

   (c) To produce a software implementation of the new methodology to encourage its adoption by the laboratories of the ERMES network.

## 1.5 Research methodology

The research methodology followed is outlined next:

An extensive *literature review* of the techniques available for vehicle emission measurement, and the ways in which the resulting emissions data can be used for the development of *emission factors* (*i.e.*, of functional relations between vehicle operation parameters and their emission behaviour) was performed. A strong focus was placed on those techniques that are able to produce continuous streams of *instantaneous data*. The special characteristics of instantaneous emission signals were investigated, as well as the distorting effects that compromise their accuracy.

An *expert consultation* process[2] was initiated by EC–JRC to study the problem of instantaneous emission signal accuracy and to explore the possibility of establishing harmonised approaches to be shared among ERMES laboratories. As a result of this process, EC–JRC took the initiative of drafting a methodological report on the topic and coordinating future developments.

A *study of signal compensation strategies* based on data post-processing was performed with the aim of developing a new, comprehensive signal compensation method. Early methodology concepts were initially applied to historical datasets extracted from the database of the VELA laboratories of IET.

An *experimental campaign* was designed and executed once the compensation methodology had reached a sufficient level of maturity. The experimental campaign included the measurements required in order to obtain the necessary data for further development and validation of the new compensation methodology, as well as those experiments needed for the physical modelling of the VELA 1 test facility (a chassis dynamometer laboratory used to measure the emissions of internal combustion engine passenger cars). These experiments were performed with the technical assistance of Dr Savas Geivanidis.

[2]Said process involved Dr Martin Weilenmann of the Swiss Federal Laboratories for Materials Testing and Research (EMPA), Dr Savas Geivanidis and Dr Leonidas Ntziachristos of the Laboratory of Applied Thermodynamics (LAT) at Aristotle University of Thessaloniki (Greece), Dr Stefan Hausberger of the Technical University of Graz (TUG, Austria), and Dr Panagiota Dilara and Dr Georgios Fontaras of EC–JRC.

## 1.6 Structure of this dissertation

This academic dissertation is divided into seven chapters, the first of them being this introduction which now concludes.

*Chapter 2*, 'Measuring the emissions of road vehicles', critically reviews the different techniques available for the measurement of road vehicle emissions in relation to the development of *emission factors* found in emission models. Each technique is assessed from a modelling perspective, emphasising those techniques that produce continuous streams of instantaneous data (namely engine and chassis dynamometer measurements, and PEMS). This review is adapted from a journal article co-authored by the author of this dissertation (Franco *et al.* 2013).

*Chapter 3*, 'Distorting effects of instantaneous vehicle emission signals', discusses the distorting effects that compromise the accuracy instantaneous vehicle emission signals. The most relevant distorting effects (namely the time misalignments among signals output by different instruments, the variable transport times of exhaust gas associated with non-steady flow rates, the mixing of exhaust gas within the exhaust system and the 'pipe' elements of the measurement setup, and the dynamic response of gas analysers) are described and assessed with regard to their impact upon the accuracy of the emission signals themselves, and that of the emission factors derived from them.

*Chapter 4*, 'Compensation of instantaneous vehicle emission signals', begins with a proposal of a *methodological framework* for the advanced or 'expert' compensation of instantaneous vehicle emission signals. This framework is used to support the subsequent analysis of its constituting methodological elements. The chapter concludes with a review of existing signal compensation methodologies. This review places a special focus on compensation methods based upon physical modelling following *systems theory* practice, which were considered as a benchmark for eventual new developments.

*Chapter 5*, 'The $CO_2$ tracer method', contains the complete description of the instantaneous signal compensation methodology that constitutes the main original contribution of this dissertation. The description covers both theoretical and practical aspects.

*Chapter 6*, 'Results and discussion', presents the results of an actual application of the $CO_2$ tracer method to instantaneous emission datasets obtained from an experimental campaign carried out at the VELA facilities (Vehicle Emissions Laboratories) of IET. It also discusses the $CO_2$ tracer method in relation to earlier methodologies, and presents a validation of the method.

*Chapter 7*, 'Conclusions', presents the conclusions of our research and is the final chapter of this dissertation.

# Chapter 2

# Measuring the emissions of road vehicles

Air pollution is a significant risk to human health and to the environment. Outdoor air pollution is estimated to cause 3.7 million annual premature deaths worldwide (WHO 2014). Road transport often appears as the single most important source of urban pollutant emissions in source apportionment studies (*e.g.*, Maykut *et al.* 2003; Querol *et al.* 2007). In the coming decades, road transport is likely to remain a large contributor to air pollution, especially in urban areas.

For this reason, major efforts are being made by regulators, the automotive industry and the scientific community in order to reduce polluting emissions from road transport. These include new powertrains and emission after-treatment technology improvements, fuel refinements, optimised urban traffic management methods, and the implementation of tighter emission standards (EC 2011b).

## 2.1 Emission models and emission factors

Pollutant emissions need to be accurately estimated to ensure that air quality plans are designed and implemented appropriately. Road vehicle emissions are particularly challenging in this regard because they depend on many parameters, such as vehicle characteristics and emission control technology, fuel specifications,

and ambient and operating conditions (gearshift strategy, temperature of engine and after-treatment devices and others). Due to this complexity, and to the variety of vehicle types available in the market, *emission models* are necessarily used to perform the calculations of road transport emissions that support regional or national *emission inventories*.

Smit, Ntziachristos and Boulter (2010) proposed a classification of vehicle emission models in five major categories according to the *input data* required. These range from models which only require mean travelling speed to estimate emissions and models that need traffic situations (*i.e.*, qualitative assessments of driving conditions) to express emissions, to models which require second-by-second engine or vehicle state data to derive emission information for the complete driving profile. Regardless of the differences among practical implementation, every road vehicle emission model will be based on *empirical emissions data*, and it will provide a collection of *emission factors* (EFs), which are functional relations between pollutant emissions and the transport activity that causes them.

This chapter is not intended as a review of the existing vehicle emission models,[1] but rather as a review of how *emissions data* may be collected and presented in the form of EFs. We will therefore examine the *experimental techniques* used to measure road vehicle emissions in relation to the development of EFs found in emission models. The emission measurement techniques covered include those most widely used for road vehicle emissions data collection, namely chassis and engine dynamometer measurements, remote sensing, road tunnel studies and portable emission measurements systems (PEMS). An earlier, similar review was performed by Faiz, Weaver and Walsh (1996). Strong points and limitations are presented for each method, together with literature examples of successful implementations. The main advantages and disadvantages of each method with regard to emissions modelling are also presented.

### 2.1.1 European emissions modelling: the ERMES group

The development of accurate EFs found in road vehicle emission models is a joint enterprise among several parties that requires intensive testing to adequately cover all the relevant vehicle types and driving conditions, and substantial research

[1] Kousoulidou *et al.* (2010d) recently performed a review of vehicle emission models and inventory tools used worldwide.

and modelling efforts to keep up with technological advances. Measurement and modelling methodologies need to be improved to accurately reflect real-world emissions, and this needs to be accomplished with limited resources.

In the European context, these circumstances led to the creation of the ERMES group (European Research group on Mobile Emission Sources) in 2009 in an effort to bring together all European research groups working on transport emission inventories and models, as well as funding agencies and other stakeholders, under the coordination of the European Commission Joint Research Centre (EC–JRC). The ERMES group aims to support a permanent network of mobile emission modellers and users, to coordinate research and measurement programmes for the improvement of transport emission inventories in Europe and to become a reference point for mobile emissions modelling and related topics in Europe while maintaining and improving international contacts (table 2.1).

**Table 2.1:** Selected ERMES group stakeholders

| **Laboratories and member state representatives** | **Vehicle emission modellers** |
|---|---|
| • *Umwelt Bundesamt* (Germany)<br>• IFSTTAR (France)<br>• TNO (the Netherlands)<br>• EMPA (Switzerland)<br>• ARPA Lombardia (Italy)<br>• University of Leeds (United Kingdom)<br>• INSIA-UPM (Spain)<br>• *Umweltbundesamt* GmbH (Austria)<br>• *Trafikverket* (Sweden)<br>• KLIF (Norway)<br>• CASANZ (Australia) | • LAT, Aristotle University of Thessaloniki (Greece)<br>• Technical University of Graz (Austria)<br>• INFRAS (Switzerland) |
| **European Commission and others** | **Industry representatives** |
| • European Commission – DG CLIMA<br>• European Environment Agency (EEA) | • Conservation of Clean Air and Water in Europe (CONCAWE)<br>• European Automobile Manufacturers' Association (ACEA)<br>• Ford Motor Company<br>• AVL MTC |
| | **ERMES group chair** |
| | • European Commission – DG JRC |

The three-level structure adopted by the group (schematically represented in figure 2.1) comprises an executive board—composed of a reduced number of senior scientists in charge of drafting the work programme and monitoring its progress—, a working group on models and emission factors—which includes the JRC, the financing EU Member States, laboratories and national experts—and a broad contact group including the European Environment Agency (EEA), relevant

Directorate-Generals of the European Commission, industry representatives and all other interested parties (Franco, Fontaras and Dilara 2012).

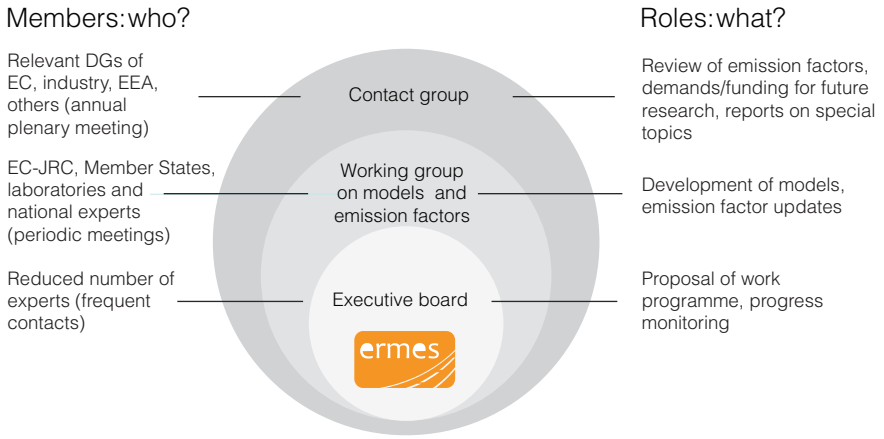


**Figure 2.1:** Structure of the ERMES group

### 2.1.2 ERMES models: COPERT and HBEFA

COPERT (Gkatzoflias *et al.* 2007) and the Handbook of Emissions Factors (HBEFA; de Haan and Keller 2004) are the two leading emission models in Europe. COPERT is the main road transport emissions model of the EMEP/CORINAIR Atmospheric Emissions Inventory Guidebook (AEIG), and it is used by several European member states to compile their official national inventories of emissions from road transport. HBEFA is mostly meant for use at finer geographic scales (down to street canyon level) and requires more detailed traffic data inputs than COPERT. HBEFA is mostly used in the DACH-NL-S European countries (Germany, Austria, Switzerland, the Netherlands and Sweden).

Both models estimate traffic emissions in *three large blocks*, namely emissions produced during thermally stabilised engine operation (hot emissions), excess emissions occurring during engine start from ambient temperature (cold-start and warming-up effects) and non-methane volatile organic compound (NMVOC) emissions due to fuel evaporation. Total emissions are calculated as the combination of vehicle fleet and activity data selected by the user and the libraries of emission factors included in the models.

In the case of COPERT, emission factors are speed-dependent, whereas HBEFA provides emission factors for different 'traffic situations', *i.e.*, qualitative descriptions of the traffic environment. Even though the approaches behind COPERT and HBEFA are somewhat different, both models are largely underpinned by the same experimental data, and further methodological convergence is expected under the steering of ERMES.

HBEFA and COPERT are backed up by extensive amounts of vehicle emissions test data, and they provide emission factors for a comprehensive set of vehicle categories of current and past technology. The emission factors in both COPERT and HBEFA have achieved a high level of quality over the past decade thanks to common projects such as ARTEMIS (Keller and Kljun 2007) or COST 346 (Sturm and Hausberger 2005), together with the national activities and joint funding actions between the DACH-NL-S group and JRC. Nevertheless, both models are in need of various methodological improvements (such as the one presented in this dissertation) and of frequent updates to keep up with new vehicle technologies.

## 2.2 Chassis and engine dynamometer testing

A *chassis dynamometer* simulates the resistive power imposed on the wheels of a vehicle during real driving. It consists of a dynamometer that is coupled via gearboxes to drive lines that are directly connected to the wheel hubs of the vehicle, or to a set of rollers upon which the vehicle is placed, and which can be adjusted to simulate driving resistance. A separate roller will be required for each drive axle (*i.e.*, each axle being driven by the engine).

During chassis dynamometer testing, the vehicle is tied down so that it remains stationary while a professional driver operates it according to a predetermined time-speed profile and gear change pattern shown in a monitor (the so-called *driver's aid*). The driver operates the vehicle to match the speed required at the different stages of the driving cycle (Nine *et al.* 1999). Chassis dynamometer test cycles (*cf.* section 2.2.1) are typically transient (Yanowitz, McCormick and Graboski 2000) and therefore the driver must anticipate and comply with changes in the required speed within a specified tolerance (Wang *et al.* 1997). Experienced drivers are able to closely match the target speed profile.

The load applied to the vehicle via the rollers can be controlled by the laboratory operators to simulate aerodynamic and rolling resistance (road load) for the vehicle under test, while the size of the rollers and the use of flywheels accounts for vehicle inertia. The exhaust flow rate is continuously monitored, and a proportional sample of the vehicle exhaust gas is collected in polymer bags for later analysis, or processed by chemical analysers attached to the sampling line (see figure 2.2). On-line analysers are increasingly being installed in test benches in order to record vehicle emissions with a fine temporal resolution. These analysers may either sample alone or in parallel with the bag sampling technique at the diluted gas line (that is, at the end of the dilution tunnel, where the total flow is quasi-steady and easier to measure).

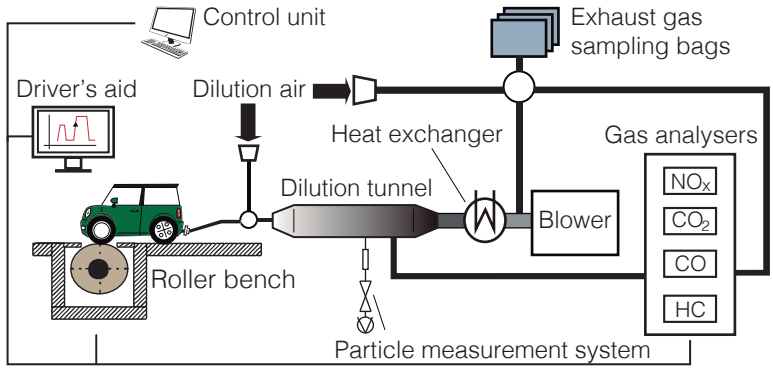


**Figure 2.2:** Schematic representation of a chassis dynamometer emissions test facility

Because dynamometer facilities are designed to meet regulatory standards, their results are viewed as highly accurate as long as proper calibration and maintenance programs are established (Traver *et al.* 2002). Also, they may be enclosed in climatically controlled test cells to simulate driving under a wide range of temperatures, including sub-zero tests.

A disadvantage of a chassis dynamometer testing is that it does not necessarily represent real-world emissions of individual vehicles. This is due to the limited range of test conditions (*e.g.*, the set ambient temperatures and the preconditioning routines, the absence of road gradients) and to the fact that a dynamometer is implemented instead of actual driving. In particular, the driving resistance values that simulate road load are obtained from vehicle coast-down tests often performed under artificially favourable conditions, thus frequently yielding fuel consumption and emission results below real-world levels (Mellios *et al.* 2011). Moreover, chassis

dynamometer test results may not be representative of the emissions of entire vehicle fleets because typically only a few vehicles from each technology class are tested for modelling purposes.

An *engine dynamometer* is a device that simulates the resistive power directly at the engine power output. In an engine dynamometer test cell, the dynamometer shaft is directly connected to the engine shaft and it measures power at the flywheel of the engine, where no transmission or driveline losses influence the results. Fully transient dynamometers may absorb or place any specified load (within limits) on the engine, even during load and speed change conditions. Engine test cells may also be climatically controlled. Emission measurements on an engine dynamometer require removing the engine and the exhaust gas after-treatment system from the vehicle (Oh and Cavendish 1985; Artelt *et al.* 1999).

Heavy-duty vehicle (HDV) engines can be coupled to many different chassis and body types. Heavy-duty *type-approval* regulations have historically relied upon engine dynamometer testing because it would be impractical to type-approve all the possible combinations. A disadvantage of this approach is that the emissions of the complete vehicle are not reflected in engine testing, even though modern engine test benches can be made to run any real-world engine load test cycle by simulating the vehicle to get torque and engine speed curves, either off-line or as hardware-in-the-loop simulations (HILS; *cf.* Lee 2003). In the past few years, the increasing technological sophistication of engine and after-treatment control systems of HDVs has made it cumbersome to perform engine dynamometer tests independently of manufacturers, which in turn continue to use this technique for engine and after-treatment device development, both for heavy-duty and light-duty vehicles (LDVs). Chassis dynamometer testing has thus become the primary source of emissions data for the development of EFs for recent-technology HDVs (*e.g.*, the current EURO VI technology class).

### 2.2.1 Test cycles

A (standard) emissions test cycle (or driving schedule) is a predefined driving profile that the vehicle or engine under test has to follow. Test cycles last for *several minutes*, and often comprise several parts (or sub-cycles) that represent different driving conditions (*e.g.*, urban or highway driving). Test cycles are an integral part of all chassis and engine dynamometer tests, and their representativity and completeness

(*i.e.*, their ability to statistically represent the driving conditions under study) are essential to achieve good testing results (André and Rapone 2009). The number of engine and vehicle dynamometer test cycles used worldwide for emission and fuel consumption measurements is continuously expanding to cover regulatory needs, while also trying to simulate real-world driving conditions (André *et al.* 2006).

Two categories of test cycles may be used in chassis or engine dynamometer tests, namely *steady-state* (or modal) and *transient* cycles: *steady-state test cycles* involve running the engine or vehicle under a number of fixed operating points or 'modes', each one of them defined by a certain constant engine speed and load. For each mode, the engine or vehicle is operated for a sufficient amount of time to produce relatively stabilised emission rates. When two or more modes are included in the test cycle, the emissions measurements from each mode are typically combined using a weighted averaging scheme, with specific definitions of each mode and weighting schemes differing from one test cycle to another (Artelt *et al.* 1999). On the other hand, *transient test cycles* include variations in the operating conditions as part of the test procedure and they are regarded as more representative of real-world operation because they can be designed to account for real-world situations such as idling, acceleration and deceleration. Detailed technical information on the most commonly used standard driving cycles can be found in the literature (CONCAWE 2006a, 2006b; Barlow *et al.* 2009).

Chassis dynamometer test cycles are predominantly transient. This is the case of type-approval cycles such as the FTP and SFTP (Federal Test Procedure and Supplemental Federal Test Procedure, used for emission certification of LDVs in the USA) and the NEDC (New European Driving Cycle, used for emission testing and certification of all Euro 3 and later LDV models in Europe). The latter has often been criticised for being too smooth and underloaded for typical vehicle operation, as it covers only a small area of the operating range of engines (Kågeson 1998; Mellios *et al.* 2011; Weiss *et al.* 2011a).

In general, type-approval cycles underestimate real-world emissions because they exhibit low speed dynamics to ensure that their trace can be followed by the less powerful vehicles, and also because manufacturers are able to optimise the emission performance for specific operating points (Ntziachristos and Samaras 2000). In order to address some of the shortcomings of current type-approval test cycles, a new transient chassis dynamometer test cycle (Worldwide harmonised Light-duty

driving Test Cycle, WLTC) and its accompanying test protocols (WLTP) are being developed within the framework of a larger UNECE project set to produce a global technical regulation for harmonised testing of LDVs.

Besides standard driving cycles used for regulatory purposes, there are many others that characterise driving in specific areas (Esteves-Booth *et al.* 2001) or a particular technology (Rapone *et al.* 2000). From the EF development perspective, the so-called *real-world cycles* provide the most valuable emissions data thanks to a wider coverage of engine operating points in comparison to type-approval cycles. Examples of real-world cycles are the test cycles for LDVs and HDVs included in the default database of the MOVES model (USEPA 2012), the ARTEMIS suite of LDV cycles (André 2004) and the recently developed ERMES test cycle (figure 2.3) which was specifically designed for emission modelling purposes. The short duration of the ERMES cycle is an advantage in terms of testing schedule flexibility and costs of individual test runs (Knorr, Hausberger and Helms 2011).

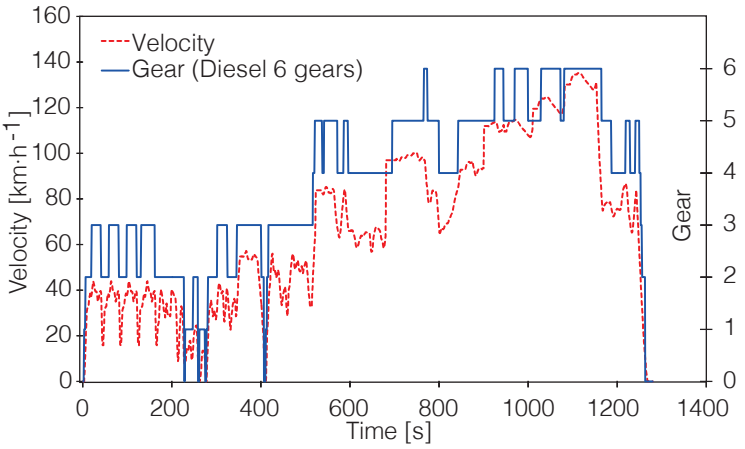


**Figure 2.3:** Time-velocity profile of the ERMES chassis dynamometer test cycle

Engine dynamometer test cycles are predominantly modal. Some of the main modal test cycles used around the world for the type-approval of current-technology heavy-duty engines include the European Stationary Cycle (ESC; applicable in Europe, and comprising 13 modes) and the Supplemental Emissions Test (applicable in the USA, also comprising 13 modes). A few transient test cycles are also in use, such as the European Transient Cycle (ETC) and the US heavy-duty engine Federal Test

Procedure (FTP). For newer technology engines (EURO VI and beyond), the World Harmonised Stationary Cycle (WHSC) and its transient counterpart (WHTC) have been proposed by the UNECE GRPE group in an effort to create global cycles that reproduce typical driving conditions in the EU, USA, Japan and Australia (Steven 2001).

### 2.2.2 EF development from dynamometer laboratory data

*Chassis dynamometer* testing has achieved a high degree of standardisation and is arguably the most proven technology for vehicle emissions measurements. In order to obtain robust EFs (*i.e.*, ones that are unlikely to change within the accepted uncertainty if there was repetition of the original measurement programme or modelling activity; *cf.* IPCC 2003), a sufficiently large number of vehicles should be tested repeatedly under different driving cycles.

*Engine dynamometer* testing is somewhat less useful for EF development because it produces results in units of quantity of pollutant emitted per unit of engine energy output (such as $g \cdot kWh^{-1}$), which are not directly relevant to real-world activity patterns. To estimate total emissions using this type of EF, one needs to estimate or calculate the engine power profile over a trip travelled and apply a relevant EF.

A straightforward approach to EF development is to plot the aggregated—or 'bag'—results of various driving cycles with respect to the mean speed or another aggregated kinematic parameter (*e.g.*, mean acceleration or relative positive acceleration) of the specific cycle and then fit a polynomial trend line to the experimental data using mathematical regression. The resulting formula of the trend line is the EF that expresses vehicle emissions as a function of the selected parameter. A disadvantage of such a simple approach is that it may not adequately capture the impact of different driving cycles upon emission performance.

An illustration of this situation is provided in figure 2.4 (see right hand column of this page), where the mass emissions of $NO_x$ (in $g \cdot km^{-1}$) over forty-one different driving cycles and sub-cycles for fifteen different Diesel Euro 4 passenger cars of similar engine capacity are summarised as a function of mean cycle or sub-cycle velocity. Figure 2.4 shows the mean, maximum, and minimum recorded value for each sub-cycle to illustrate the variability of the emission levels within a given vehicle class, and also the variability of average emission levels from different test cycles with similar average velocities.[2]

The observed variability is much higher for CO and HC and lower for $CO_2$ and fuel consumption than it is for $NO_x$ (Boulter and McCrae 2007; Zallinger 2010), and it is generally higher at lower mean velocities (Choi and Frey 2009, 2010). In any case, the development of robust EFs from chassis dynamometer data requires the measurement of a sufficient number of vehicles *and* an adequate selection of driving cycles that are representative of the driving conditions being modelled.

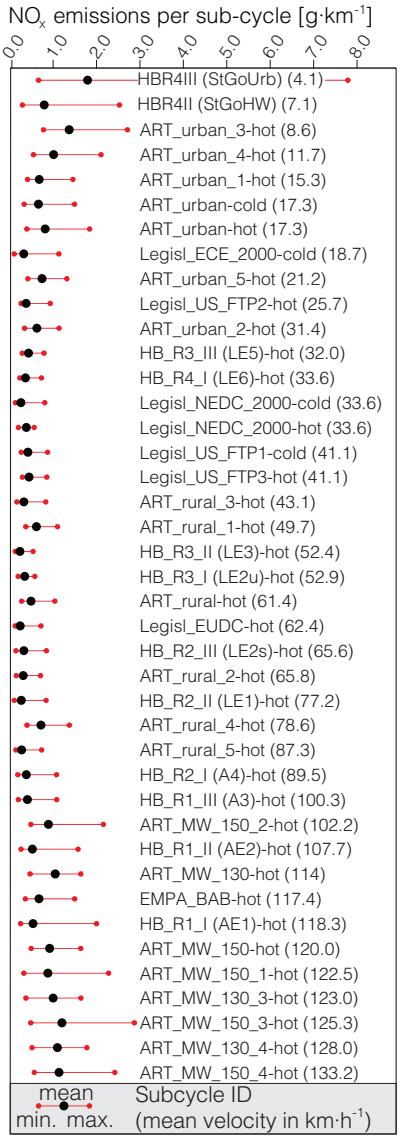


**Figure 2.4:** Illustration of the variability of chassis dynamometer test results

[2] Source: Artemis 300 database (many thanks go to Stefan Hausberger for providing the data an the idea as to how to illustrate this point).

Whenever instantaneous data from on-line analysers (typically with a sampling frequency of 1 Hz or higher) are available in addition to aggregated (or 'bag') values, other, more elaborate approaches to EF development may be considered. In such cases, measured emission values can be related to recorded instantaneous kinematic parameters or engine covariates. This is done in the MOVES model, which uses the metric of vehicle-specific power (VSP) and instantaneous velocity to bin instantaneous data and estimate EFs, and also in PHEM (Passenger car and Heavy duty vehicle Emission Model), which uses modal chassis and engine dynamometer test data to produce engine emission maps that predict pollutant mass emissions as a function instantaneous engine speed and engine power, normalised by their maximum rated values (see figure 2.5).

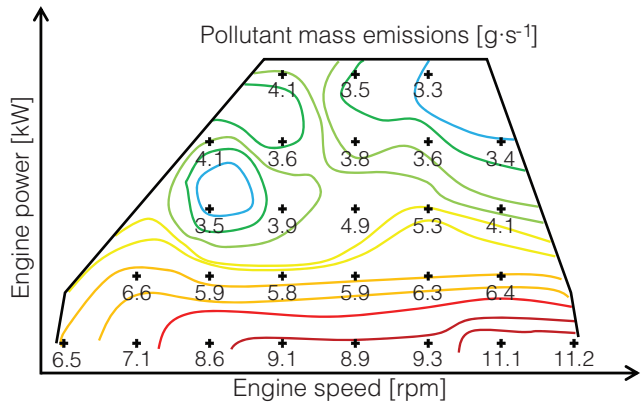


**Figure 2.5:** Example of engine emission map [adapted from Kousoulidou *et al.* (2010d)]

An advantage of EFs derived from *instantaneous emissions data* is that they allow for the *simulation* of fuel consumption and emissions for any driving pattern and vehicle configuration (Kousoulidou 2011). For such applications, the instantaneous mass emissions for a non-measured driving pattern can be interpolated from measured data. However, the creation of engine emission maps requires additional *data post-processing* efforts to fine-tune the results. For example, maps derived from modal data may have to incorporate correction factors to account for the excess emissions typical of transient states, or be calibrated with 'bag' results (Hausberger *et al.* 2009).

Additional complications arise if *transient data* are used to develop the instantaneous EFs. In this case, the fine allocation of instantaneous mass emissions to engine state data poses a technical challenge because pollutant concentrations are affected by a number of distortions including mixing of the exhaust gas, variable transport delays and dispersion due to the finite dynamic response characteristics of gas analysers. As pointed out in chapter 1, all of these effects result in measured emission signals which are smoothed, dynamically delayed instances of the 'true' signals at the catalyst-out point. A number of methodological proposals have been made to address this issue through data post-processing [see, for example, the work of Weilenmann, Soltic and Ajtay (2003); Ajtay and Weilenmann (2004) and Geivanidis and Samaras (2008)], but they are not applied in routine measurements.[3]

### 2.2.3 Chassis and engine dynamometer applications

*Chassis dynamometer* measurements are used for the *type-approval* of road vehicles and engines (*i.e.*, to check and certify the compliance with legal emission limits). Scientific studies involving chassis dynamometer measurements are conducted for several other purposes, including the investigation of the emission characteristics of specific types of vehicles or pollutants, the assessment of emission control technologies or the analysis of the emissions performance of different types of fuels.

Chassis dynamometer testing can cover a wide range of pollutants depending on the type of analysers used to process vehicle exhaust. As far as the type of vehicles tested is concerned, chassis dynamometer tests are more commonly used for motorcycles, passenger cars and light commercial vehicles (Pelkmans and Debal 2006; Fontaras *et al.* 2007; Fontaras, Pistikopoulos and Samaras 2008; Chiang *et al.* 2008) than for HDVs (Wang *et al.* 1997; Morawska *et al.* 1998; Whitfield and Harris 1998; Ramamurthy and Clark 1999; Clark *et al.* 2002), because only the more costly HDV chassis dynamometer laboratories can accommodate these larger vehicles.

Chassis dynamometer studies have been used to investigate the emission profiles of several pollutants from different types of vehicles under various *operating conditions*. For instance, Yanowitz *et al.* (1999) reported the emissions of regulated pollutants from twenty-one in-use Diesel HDVs as measured on a chassis dynamometer for

[3] One such methodological proposal—described in chapter 5—is the main original contribution of this dissertation.

three different standard driving cycles. Mohr, Forss and Steffen (2000) carried out an experimental study on particulate emissions of gasoline vehicles with three passenger cars at a chassis dynamometer. Durbin *et al.* (2002) investigated the variation of ammonia emissions across different driving cycles. Soltic and Weilenmann (2003) studied the total amount and the partitioning of $NO_x$ emissions over different test cycles for sixteen Euro 2 light-duty vehicles. Heeb *et al.* (2003) reported the emissions of methane, benzene and the alkyl benzene class compounds for gasoline passenger cars from Euro 0 to Euro 3 technology class over the US urban driving cycle (FTP), measured by chemical ionisation mass spectrometry (CI-MS) under cold and hot engine conditions.

In order to assess the influence of *cold engine start events* upon emissions, Weilenmann *et al.* (2005) measured and analysed benzene and toluene emissions at various ambient temperatures for Euro 3 gasoline cars, Euro 2 Diesel cars and pre-Euro 1 gasoline cars over a repetitive urban real-world test cycle. More recently, Livingston, Rieger and Winer (2009) used a chassis dynamometer equipped with Fourier Transform Infrared Spectroscopy (FTIR) analysers to measure tailpipe ammonia emissions from a random sample of light and medium-duty vehicles, while Adam *et al.* (2011) investigated the time-resolved emissions of several hydrocarbons and other unregulated pollutants of a medium-sized truck using state-of-the-art spectrometers, and Fontaras *et al.* (2013) investigated the emission profile of Diesel and gasoline Euro 5 passenger cars over several test cycles.

Chassis dynamometer studies have been used to assess the performance characteristics of different *emission control technologies*. For example, Huai *et al.* (2004) measured $N_2O$ emissions from different vehicle technologies ranging from non-catalyst to super-ultra-low-emission vehicles (SULEV) over the FTP and other, more aggressive cycles. Heeb *et al.* (2006a, 2006b) studied the efficiency of catalytic reduction of NO and the selectivity towards $NH_3$ and analysed the parameters with impact upon the $NH_3$ output of a three-way catalyst equipped gasoline LDV during real-world driving. Olfert, Symonds and Collings (2007) studied the modal particle emissions of a passenger car equipped with a Diesel oxidation catalyst (DOC). Bergmann *et al.* (2009) evaluated the efficiency of a passenger car Diesel particulate filter (DPF) over NEDC and a custom acceleration-deceleration chassis dynamometer cycle, while Biswas *et al.* (2008, 2009) studied the particulate emissions of Diesel HDVs retrofitted with recent-technology after-treatment systems (DPF and selective catalytic reduction, SCR) over steady-state and transient cycles.

Repeated chassis dynamometer testing is an excellent way to assess the *influence of different fuels* upon vehicle emissions, because the repeatable conditions allow even small emission and consumption differences to be observed. Chao *et al.* (2000) used chassis dynamometer measurements to study the effect of an additive containing methanol on the emission of carbonyl compounds from a HDV Diesel engine. Some chassis dynamometer studies (Wang *et al.* 2000; Fanick and Williamson 2002; USEPA 2002) compared exhaust emissions from in-use heavy-duty trucks fuelled with biodiesel blends with those from trucks fuelled with Diesel fuel.

The impact upon both particle and carbon dioxide emissions of alternative fuels such as liquefied petroleum gas (LPG) and unleaded gasoline was analysed by Ristovski *et al.* (2005). Peng *et al.* (2008) examined the effect of biodiesel blend fuel on aldehyde emissions in comparison with those from Diesel fuel. Aslam *et al.* (2006) studied the performance of compressed natural gas in comparison with gasoline. Nelson, Tibbett and Day (2008) reported the emissions of a range of toxic compounds from twelve in-use vehicles which were tested using urban driving cycles developed for Australian conditions and Diesel fuels with varying sulphur contents. More recently, Kousoulidou *et al.* (2010b) studied the impact of biodiesel on the regulated pollutant emissions and fuel consumption of a modern passenger car, and Fontaras *et al.* (2012) assessed the on-road emissions of four Euro V Diesel and CNG waste collection trucks. A study by Kousoulidou *et al.* (2012) used chassis dynamometer test data to provide correction factors for pollutant emissions when biodiesel is used on passenger cars at different blending ratios.

Chassis dynamometer measurement data have also been used as an input to specific *emission models*. For example, the study of Kear and Niemeier (2006) used chassis dynamometer test data to derive a model aimed at developing operational correction factors for distance-based HDV Diesel particle EFs measured on standard test cycles for real-world conditions. The study of Fontaras *et al.* (2007) presented the application of a tool for predicting $CO_2$ emissions of vehicles as measured on a chassis dynamometer under different operating conditions, and these results were directly used to represent hybrid EFs in COPERT. In the context of the DECADE project—carried out under the 5$^{th}$ Framework Programme of the European Commission—a software package was developed to predict vehicle fuel consumption and emissions for a given distance-speed profile. Specific LDVs were subjected to measurements on engine dynamometers in order to give input to the model (Pelkmans and Debal 2006).

Engine dynamometer test data have been found to be especially accurate for the simulation of *instantaneous fuel consumption*. Moreover, the upcoming HDV $CO_2$ monitoring regulation is expected to rely upon a combination of vehicle component measurement and modelling and vehicle simulation (Hausberger *et al.* 2012).

Newer powertrain configurations such as Hybrid Electric Vehicles (HEVs) and full-electric vehicles (EVs) need modified test benches to evaluate the electric power flows among the driveline components. UNECE Regulation 101 (UNECE 2005) defines standard test procedures for the measurement of fuel consumption and $CO_2$ emissions from passenger cars and LDVs, including HEVs and plug-in hybrid electric vehicles (PHEVs). This regulation also proposes a method to measure the *electric range* of EVs and PHEVs. Silva, Ross and Farias (2009) proposed a methodology based on the SAE J1711 standard to produce dynamometer-based EFs for PHEVs, including life cycle assessment considerations to make comparisons fair among different vehicle technologies. In general terms, chassis dynamometers (coupled with some degree of hardware simulation) capture the emissions of newer powertrain configurations better than engine dynamometers (ICCT 2012).

### 2.2.4 Summary

The characteristics of engine and chassis dynamometer measurements are summarised in tables 2.2 and 2.3.

**Table 2.2:** Summary of vehicle emission measurements in chassis dynamometer laboratories

| Applications | Characteristics |
|---|---|
| *General*<br>• Type-approval and general testing of LDVs.<br>• General testing of HDVs.<br>• More commonly used for LDVs than for HDVs.<br>*EF development*<br>• Provides high-resolution EFs.<br>• The quality of EFs is linked to the representativity of the test cycle used.<br>• The use of standardised cycles leads to good repeatability and comparability of results (slightly worse than engine dynamometer testing). | *Advantages*<br>• Proven technology, highly automated and economically optimised. Good precision and repeatability.<br>• The complete vehicle is measured, leading to better representativeness for on-road duty cycles (as compared to engine dynamometers).<br>• Emission measurements are obtained in units that are more useful for emission inventory purposes.<br>• Relatively inexpensive (especially for LDVs).<br>*Disadvantages*<br>• Driving cycles/dynamometer load may not be representative of real-world conditions. Limited flexibility to test alternative driving conditions.<br>• Dilution conditions not representative of real world (especially for particle number emissions). |

**Table 2.3:** Summary of vehicle emission measurements in engine dynamometer laboratories

| Applications | Characteristics |
|---|---|
| *General*<br>• Type-approval of heavy-duty engines.<br>• Applied to LDV engines in the development phases of the engine and for the testing of after-treatment devices.<br>*EF development*<br>• Provides high-resolution EFs.<br>• Highest precision and repeatability.<br>• The quality of EFs is linked to the representativity of the test cycle used.<br>• More commonly used for HDVs than for LDVs (modal test results used to fill engine maps). | *Advantages*<br>• Proven technology, highly automated and economically optimised.<br>• The use of standardised cycles leads to good repeatability and comparability of results.<br>*Disadvantages*<br>• Results are expressed as quantity of pollutant per unit of mechanical energy delivered by the engine (*e.g.*, in $g \cdot kWh^{-1}$); these units are not directly relevant to real-world activity patterns.<br>• Does not necessarily represent real-world emissions, as the influence of the whole vehicle is ignored and only a limited number of vehicles under a limited range of conditions are tested.<br>• Requires engine disassembly from chassis leading long installation times and high costs.<br>• Test cycles utilised for testing may not be representative of real-world driving conditions; susceptible to 'cycle-beating'.<br>• After-treatment systems are not always taken into account; thermal conditions of the after-treatment systems are different from real-world ones. |

## 2.3 Remote sensing

In remote sensing (also called 'roadside measurement'), instantaneous ratios of pollutant concentrations are determined as vehicles pass by a measurement station on the roadway (Bishop *et al.* 1989). Remote sensing equipment is able to take several readings of the ratios of concentrations for each exhaust plume analysed, correct for background levels and report a mean value for each passing vehicle. In remote sensing measurements, infrared and ultraviolet light of specific wavelengths from a source passes through the exhaust plume to a detector, wherein the amount of light absorbed is proportional to the concentration of CO, $CO_2$ or THC (measured in the IR band) and $NO_x$ (measured in the UV band; *cf.* Bishop and Stedman 1996). Remote sensing can be used to determine the molar ratios of pollutants, offering a quick and effective method of monitoring exhaust emissions from in-use vehicles under real-world driving operation.

The major advantage of remote sensing is that it enables the monitoring of the emissions of large numbers of vehicles (up to thousands per day). It also offers the necessary resolution to identify emission levels of single vehicles—whose emission technology may be determined by video recording licence plates and cross-referencing them with vehicle registration databases—and not just the average fleet-wide emission level. This has made this technique especially popular for the identification of high emitters (Jiménez *et al.* 2000; Chan *et al.* 2004; Ko and Cho 2005). On the other hand, remote sensing only gives an uncertain instantaneous estimate of emissions at a specific location, is a rather 'fair weather' technology (Frey and Eichenberger 1997) and it cannot be used across multiple lanes of heavy traffic. In most cases, approximately half of the data collected are valid. Moreover, measurements of exhaust emissions by remote sensing are influenced by many factors, such as the physical characteristics of sampling sites, sampling times and operating mode of the vehicles (Sjödin and Lenner 1995; Sadler *et al.* 1996), and even the visible presence of the measurement instruments on the roadside may have an influence on the behaviour of some drivers as they approach the measurement site. Thus, the uncertainty of emissions factors derived from remote sensing studies is large, and their resolution is limited as this technique can only record 'snapshots' of vehicle emissions and does not provide insight into how emissions vary at different points of a trip (Borken-Kleefeld *et al.* 2012).

### 2.3.1 EF development from remote sensing data

In remote sensing measurements, exhaust plumes are immediately diluted with ambient air, and so the actual concentrations of pollutants at the tailpipe cannot be directly measured. However, assuming that dilution is turbulent and happens instantaneously, the ratios of pollutant concentrations for a given plume should be preserved (Bishop and Stedman 1996), and it is these that are measured and reported by remote sensing equipment (*e.g.*, CO to $CO_2$; *cf.* Jiménez *et al.* 2000). By assuming stoichiometric combustion conditions and mean fuel characteristics (carbon mass fraction and ratio of H to C), one can calculate an expected concentration of $CO_2$ at the tailpipe (Heywood 1988), and thus the tailpipe concentration of a generic pollutant $P$ can be estimated by means of equation 2.1 (Jiménez 1999).

$$[P]_{tailpipe} = \left[ \frac{[P]_{RS}/[CO_2]_{RS}}{1 + [CO]_{RS}/[CO_2]_{RS} + [HC]_{RS}/[CO_2]_{RS}} \right] \cdot [CO_2]_{stoich} \tag{2.1}$$

In equation 2.1, $[CO_2]_{stoich}$ is the stoichiometric concentration of $CO_2$ for the fuel being considered, and the ratios of pollutant concentrations to $CO_2$ with the $RS$ subscript are measured by the remote sensing instrument. The assumption of stoichiometric combustion is correct for properly-functioning gasoline vehicles, but in Diesel vehicles (and frequently in gasoline direct injection vehicles) lean-burn mixtures are used. In these cases, $CO_2$ does not perform well as a reference gas to estimate tailpipe pollutant concentrations.

Remote sensing measurements can also be used to develop fuel-based EFs by measuring the ratios of concentrations of pollutants and carbon-containing species ($CO_2$, CO and HC) in the vehicle plumes and referring them to the amount of fuel consumed. Since the conversion efficiency of elemental carbon in fuel to $CO_2$ is consistently above 99% for normal operation of both gasoline and Diesel vehicles, it is reasonable to assume that the carbon mass in the exhaust plume is mostly in the form of $CO_2$ and CO, and then the measurement of other carbon-containing compounds can be omitted. Thus, it is possible to estimate an emission factor for $P$ by means of equation 2.2 (Singer and Harley 1996).

$$E_P = \frac{\text{Estimated mass emission of P}}{\text{Estimated fuel consumption}} = \left[ \frac{[P]_{RS}/[CO_2]_{RS}}{1 + [CO]_{RS}/[CO_2]_{RS}} \right] \cdot \frac{M_P \cdot w_C}{M_C} \tag{2.2}$$

In equation 2.2 above, $E_P$ is given in kg of $P$ per kg of fuel burned, $w_C$ is the weight fraction of carbon in the fuel considered and $M_P$ and $M_C$ are the molecular/atomic masses (in $g \cdot mole^{-1}$) of $P$ and elemental carbon, respectively. For the purposes of area-wide emissions estimation, this fuel-based approach may be adequate, but not enough for meso- or micro-scale emission inventories (Cadle and Stevens 1994). A shortcoming of this approach is that it is not straightforward to associate roadside emission concentrations with the engine states that produce them because the latter are not recorded. EFs can be expressed in qualitative terms of vehicle operation, such as emissions over 'acceleration', 'steady-speed', and the like (primarily based on the location of the remote-sensing equipment used). They can also be linked to estimated kinematic parameters such as vehicle-specific power (Frey, Zhang and Rouphail 2010). An estimation of instantaneous fuel economy is required to convert fuel-based emissions to distance- or time-based estimates.

The application of remote sensing to the derivation or validation of disaggregate EFs (*i.e.*, broken down by vehicle category) requires additional data for each passing vehicle to allocate measured EFs to the vehicle class (notably engine type and year of first registration, which may be determined after the measurement if licence plate recognition is implemented). The EFs estimated using a fuel-based approach become more uncertain for pollutants that are characterised by concentrations close to background levels (due to a low signal-to-noise ratio of the recorded concentrations), which in turn are affected by older, diluted exhaust plumes.

### 2.3.2 Remote sensing applications

Remote sensing studies of road vehicle emissions abound in the literature. Singer and Harley (1996) built a large database of on-road vehicle emissions to estimate fuel-based EFs of CO and HC using a remote sensing device. Yu (1998) developed the ONROAD emissions estimation model, which established a relationship between the emission rate and the instantaneous speed profile of a vehicle based on in-use CO and HC emissions data collected from five highway locations in the Houston

area (Texas, USA) using remote sensing. In one of their multiple applications of the technique, Stedman and Bishop (1997) used remote sensing to evaluate the effectiveness of a vehicle inspection and maintenance programme in the metropolitan area of Denver (Colorado, USA). A database of EFs vehicles based on remote sensing measurements of CO, HC and NO was developed in Hong Kong for both gasoline (Chan *et al.* 2004) and Diesel vehicles (Chan and Ning 2005). In Mexico City—where the availability of data used in traditional on-road mobile source estimation methodologies is limited—the remote sensing technique was used within a scientific study by Schifter *et al.* (2005) as an alternative method to estimate motor vehicle emissions. Guo *et al.* (2007) performed on-road remote sensing measurements on over 32,000 gasoline vehicles at five sites in Hangzhou, China, and derived average EFs for CO, HC and $NO_x$ specific of model year, technology class and vehicle type. Westerdahl *et al.* (2009) conducted measurements in three different environments (on-road, roadside and ambient) in Beijing (China) and derived CO, black carbon and ultrafine particle number fuel-based EFs for on-road LDVs and HDVs. Wehner *et al.* (2009) measured number size distributions of exhaust particles and thermodynamic parameters under real traffic conditions with roadside measurements using a Diesel and a gasoline passenger car driven under different conditions and calculated distance-based EFs for primary emissions of particles.

Remote sensing has been employed in several *emission model comparison and validation* processes. Ekström, Sjödin and Andreasson (2004) used on-road remote sensing measurements for gasoline and Diesel passenger cars and HDVs to evaluate the COPERT III model. Hueglin, Buchmann and Weber (2006) found good agreement between the average real-world road traffic EFs obtained from long-term roadside air quality measurements at a monitoring site of the Swiss national air pollution monitoring network and the corresponding EFs from the HBEFA model. An evaluation of the International Vehicle Emission (IVE) model—which was developed by USEPA to estimate emissions from motor vehicles in developing countries—was performed by Guo, Zhang and Shi (2007) using on-road remote sensing measurements.

Remote sensing can also provide interesting results about *real-world driving conditions* that are difficult to replicate in the laboratory. For example, some studies were specifically targeted at the effects of altitude upon vehicle emissions (Bishop *et al.* 2001; Burgard *et al.* 2006). Akin to tunnel studies, remote sensing campaigns can be used to assess *emission trends* and to evaluate the effects of emission control

standards upon air quality (Schifter *et al.* 2007; Carslaw *et al.* 2011), or to support and orient air quality policies (Xie *et al.* 2005).

### 2.3.3 Summary

The characteristics of the remote sensing technique for the measurement of vehicle emissions are summarised in table 2.4.

**Table 2.4:** Summary of remote sensing of vehicle emissions

| Applications | Characteristics |
|---|---|
| *General*<br>• Real-world validation of EFs.<br>• Investigation of the relationship between instantaneous emissions and local/regional air quality levels.<br>*EF development*<br>• Disaggregated EFs require vehicle registration data.<br>• Time- or distance-based EF development requires assumptions that increase uncertainty. | *Advantages*<br>• Easy setup.<br>• Possibility of measuring a large number of on-road vehicles (in the range of thousands per day).<br>*Disadvantages*<br>• Only gives an instantaneous estimate ('snapshot') of emissions at a specific location, and cannot be used across multiple lanes of heavy traffic. Measurements are affected by adverse weather conditions.<br>• Values expressed with reference to $CO_2$.<br>• Laborious procedure to assign emissions to vehicle type/technology. |

## 2.4 On-road (chase) measurements

During on-road (also called chase or plume chase) measurements, individual vehicles are followed by a mobile laboratory—usually on board of a van or trailer—that is instrumented with gas and aerosol measurement equipment (ideally instruments with fast time response and high sensitivity, such as laser spectrometers), plus meteorological and positioning instruments, and even video recording equipment to monitor traffic situations (Shorter *et al.* 2005). In a similar fashion as in remote sensing studies, $CO_2$ is used as a tracer of combustion, and the results indicate the relative concentration of the pollutant of interest per $CO_2$ concentration value. These mobile laboratories are able to capture the exhaust plume of the vehicle being followed, thus providing real-world emissions data under a wide range of operating and environmental conditions. Mobile emission laboratories make it possible to

study a statistically representative sample of vehicles for fleet characterisation. One disadvantage is that such measurements are best conducted on a test track due to traffic safety considerations. Moreover, they are limited by a minimum distance of about ten metres between the laboratory and the vehicle being chased—unless the laboratory is mounted on a trailer; see (Morawska *et al.* 2007)—and a maximum chase speed of approximately 120 kilometres per hour.

### 2.4.1 EF development from on-road measurement data

On-road measurements allow for the calculation of fuel-based EFs. The derivation of EFs is analogous to remote sensing applications discussed in section 2.3.1. In some practical instances, mobile laboratories may sample within traffic without following a particular vehicle to get average on-road emission levels, or be parked at specific locations to perform roadside or background measurements (Pirjola *et al.* 2004).

### 2.4.2 On-road measurement applications

Chase measurements are especially valuable for the study of particulate emissions (Kittelson *et al.* 2006; Canagaratna *et al.* 2004; Morawska *et al.* 2007) because they allow the study of secondary formation after the exhaust, and also due to the fact that—unlike measurements in dilution tunnels used in dynamometer studies—they are not affected by artefact nucleation modes (Maricq, Podsiadlik and Chase 1999). This technique has also been used to investigate the influence of real-world driving upon vehicle emissions of other pollutants. For example, Shorter *et al.* (2005) used chase measurements to study the NO and $NO_2$ emissions profile of the New York City Transit bus fleet, and a follow-up study by Herndon *et al.* (2005) included $SO_2$, $H_2CO$ and $CH_4$.

### 2.4.3 Summary

The characteristics of the on-road technique (vehicle chase) for the measurement of vehicle emissions are summarised in table 2.5.

**Table 2.5:** Summary of on-road (chase) measurement of vehicle emissions

| Applications | Characteristics |
|---|---|
| *General*<br>• Real-world validation of EFs.<br>*EF development.*<br>• The disaggregation of EFs by vehicle technology class requires vehicle registration data. | *Advantages*<br>• Data are collected under real-world conditions in the driving environment, capturing details that are overlooked in standard cycles.<br>• Real-world dilution taken into account (relevant for particle emissions).<br>*Disadvantages*<br>• Testing may pose a hazard to traffic safety; best conducted on closed tracks.<br>• Expensive and time-consuming tests.<br>• Limitations in linking emission measurement to driving condition.<br>• Uncertainty induced by the unknown dilution ratio between the tailpipe and the sampling point. |

## 2.5 Tunnel studies

Tunnel studies involve measuring the total flux of pollutants from vehicles passing through a tunnel and correlating it to traffic flow (Jamriska *et al.* 2004; Hueglin, Buchmann and Weber 2006). Pollutant measurements are typically performed at the entrance and exit of tunnels with separate bores for each direction. Total pollutant emissions may be calculated by estimating the air flow through the tunnel and multiplying it by the difference in pollutant concentrations between the outlet and inlet. Wind speeds and through-traffic are also recorded.

An advantage of tunnel studies is that, contrary to roadside or chase experiments, the wind conditions in road tunnels are well defined, and so average absolute levels of emissions (rather than estimations based on $CO_2$) can be obtained. Tunnel studies are thus able to capture a cross-section of the on-road vehicle fleet and represent real-world operation conditions at the location of the tunnel. These, in turn, may not be typical of real-world urban driving, since tunnels are usually traversed at steady speeds (El-Fadel and Hashisho 2000).

An additional benefit of tunnel studies is that they can cover not just tailpipe emissions, but also *brake lining wear, tyre wear and emissions of secondary particulate matter* coming from chemical transformations within the tunnel. A notable disadvantage of tunnel studies is the difficulty to apportion emissions to specific

vehicle classes unless different tunnel bores are dedicated to them (Geller *et al.* 2005). Furthermore, induced wind speed effects in the tunnel due to the movement of large vehicles may affect the driving resistance—and therefore the emissions—of lighter cars (Corsmeier *et al.* 2005).

### 2.5.1 EF development from tunnel studies data

Tunnel studies can be used to derive aggregated real-world EFs. These may be either distance- or fuel-specific (if a carbon balance can be assumed). The EFs from tunnel measurements may be calculated according to the method of Pierson (Pierson and Brachaczek 1983; Pierson, Gertler and Robinson 1996) (equation 2.3), where $EF_{veh}$ is the average EF (in $mg \cdot vehicle^{-1} \cdot km^{-1}$), $C_{out}$ and $C_{in}$ represent the pollutant mass concentrations (in $mg \cdot m^{-3}$) at the exit and entrance of the tunnel, respectively. $A$ is the tunnel cross-sectional area (in $m^2$), $U$ is the wind speed (in $m \cdot s^{-1}$), $t$ is the sampling duration (in $s$), $N$ is the total number of vehicles during the sampling period and $L$ is the distance between the two monitoring stations (in $km$). When using this equation, one assumes that the movement of air and vehicles causes uniform mixing and distribution of pollutants throughout the tunnel (El-Fadel and Hashisho 2001).

$$EF_{vehicle} = \frac{C_{out} - C_{in}}{N \cdot L} \cdot A \cdot U \cdot t \tag{2.3}$$

In a similar fashion to remote sensing and chase experiments, *fuel-based EFs* may be calculated from road tunnel experiments using the carbon balance of the major carbon-containing exhaust constituents (Miguel *et al.* 1998; Kirchstetter *et al.* 1999; Kean, Harley and Kendall 2003).

### 2.5.2 Tunnel study applications

Several tunnel studies have been conducted to measure and analyse gaseous and particulate pollutants emitted by road vehicles. The majority of these studies were aimed at obtaining representative EFs using mass balance techniques (Ingalls, Smith and Kirksey 1989; Sjödin and Lenner 1995; Staehelin *et al.* 1995, 1997; Rogak *et al.* 1998; Sjödin *et al.* 1998; Sturm *et al.* 2003).

Allen *et al.* (2001) measured particulate matter emissions in a tunnel in the San Francisco Bay area (California, USA) and determined the chemical composition of sampled particulate, as well as separate EFs for HDVs and LDVs. Abu-Allaban, Rogers and Gertler (2004) measured size distributions of particle emissions in a Pennsylvania (USA) highway tunnel using a scanning mobility particle sizer, and were able to determine EFs for LDVs and gasoline HDVs. Cheng *et al.* (2006) calculated a real-world EF for $PM_{2.5}$ in the Shing Mun tunnels (Hong Kong), while Ho *et al.* (2009) calculated vehicle EFs for seventeen gas and particulate polycyclic aromatic hydrocarbons (PAHs) at the same location. Sánchez-Ccoyllo *et al.* (2009) calculated EFs for fine particles, coarse particles, inhalable particulate matter and black carbon, as well as size distribution data for inhalable particulate matter from measurements at two different tunnels in São Paulo (Brazil).

Because the dispersion of pollutants is prevented by the confined space, tunnels offer a suitable microenvironment for *model evaluations*. Tunnel studies have thus been used to validate EFs found in road transport emission models by comparing the results of the measurements with the calculated pollutant concentrations based on the corresponding EFs for the mix of vehicles operating in the tunnel (Hsu *et al.* 2001; Hausberger *et al.* 2003; Colberg *et al.* 2005a; Singh and Sloan 2006). One disadvantage of this approach is that it only provides a lump average of all vehicle categories operating through the tunnel, which are frequently heterogeneous.

Tunnel studies have also been used to evaluate the impact of *real-world sources of variability* that are difficult to reproduce on the test bench, such as the effect of *road gradient* (Kean, Harley and Kendall 2003; Colberg *et al.* 2005b; Chang, Lin and Lee 2009), or diurnal and seasonal traffic emission variations (Grieshop *et al.* 2006). Also, repeated measurements in tunnels over long periods of time have been used to assess the impact of technological and legislative improvements upon *emission trends* (Kean *et al.* 2002; Stemmler *et al.* 2005; Vollmer *et al.* 2007; Ban-Weiss *et al.* 2008; Kean *et al.* 2009).

### 2.5.3 Summary

The characteristics of tunnel studies for the measurement of vehicle emissions are summarised in table 2.6.

**Table 2.6:** Summary of tunnel studies for the measurement of vehicle emissions

| Applications | Characteristics |
|---|---|
| *General*<br>• Real-world validation of EFs.<br>• Assessment of long-term emission trends (experiments that share the same setup and location).<br>• Particle emission measurements under controlled dilution conditions.<br>*EF development*<br>• Cannot provide disaggregated EFs.<br>• Can cover brake lining wear and tire wear and emissions of secondary particulate matter coming from chemical transformations within the tunnel. | *Advantages*<br>• Monitoring of a large number of vehicles under real-world driving conditions.<br>• Real-world dilution taken into account (important for particle emissions).<br>• Covers both tailpipe and non-tailpipe sources (may be a disadvantage if only one source needs to be monitored).<br>*Disadvantages*<br>• Results are lump averages of vehicles passing through the tunnel.<br>• Differences in traffic composition, experimental setups and assumptions of pollutant dispersion models have a large influence on the results.<br>• Tunnels are usually traversed at a semi-constant speed which is not a typical traffic situation. |

## 2.6 On-board measurements (PEMS)

Portable emissions measurement systems (PEMS) are complete sets of emission measurement instruments that can be carried on board of the vehicle under study (Vojtíšek-Lom and Cobb 1997; Frey *et al.* 2003). Such systems can provide instantaneous emission rates of selected pollutants with satisfactory levels of accuracy. A PEMS unit is usually comprised of a set of gas analysers with heated sampling lines directly connected to the tailpipe, plus an engine diagnostics scanner designed to connect with the on-board diagnostics (OBD) link of the vehicle and an on-board computer that provides data regarding emissions, fuel consumption, vehicle speed, engine speed and temperature, throttle position and other parameters. PEMS typically measure instantaneous raw exhaust emissions of $CO_2$, CO, $NO_x$ and THC. Portable *particle mass* analysers have become commercially available after extensive testing (Mamakos *et al.* 2011), and particle number analysers are expected to follow suit.

Exhaust flow meters are attached to the tailpipe (alternatively, the exhaust flow rate can be calculated from engine operating data, known engine and fuel properties and measured $CO_2$ concentrations in the exhaust gas) while a GPS and a weather station are normally installed on the external area of the vehicle. In some cases,

other instruments may be used, namely accelerometers to record instantaneous acceleration (Oprešnik *et al.* 2012), altimeters or video/photographic equipment to document traffic conditions during test runs.

In heavy-duty trucks, PEMS equipment is often mounted inside the trailer (if present), while in the case of buses and LDVs the main unit is installed in the cabin of the vehicle to avoid contamination, excessive vibrations and overheating of the equipment (figure 2.6). The connections of the PEMS to the vehicle are typically reversible, and no further modifications are necessary in many cases.

**Figure 2.6:** Passenger car instrumented with PEMS

In the past few years, PEMS have experienced a remarkable technological development, with significant reductions in size, weight, and piping and cabling complexity; improved gas measurement principles, reduced analyser response times and an overall performance similar to conventional fixed laboratory equipment. The main advantage of on-board methods is that they can provide long series of emissions data for a particular vehicle driven under a wide range operational/duty cycles and driving and ambient conditions (Cicero-Fernández, Long and Winer 1997), including some that would otherwise be difficult to replicate in the laboratory (*e.g.*, large road gradients). The installation of PEMS on several vehicles of various categories can lead to a large database of emission values from vehicles of different technologies driven under different driving and environmental conditions.

PEMS are relatively simple and inexpensive, and can be installed on a wide variety of vehicles. They can be especially convenient for HDVs, considering that dynamometer test beds have limitations in terms of vehicle size and that they become expensive for high engine power applications. PEMS are thus becoming an important regulatory tool for HDVs. USA authorities have introduced additional emission requirements based on PEMS testing and the 'not to exceed' (NTE) concept, whereby emissions averaged over a time window must not exceed specified values for regulated pollutants while the engine is operating within a control area under the torque curve. The corresponding test procedures and the portable instrumentation performance requirements are laid down in (USEPA 2005). In Europe, PEMS can be applied to verify the in-service conformity of EURO V and EURO VI heavy-duty engines with the applicable emissions standards (EC 2011a, 2012), and the EC is currently working with stakeholders to include PEMS testing as part of the type-approval process of Euro 6 passenger cars (Weiss *et al.* 2013).

Older PEMS were inferior to laboratory systems in terms of measurement accuracy, but new generations of portable instruments have come to rival laboratory-grade systems in EF development applications. The main limitations of PEMS include the reduced range of measurable pollutants, the added mass (of approximately 30 to 70 kg) that may bias the measurement (especially for light-weight cars), and the reduced reproducibility due to real-world sources of variability. Also, the range of pollutants that can be measured with PEMS is still limited in comparison to laboratory measurements.

### 2.6.1 EF development from PEMS data

The development of EFs from PEMS data is analogous to the procedure followed with chassis dynamometer data. Mean speed-based EFs may be derived by dividing a large PEMS dataset into small sections (data bins) and plotting the mass emissions against the mean speed of each data bin. A regression curve may then be fitted to the thus produced cloud of data points. Rubino *et al.* (2007) and Weiss *et al.* (2011a, 2011b) used a 'moving averaging window' approach to derive distance-based EFs from PEMS datasets.

Alternatively, an instantaneous *engine emission map* model approach may be used, whereby 'emission map' EFs are developed from the instantaneous PEMS data

and the engine states recorded via the OBD link. A practical application of this principle was developed by Kousoulidou *et al.* (2010a, 2010c), who developed a tool for the creation of engine emission maps from on-board data, which were then used as input to a vehicle simulation tool. As will be shown in chapter 3, the use of transient PEMS data for the direct derivation of engine emission maps is hindered by the difficulty to accurately allocate emissions to measured vehicle or engine states. Moreover, it is difficult to make on-board engine power or torque measurements (in contrast to chassis dynamometer testing). Readings from the OBD of the vehicle can be quite inaccurate in absolute terms, and the application of torque measurement systems (such as resistance strain gauges) is cumbersome and difficult to calibrate on the road, while a calculation from the measured velocity signal is affected by the uncertainty of road gradient. These problems can be overcome if PEMS tests are planned properly and all relevant data (road gradient, vehicle mass and frontal area, *etc.*) are recorded and taken into account during the post-processing of measured data. If these conditions are met, PEMS become a reliable source of real-world emissions data and a useful tool for the validation of EFs derived from laboratory data.

### 2.6.2 PEMS applications

PEMS have been used to study the behaviour of exhaust emissions under real-world operation, for EF derivation and validation, for the improvement of emission models, and for the investigation of the emissions performance of new powertrains and after-treatment systems. Vojtíšek-Lom and Cobb (1997) made an early demonstration of the feasibility of PEMS. A simple on-board measurement system was employed by Miyazaki, Takada and Iida (2002) to evaluate the $NO_x$ emissions of a medium-duty vehicle. Another version of these simple systems was implemented and tested by Hawirko and Checkel (2002) using a vehicle fuelled either with gasoline or natural gas under a wide range of driving conditions in the region of Edmonton (Canada). In these early applications of PEMS, the authors used an on-road setup to record ambient conditions, driving behaviour, vehicle operating parameters, fuel consumption and exhaust emissions results for a small set of repeated commuting trips to illustrate the capabilities of the on-board measurement approach.

The issue of the *accuracy and repeatability* of PEMS has been covered by a number or research studies that compare the performance of PEMS to fixed laboratory

equipment (Daham *et al.* 2005; Dearth *et al.* 2005; Pelkmans and Debal 2006; Gierczak *et al.* 2006; Durbin *et al.* 2007; Rubino *et al.* 2010; Liu *et al.* 2010) or to a reference mobile laboratory (Johnson *et al.* 2009a, 2009b). Moreover, Zhang and Frey (2008) evaluated the response time of a commercial PEMS, and found that it led to deviations which could be corrected through adequate data post-processing. Judging from the results of these studies, it can be concluded that PEMS are a robust tool to measure vehicle emissions that exhibits acceptable agreement with results from reference measurement instruments.

The technological development of PEMS is seeing interesting advances that position it as an interesting alternative to conventional testing equipment. This is especially true when effects that are not typically captured under controlled laboratory conditions need to be investigated. Among those effects is the impact of sudden accelerations leading to so-called *emission events* (peaks of high emissions). On-board systems have also been employed to evaluate the *effect of ambient temperature* upon exhaust EFs; for instance, Hawirko and Checkel (2003) analysed a series of trips over a one year period with temperatures ranging from $-25$ to $+20$°C.

The influence of *driver behaviour* upon emissions was studied by Nam, Gierczak and Butler (2003), who also derived a custom driver aggressiveness indicator calculated from instantaneous speed and acceleration based on PEMS data. Unal, Rouphail and Frey (2003, 2004) used PEMS to evaluate the effects of signal timing and coordination on emissions for arterial corridors, and to identify emission hotspots. Chen *et al.* (2007) studied the impact of speed and acceleration upon fuel consumption and emissions of HDVs in an urban area in Shanghai (China) using PEMS, finding that congestion conditions—characterised by low-speed with frequent acceleration and deceleration—led to sharp increases in the emissions of CO and THC. Frey, Zhang and Rouphail (2008) used PEMS data from ten different vehicles and three different routes to study the influence of routing on emissions, finding that total emissions of NO varied significantly from trip to trip and from route to route due to variations in mean speed.

PEMS have been used within studies aimed at evaluating the on-road performance of different *emission control technologies* and the emission performance of different *blends of fuels*. For example, Lenaers and Van Poppel (2005a) used an on-board measuring system capable of determining emissions of ammonia to evaluate the emissions performance of a city bus equipped with selective catalytic reduction (SCR). The same authors also investigated the real-world PM emissions reduction

from a city bus retrofitted with a continuously regenerating trap (CRT) using an on-board emission measurement system that performed measurements before and after the installation of the CRT (Lenaers and Van Poppel 2005b). Tzirakis *et al.* (2006) investigated the emissions from a EURO IV heavy-duty vehicle fuelled by Diesel and Diesel/biodiesel blends using on-board emission measurements performed in real-world driving conditions that included altitude differentiations. Lenaers and Van Poppel (2007) also used PEMS to evaluate the real-world emissions performance of two Euro II buses retrofitted with two different combined solution systems for the simultaneous reduction of $NO_x$ and PM. Frey *et al.* (2007) performed a comparison of fuel consumption and emission variations for Diesel and hydrogen fuel cell buses that operate on identical routes. Frey and Kim evaluated the impact of biodiesel on the real-world emissions of dump trucks (2006) and cement mixers (2009). Graver, Frey and Choi (2011) evaluated the real-world energy use and emissions of a retrofitted PHEV using a combination of PEMS and a data logger for the hybrid system.

Portable instruments have also been employed in the *validation of models* based on dynamometer cycles. Silva *et al.* (2006) compared the outputs of three of these models—EcoGest, Comprehensive Modal Emission Model (CMEM) and Advanced Vehicle Simulator (ADVISOR)—with fuel consumption and emissions data obtained using on-board instruments, and concluded that models could be used with relatively high confidence to predict fuel consumption and $CO_2$ emissions. More recently, Kousoulidou (2011) used experimental data obtained from PEMS runs for the development of EFs, and found good correlation with the corresponding values provided by COPERT. Moreover, said author produced *engine emission maps*—which were initially developed from PEMS data and further enhanced through artificial neural network computing—that were then used to simulate the experimental PEMS runs under ADVISOR.

A different approach to on-board measurements (one that cannot be labelled as PEMS, since it is not a portable setup) was taken by a group of researchers at the Center for Environmental Research & Technology of the University of California Riverside (Cocker *et al.* 2004a, 2004b) who developed a complete emissions laboratory inside a heavy-duty trailer that acts as a load for the vehicle under test. This Mobile Emissions Laboratory (MEL) included a full-flow dilution tunnel, and was built to comply with legal requirements in the USA. Shah *et al.* (2004, 2006) used the MEL to illustrate the differences in exhaust emissions between cruising and

congested traffic conditions, while Durbin *et al.* (2008) used it to study the $NO_x$, PM, THC and CO emissions of several HDVs under real-world operation.

### 2.6.3 Summary

The characteristics of PEMS for the measurement of vehicle emissions are summarised in table 2.7.

**Table 2.7:** Summary of vehicle emissions measurements using PEMS

| Applications | Characteristics |
|---|---|
| *General*<br>• Used for research purposes: investigation of the influence of driving conditions, new fuels and powertrains, in-use efficiency of after-treatment systems.<br>• Real-world validation of EFs.<br>• Type approval/in-use compliance of heavy-duty vehicles.<br>*EF development*<br>• Provides high-resolution EFs.<br>• EF development based solely on PEMS is possible (with limitations); PEMS data may be used to develop real-world engine maps.<br>• Influence of ambient parameters is not controlled; accurate road gradient data are needed to interpret emissions data. | *Advantages*<br>• Data are collected under real-world conditions in the driving environment, capturing details that are overlooked in standard cycles.<br>• PEMS systems are relatively simple and inexpensive and can be installed in a wide variety of vehicles.<br>• The connections of the portable system to the vehicle are typically reversible, and no modifications are necessary in most cases.<br>*Disadvantages*<br>• Lack of reproducibility due to the variable driving and environmental conditions.<br>• Installation is complex, can only be installed on a limited number of vehicles. |

## 2.7 Summary of EF development

Road vehicle EFs are empirical functional relations that predict the quantity of a pollutant that is emitted per distance driven, energy consumed, or amount of fuel used during a road transport activity. EFs are typically derived for vehicle categories (but they also exist for single vehicles, or even an entire fleet), and they depend on many parameters such as vehicle characteristics and emission control technology, fuel specifications, and ambient and operating conditions (cold-start, cruising, acceleration, *etc.*).

The emission profiles of vehicles and their dependency on operating conditions can be determined under *controlled conditions* in laboratories (engine and chassis dynamometer studies; discussed in section 2.2) or under *real-world conditions* (tunnel, remote sensing, on-road and on-board measurements; discussed in sections 2.3 to 2.6).

Road vehicle emission measurements for *modelling purposes* are mostly performed under *controlled conditions* in laboratories. These measurements are performed either on chassis or engine dynamometer facilities. In these cases, test operators have control over the *test cycle* being followed, the environmental conditions and other parameters, thus contributing to the repeatability and reproducibility of the results.

On the other hand, measuring emissions under *real-world conditions*—be it with tunnel, remote sensing, on-road or on-board measurements—yields valuable data regarding the actual emissions behaviour of road vehicles as they operate outside the boundaries of the emissions laboratory. The results of real-world techniques are typically less precise and reproducible than those of engine and chassis dynamometer studies. This is due to the absence of a standard test cycle and to the presence of additional sources of variability such as environmental or traffic conditions, driver behaviour or highly transient operation. Moreover, real-world techniques exhibit other technical shortcomings that limit their applicability to EF development. Still, the data produced by these measurements can play an important role in the identification of gaps in emission models and the establishment of model development priorities. Real-world emission measurements are also essential towards the validation of EFs gained from laboratory testing.

The quality of the application of any road vehicle emission model largely depends on the representativity of the EFs it contains. This refers to the accuracy with which the EF can describe the actual emission level of the particular vehicle type and the driving condition it is applied to. For example, an EF based on the mean speed of vehicles may be representative for the estimation of emissions at a national level, but its representativity will decrease when trying to assess the impacts of local traffic measures (*e.g.*, a local traffic intervention with large impacts on the stop-and-go pattern of vehicles but not affecting their mean travelling speed). EFs are usually developed on the basis of experimental data collected in vehicle emission measurement campaigns. The measurement technique selected, along with other specifics of each campaign—including the criteria for vehicle selection and the

driving conditions imposed—all have an impact upon the quality of the EFs later derived.

### 2.7.1 Instantaneous vehicle emissions modelling

The experimental data that support vehicle emissions modelling are produced by the measurement techniques discussed in this chapter. With regard to the *time resolution* of emission factor development, there are two basic approaches; one is based on aggregated emissions data (*e.g.*, 'bag' cycle or sub-cycle results from engine and chassis dynamometer testing, or trip or sub-trip averages from PEMS testing) and the other relies on instantaneous emissions data. This dissertation is concerned with the latter, and thus in the remaining chapters we will focus on the emission measurement setups that are able to provide long streams of instantaneous data[4] (see table 2.8).

**Table 2.8:** Sources of instantaneous and aggregated data, by measurement setup

| Measurement setup | Source of instantaneous data | Source of aggregated data |
|---|---|---|
| Chassis or engine dynamometer laboratory with diluted gas sampling | Online analysers at dilution tunnel. The determination of exhaust flow can be omitted. | Sampling bags, calculation from instantaneous data. |
| Chassis or engine dynamometer laboratory with raw gas sampling | Online analysers at raw gas line. Exhaust flow is calculated or measured at the tailpipe. | Sampling bags, calculation from instantaneous data. |
| PEMS | Portable analysers and flow meter at tailpipe line. | Calculation from instantaneous data. |

*Aggregated or integrated emissions modelling* is supported by databases of measured emissions. Statistical regression techniques are applied to measured data to obtain the EFs as function of the average cycle speed (as is done *e.g.*, in COPERT) or other kinematic parameters of the cycle or trip that generated the data. Such models allow the estimation of the emissions of cycles or trips that were not measured (*e.g.*, through interpolation), but they are severely limited when it comes to matching emissions to engine states (*i.e.*, to produce engine emission maps). Emission models based on

[4]It is assumed that instantaneous emissions data are those with a time resolution of at least 1 Hz This excludes on-road and roadside measurements, because they only provide 'snapshots' of the instantaneous emission behaviour of vehicles.

aggregated dynamometer cycle measurement results only provide good results for *traffic situations* for which the driving pattern used to fill the bag is representative. In addition, their results are restricted to the parameter setting of the tests. Thus, no variations of load, slope, *etc.* are possible, and if driving behaviour or any of these parameters change, additional measurements have to be made to predict the emissions under the new conditions.

*Instantaneous vehicle emissions modelling* represents a step forward from aggregated modelling. PHEM (for heavy-duty vehicles) is an example of this type of model. Instantaneous emissions models need to accurately allocate (or 'map') instantaneous mass emissions of pollutants to their generating vehicle or engine state. Engine states are typically determined by instantaneous engine speed and power (or similar values) for engine dynamometer measurements, and by instantaneous speed and acceleration for chassis dynamometer and PEMS tests. A key advantage of instantaneous vehicle emission modelling is that they it makes it possible to use *simulation techniques* to integrate new, not previously measured driving patterns or parameter settings over the map and generate emission factors. Instantaneous emissions models are also able to account for the dynamicity of driving cycles (*cf.* section 2.2.1), and improve the modelling of short *emission events* that make up a substantial part of the emissions produced by engines equipped with current emission control technologies. Moreover, they allow emissions to be spatially resolved, which can potentially lead to improvements in the prediction of air quality levels (Boulter and McCrae 2007).

The increased time resolution of emissions data is an ongoing general modelling and regulatory trend.[5] In the chapters that follow, we will show that the increased *time resolution* of emissions data signals output by vehicle emission measurement equipment does not necessarily imply an increase in *instantaneous accuracy*, and that accurate modelling of the instantaneous emissions or road vehicles requires careful post-processing of data.

[5]This is illustrated by the emergence of PEMS as a regulatory tool for vehicle certification and in-service conformity checks; see p. 39.

# Chapter 3

# Distorting effects of instantaneous vehicle emission signals

Modern vehicle emissions measurement equipment can output emissions data with a fine temporal resolution. Most gas analyser benches report pollutant mass emissions at 1 Hz, and some models go up to 10 Hz. Due to a number of *distorting effects* , these mass emission signals are different from those that would be measured at the tailpipe or catalyst-out point. In other words, high temporal resolution does not equate with high instantaneous accuracy.

In this chapter, we will discuss the aforementioned distorting effects and their impact upon the instantaneous and overall accuracy of vehicle emission signals. Despite being well known by emissions test bench operators, these distorting effects have not been extensively addressed in the literature (*cf.* section 4.4 on pp. 85—88). A plausible explanation for this situation is that, in spite of their fairly widespread availability, instantaneous emission test data are rarely used to develop instantaneous engine emission maps, but rather aggregated and reported at cycle or sub-cycle level (*e.g.*, as type-approval test results). Moreover, whenever emissions data are averaged over large enough data windows (*i.e.*, substantially larger than the sum of transport times and the response time of the analyser) to produce emission factors, the distortions become less of a problem because, given the fact that mass emissions are conserved throughout the measurement setup, integrated values will follow results calculated from instantaneous data very closely. Also, it is possible to

eliminate these distortions altogether by using *steady-state test cycles* and matching the recorded emissions to their generating vehicle or engine state once they are stabilised, but this comes at the expense of obtaining test results that are less representative of real-world operation.

Therefore, if we wish to create emission factors in the form of engine emission maps from *instantaneous, transient emissions data*, emission signals need to be adequately post-processed to make up for the distortions brought about by the transport time of sampled emissions from the tailpipe to the analysers and the dynamic response characteristic of the analysers. For proper instantaneous EF development, instantaneous emission signals ought to be properly time-aligned, and their features lost due to measurement distortions reconstructed at least up to the tailpipe or, ideally, up to the catalyst-out point.

## 3.1 Vehicle emission measurement signals and systems

In this section, we will use basic concepts of *systems theory* to describe the main characteristics of the signals and systems that we work with in the context of vehicle emissions modelling. A *signal* is a function or data series that represents a physical magnitude or variable. Signals contain information about the phenomenon that produces them. A *system* can be defined as a combination of components that act together and perform a certain objective (Ogata 2002).

From a systems theory perspective, we can deal with a wide array of signals and systems. Fortunately, the range of signals and systems that we will encounter in the context of vehicle emissions modelling is limited, which will allow us to simplify our modelling task. In the sections that follow we will briefly discuss the main characteristics of the aforementioned signals and systems.

### 3.1.1 Vehicle emission measurement signals

In this section we will introduce the type of signals that are of interest in the context of vehicle emissions modelling, and we will discuss some of its more relevant characteristics.

#### *3.1.1.1 Physical magnitudes*

The most important physical magnitudes in vehicle emissions modelling are the *mass emission rates* of the pollutants being modelled (*i.e.*, the quantity of each pollutant that is being emitted over time). For gaseous pollutants, the mass emission rate is calculated as the multiplication of a pollutant concentration signal (measured by an exhaust gas analyser) and an exhaust gas volume flow signal (measured at the tailpipe or at the dilution tunnel). Therefore, an accurate knowledge of *pollutant concentrations* in the exhaust gas is as important as a reliable *volume flow* signal in order to support the compensation of instantaneous emission signals. Volume flow can be calculated from the exhaust *mass flow*, pressure and temperature. The exhaust *mass flow* may be directly measured at different points of the measurement chain (*e.g.*, at the tailpipe, at the dilution tunnel or at the air intake of the engine using one of the several available measurement principles (see table 3.1).

**Table 3.1:** Air flow measurement methods in vehicle emissions modelling

| Method | Notes |
|---|---|
| Critical orifice (Venturi) | Cannot deal with pulsations in tailpipe measurements. Resolution is low at low flows (flow is proportional to the square of differential pressure). |
| Pitot tube | Needs to be sophisticated to deal with pulsations in tailpipe measurements. Resolution is low at low flows. |
| Hot wire anemometer (thermal principle) | Works well for intake air, some effort is needed to install it. Causes disturbances in intake pressure. Not applicable to tailpipe measurements due to soot. |
| Ultrasound, annubar | Acceptable performance for tailpipe measurements, some thermal problems at high loads. |
| Synthetic (OBD/ECU) | OBD signals can be delayed. Direct (manufacturer) ECU access is preferable. |
| Propeller anemometer | Not applicable to tailpipe measurements due to contamination. |
| Vortex | Not applicable to tailpipe measurements due to pulsations. |

The *pressure* in the gas transport system of vehicle emission measurement setups is close to ambient pressure and approximately constant. The *temperature* of the exhaust gas, however, is a function of both time (vehicle operation) and location within the measurement setup (*e.g.*, it will be higher at the tailpipe point than at the dilution tunnel; and it will be lower at idling than under full-load acceleration). The temperature within the gas transport system cannot be measured or calculated at every point, but a good approximation may be the mean of the temperature at

the input and the output of the measurement setup sub-system considered. This approximation may not be applicable for the exhaust system of the vehicle, where the signal at the catalyst outlet cannot be easily measured for economic and technical reasons. A model for the average temperature based on the temperature at the tailpipe may be more appropriate in this situation (Ajtay and Weilenmann 2004).

Another set of important physical magnitudes are those related to *vehicle or engine states*. Vehicle speed and acceleration, engine rotational speed, power and torque are the usual physical magnitudes related to the development of EFs. Other signals such as catalyst temperature or status of the after-treatment systems are also of interest in some cases. All of these signals are measured at the chassis or engine dynamometer, or reported by the ECU of the vehicle.

#### 3.1.1.2 Time domain characteristics

A signal $u(t)$ will be a *continuous-time signal* if the time variable $t$ is a continuous variable. Conversely, if $u(t)$ is defined discretely in the time domain, it will be a discrete-time signal. When a discrete-time signal is defined at a *fixed sampling interval*, it takes the form of a sequence of numbers denoted by $x[n]$, where $n$ is an integer that indicates the sampling period. The vehicle emissions signals that we will deal with are discrete, because they are obtained by measurement equipment that samples a continuous-time signal. Thus, they will take the form of data arrays, which can be easily manipulated in computing environments.

#### 3.1.1.3 Stochastic components

Deterministic signals are those signals whose values are completely specified for any given time. A *deterministic signal* can be exactly predicted by a known function of time $f(t)$. On the other hand, random or *stochastic signals* are those signals that take random values at any given time and must be characterised statistically. Unlike deterministic systems, stochastic systems do not always yield the same output for a given input. The systems that we will model clearly exhibit a certain degree of stochastic behaviour, since their output cannot be predicted with complete accuracy by any model. The sources of stochastic behaviour in vehicle emission measurement systems are the mixing of exhaust gas—an inherently chaotic process—, instrument noise and other disturbances.

### 3.1.2 Vehicle emission measurement systems

In this section we will discuss the systems that are used to measure vehicle emissions, focusing on those that are able to produce instantaneous emission signals. Later in this chapter, we will study in detail how these systems affect the accuracy of measured instantaneous signals.

#### *3.1.2.1 Sub-system division*

The main vehicle emission measurement setups that are able to produce instantaneous emissions data signals (see section 2.7.1 on page 45) may be broken down into a small number of generic sub-systems: the exhaust system of the vehicle, the raw gas line, the dilution tunnel (if present) and the gas analysers including their sampling line (see table 3.2). These sub-systems are briefly described in the sections that follow.

**Table 3.2:** Measurement setup sub-system division

| | Measurement setup sub-systems | | | |
|---|---|---|---|---|
| **Measurement setup** | Exhaust system | Raw gas line | Dilution tunnel | Analysers |
| Dynamometer laboratory* with *diluted* gas sampling | ✓ | ✓ | ✓ | ✓ |
| Dynamometer laboratory* with *raw* gas sampling | ✓ | ✓ | ✗ | ✓ |
| PEMS | ✓ | ✓ | ✗ | ✓ |

* *May be a chassis or engine dynamometer laboratory*

**3.1.2.1.1 Vehicle exhaust system** The vehicle exhaust system stretches from the engine-out point to the tailpipe. The exhaust gas can take up to several seconds to travel between these two points, depending on the exhaust volume flow and on the volume of the exhaust system of the vehicle. The exhaust gas is also mixed within the exhaust system of the vehicle before being emitted at the tailpipe, especially in the silencer.

**3.1.2.1.2 Raw gas line** The 'raw'[1] gas line is a 'pipe' element that collects the exhaust gas from the tailpipe and channels it into the measurement sub-systems downstream. The raw gas line is normally kept heated at temperatures above $180°C$ to prevent the condensation of hydrocarbons. In some measurement setups, analysers sample directly from the end of the raw gas line, whereas in others an intermediate dilution process takes place.

**3.1.2.1.3 Dilution tunnel** Many chassis and engine dynamometer laboratories are equipped with a diluted or constant volume sampling setup (CVS; see figure 3.1). This method requires the vehicle exhaust to be continuously diluted with a variable flow of ambient air in such a way that total volume flow is kept constant inside a long, tubular section—the *dilution tunnel*—from which the exhaust is sampled for analysis. This is accomplished by connecting one end of the dilution tunnel to a constant volume pump (Roots type blower) driven by an electric motor or to a critical flow venturi (CFV; used in the more recent designs). A heat exchanger is also used to control the temperature of the exhaust gas-dilution air mixture (SAE 2011). By keeping the total volume flow of the diluted exhaust gas constant, CVS setups eliminate the need for measuring the rapidly changing exhaust gas volume flow at the tailpipe to calculate mass emissions from measured pollutant concentrations, and so they are able to produce very accurate overall emission values.

**3.1.2.1.4 Analysers** Electrochemical analysers are used to determine the volume concentration of the different gaseous pollutants in the exhaust gas. A small sample of the exhaust gas is drawn at a small, constant flow rate, either from the dilution tunnel (in CVS setups) or from the raw gas line (in PEMS and dynamometer laboratories with raw gas sampling). The gas is then cooled to remove the moisture and fed to the analyser cells. The measurement principle of these analysers varies according to the pollutant: total hydrocarbon emissions are typically measured by a heat flame ionisation detector (HFID), CO and $CO_2$ emissions are measured by a non-dispersive infrared (NDIR) analyser, and NO and $NO_2$ emissions are measured by non-dispersive ultraviolet (NDUV) or chemiluminiscent detector (CLD) analysers.

[1] In the context of vehicle emission measurements, 'raw' is equivalent to undiluted.

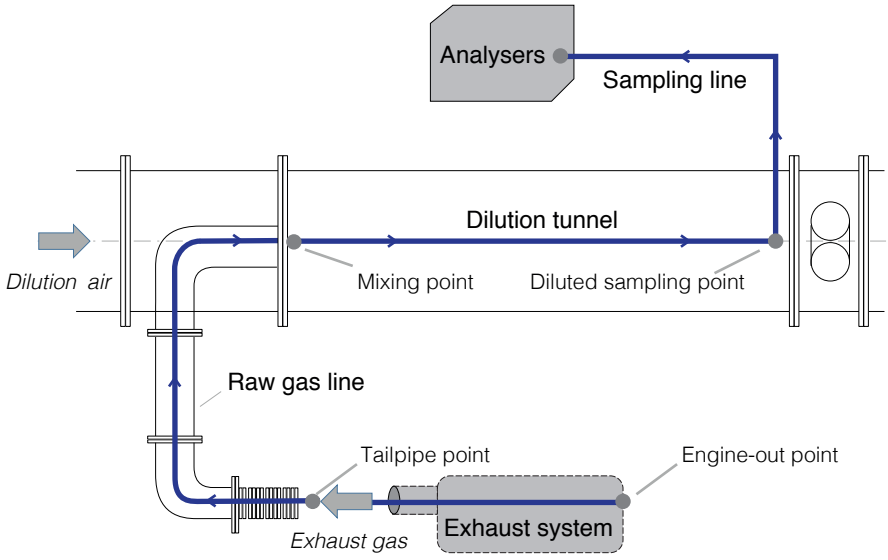


**Figure 3.1:** Schematic representation of a chassis dynamometer measurement setup with dilution (constant volume sampling) [adapted from Geivanidis and Samaras (2008)]

#### 3.1.2.2 Dynamicity

A dynamic model is a mathematical model that describes the behaviour of a system where the output $y(t)$ react with delay to a change of input $u(t)$. Such systems are said to have *memory*. A dynamic system in continuous time is described by a differential equation in $y(t)$. The output $y(t)$ is a function of a number of its own derivatives (with respect to time) and of the input $u(t)$. The order of this equation ($ntt$) corresponds to the highest derivative of the output $y(t)$ in this equation. As an example, we can consider the exhaust system of a vehicle (which includes the silencer) at a stationary exhaust flow: as pressure remains (roughly) constant, we can assume that input and output flows are equal. Assuming that the level of turbulence within the exhaust system—which acts as a gas 'mixing chamber'—is high enough to make the pollutant concentrations equal (even though the inlet concentration could be different), we can perform a mass balance and find that the output concentration $y(t)$ follows equation 3.1.

$$\dot{y}(t) = \frac{\dot{V}_{exhaust}}{V_{silencer}}[-y(t) + u(t)] \tag{3.1}$$

In equation 3.1, $u$ is the input concentration, $\dot{V}_{exhaust}$ is the exhaust volume flow and $V_{silencer}$ is the volume of the silencer.[2] This is a very simple, first-order differential equation. Two such 'mixing chambers' in series would need to be described by a second-order differential equation, and so on. For each 'mixing chamber', one order is added to the system, increasing the complexity of the differential equations that describe it. Pipes in general would need to be described using several of these chambers. However, most of the systems that we will encounter may be satisfactorily modelled with first- or second-order approximations.

If we discretise a dynamic model, the differential equation is transformed into a set of algebraic equations where the output is a function of past inputs, past outputs, or both. In the example, the output (instantaneous pollutant concentration) will be a function of a finite number of past inputs (pollutant concentrations of previous instants). Assuming that our output $y$ depends on $ntt$ previous inputs, we would have the discrete representation of our system given in equation 3.2.

[2]The volume of the silencer is used to approximate the total volume of the exhaust system.

$$y_n = d_{ntt} \cdot u_{n-ntt} \pm \cdots \pm d_3 \cdot u_{n-3} \pm d_2 \cdot u_{n-2} + d_1 \cdot u_{n-1} \tag{3.2}$$

Assuming that our output y depends on $ntt$ previous outputs and the current input, we would have the discrete representation of our system given in equation 3.3.

$$y_n = -e_1 \cdot y_{n-1} - e_2 \cdot y_{n-2} - \cdots - e_{ntt} \cdot y_{n-ntt} + d_0 \cdot u_n \tag{3.3}$$

#### *3.1.2.3 Linearity*

The systems encountered in practical applications are rarely linear. However, many systems can be modelled by means of linear approximations, thereby greatly simplifying their symbolic manipulation without much loss of accuracy. Given a system $H$ that maps input signal $u(t)$ into its corresponding output $y(t)$, then for any two inputs $u_1(t), u_2(t)$ and their respective outputs $y_1(t) = H\{u_1(t)\}$ and $y_2(t) = H\{u_2(t)\}$, the system will be linear if it satisfies the following conditions for any two scalar factors $k_1$ and $k_1$:

$$H\{k_1 \cdot u_1(t)\} = k_1 \cdot y_1(t) \tag{3.4a}$$
$$H\{u_1(t)\} + u_2(t)\} = y_1(t) + y_2(t) \tag{3.4b}$$
$$H\{k_1 \cdot u_1(t) + k_2 \cdot u_2(t)\} = k_1 \cdot y_1(t) + k_2 \cdot y_2(t) \tag{3.4c}$$

Any *linear* system will satisfy the conditions of homogeneity and additivity: in layman terms, an *homogenous* system will respond with a scaled output to a scaled input (equation 3.4a), whereas an *additive* system will produce an output that is the sum of the outputs resulting from each input signal acting alone (equation 3.4b). The conditions of homogeneity and additivity can be summarised by the *principle of superposition* (equation 3.4c), which is satisfied by all linear systems.

#### *3.1.2.4 Time variance*

A system is called *time-invariant* if a time shift (delay or advance) in the input signal causes the same time shift in the output signal. The time variance in the response

of the sub-systems of typical vehicle emissions measurement setups is due to the variability of flow (*e.g.*, the degree of mixing within the raw gas line is affected by changes in the exhaust mass flow, and so is the transport time). Some sub-systems in the vehicle emissions measurement chain are time-variant, and some others—namely those where flow is quasi-constant—may be considered time-invariant for modelling purposes. The time variance (or rather, *flow variance*) of the different sub-systems of vehicle measurement setups is summarised in table 3.3.

Time invariance is an advantage from a modelling perspective, because it means that the sub-system can be characterised with little experimental effort. Time-variant sub-systems of the measurement setup, on the other hand, will have to be characterised at several operating points (defined by flow rate), thereby increasing the number of characterisation experiments. Considered as a whole, the measurement system will be time-variant because it will contain sub-systems that are time-variant.

**Table 3.3:** Time and flow variability in sub-systems of measurement setups

| Sub-system | Flow | Travel time | Time invariance |
|---|---|---|---|
| Exhaust system | Medium, highly variable | Variable* | No |
| Raw exhaust line | Medium, highly variable | Variable* | No |
| Dilution tunnel | High, quasi-constant | Quasi-constant | Yes† |
| Diluted sampling line | Low, quasi-constant | Quasi-constant | Yes† |
| Analyser | Low, quasi- constant | / | Yes† |

**Variability is higher at lower flow rates* †*Flow can be varied, but is set for individual test runs*

### *3.1.2.5 Stability and mass conservation*

Vehicle emission measurement setups can be considered as *stable* from a systems theory perspective. This is because all finite inputs will produce a finite output. This type of stability is called BIBO (bounded input-bounded output). Moreover, in all the sub-systems of our measurement setup a constant pollutant mass flow at the input will lead—after a short stabilisation time—to a constant output of the same value (as far as there are no leaks and the analysers are well calibrated). In systems theory terms, the elements of the measurement setup are said to have unity static gain, and thus we can expect mass to be conserved through them.

## 3.2 Distorting effects and instantaneous accuracy

The three main causes that lead to the distortion of measured emissions signals (signal misalignments, mixing and transport effects, analyser response characteristics) are translated into one observable effect: the pollutant concentration signal (or the measured mass emission signal, obtained by multiplying the former by the volume flow rate and the density) is delayed, smoothed and flattened with respect to the 'true' signal that would be observed by a 'perfect' (infinitely fast) analyser located at the catalyst-out point, before the exhaust is transported and mixed within the pipes of the measurement setup (figure 3.2).

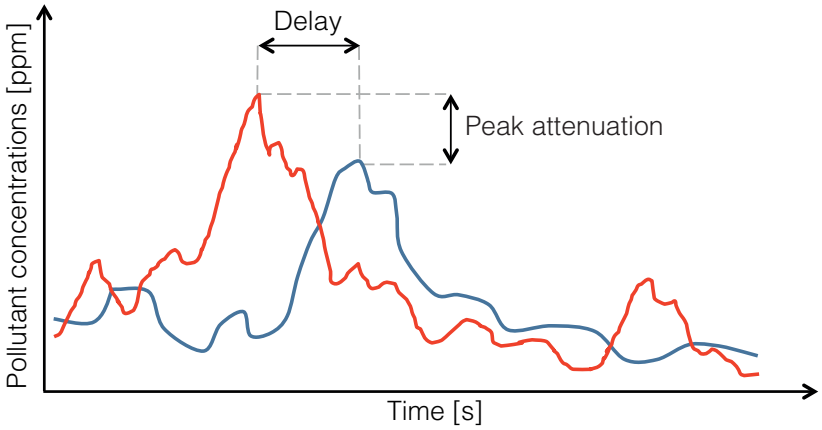


**Figure 3.2:** Illustration of the distorting effects upon pollutant concentration signals [adapted from Geivanidis and Samaras (2008)]

In the sections that follow, we will classify and describe the distorting effects that compromise the accuracy of vehicle emission signals. Whatever the measurement setup (diluted gas measurements at the dilution tunnel, raw exhaust analysers or PEMS), measured instantaneous emissions will be distorted to some extent by transport delays of the sampling system, and they will be affected by gas mixing phenomena and the finite dynamic response of the analysers. The distorting effects covered in this document take place in different points or sub-systems of the measurement setup, and some of them will have a greater impact upon accuracy than others.

### 3.2.1 Systematic signal misalignments

The signals used to build engine emission maps often come from different instruments, which may in turn be located at different points along the measurement chain, and which may lack a measured, common time reference. An improper time alignment of signals can have a large impact upon the accuracy of the reported results, and yet many times it is not adequately addressed.

#### *3.2.1.1 Primary misalignment*

The emissions of gaseous pollutants from road vehicles are reported as *mass emissions*, but these cannot be directly measured by a single instrument. Rather, they are calculated as a multiplication of two measured signals, namely pollutant concentrations and (volumetric or mass) flow rate at the tailpipe. The accuracy of reported mass emissions—be they instantaneous or aggregated over a time window—is equally dependent on the accuracy of either one of these individual signals. Moreover, it is affected by the quality of the time alignment of the pollutant concentration and the flow rate signals, which is hereinafter referred to as *primary alignment*. This distorting effect can have a significant impact upon the accuracy of the calculated instantaneous mass flow signals, especially when both the measured pollutant concentration and flow rate signals are varying rapidly[3]—as is the case in raw exhaust gas measurements—or when they are measured at different, distant physical locations along the measurement chain.[4]

Deriving a pollutant mass emission signal from the multiplication of a pollutant concentration and an exhaust flow rate signal that are not properly time-aligned has unpredictable consequences in terms of signal accuracy, as it may lead to emissions under- or over-reporting, both for instantaneous and aggregated results. A first alignment is a simple data post-processing task that does not require any modelling

[3]This effect does not affect diluted measurements, where the flow rate is kept almost constant at the measurement point for pollutant concentrations (*i.e.*, at the end of the dilution tunnel).

[4]Even if the measurement locations are very close, the alignment of concentration and flow signals will not be perfect because the changes in flow propagate as a wave (and therefore with sonic speed), whereas changes in concentration propagate with the actual transport velocity of exhaust gas along the measurement chain.

effort, and which can be easily performed by following a systematic time alignment of the signals based on shifting one signal over the other by a fixed time step.[5]

Emissions test benches (also PEMS) can output formatted data sheets that list analyser and flow meter readings in separate columns. These data are typically reported at fixed time intervals of one second, along with other measured or calculated test data. A 'clock' signal column is also provided, leading to the impression that signals are time-aligned. However, it is frequently the case that pollutant concentrations and mass flow signals are measured at different points along the measurement chain, leading to a time misalignment between the two. It is also true that most emissions test setups can be configured to apply a constant time shift to compensate this misalignment and thus report the aligned signals in the output data sheet (figure 3.3). However, this is a coarse approach, and the time shift applied may not be optimal, so it is advisable to perform a systematic alignment check before deriving mass emission signals.

| | |
|---|---|
| AMBII RPM Multiplier | 2 |
| Torque (ecm or calc) | ecm |
| Use Frictional Torque | YES |
| Mass Calc Method | EXH_FLOW |
| NDIR Delay (s) | 4 |
| NDUV Delay (s) | 4 |
| THC FID Delay (s) | 3 |
| Methane FID Delay (s) | 5 |
| SEMTECH EFM Delay (s) | 2 |
| Vehicle Interface Delay (s) | 0 |
| Engine Speed Delay (s) | none |
| Environmental Delay (s) | 0 |
| Aux Temp Delay (s) | none |
| EAI1 Delay (s) | 0 |
| EAI2 Delay (s) | 0 |
| EAI3 Delay (s) | 0 |
| Methane FID PF-CH4 value | 1 |
| Methane FID PF-C2H6 value | 0.05 |
| Vehicle Interface Type | Not Enabled - |
| Flow Meter Type | EFM |
| NOx Kh Calculation | CFR40 86.1342-94 Diesel |

**Figure 3.3:** Application of fixed time shifts via the software settings of measurement instruments. Pictured: fixed shifts among exhaust flow rate and measured pollutant concentrations as reported in a PEMS test data sheet (shifts are in seconds)

[5] This fixed time shift is typically determined from clear emission events such as the initial emissions peak following engine start.

#### 3.2.1.2 Secondary misalignment

Engine emission maps are used to predict the instantaneous mass emissions of a vehicle as a function of its operating state, which is typically characterised by the instantaneous engine speed and torque. As we try to increase the time resolution of our prediction (we assume 1 Hz to be standard practice), we will need a finer time alignment between *measured mass emissions and recorded engine states*. Since the misalignment between these signals comes into play later in the process of building engine emission maps, we will refer to it as *secondary misalignment*.

There are several ways in which the engine and mass emission signals can be time-aligned. Test bench operators tend to perform a visual time alignment, whereby the initial peak of an engine covariate (*e.g.*, engine speed) is matched to the initial emissions peak recorded (*e.g.*, $CO_2$ concentration). The most widely followed procedure for time alignment is a cross-correlation check (*cf.* section 4.1.4.3 on page 75), whereby the evolution of the cross-correlation of two data sets is calculated as one of the signals is shifted in time. This method can be used to align emissions to engine states by cross-correlating $CO_2$ emissions with engine power or torque.

The impact of signal misalignments is difficult to predict, as it may lead to over- or underreporting of mass emissions, both for instantaneous and aggregated results (*i.e.*, simulated results using the engine emission map). As will be shown in chapter 4, signal misalignments can be addressed through data post-processing.

### 3.2.2 Variable transport times

Performing a fixed time alignment (using a visual peak alignment, or a cross-correlation test) takes care of the delay imposed by the mean transport time of exhaust gas through the measurement setup. This can afford a large improvement in the alignment, but some additional gains may be obtained if one considers that transport delays are not fixed, but rather vary with flow in some sub-systems of the measurement chain. Most chassis dynamometer test cycles—especially the so-called real-world cycles like CADC (Common ARTEMIS driving cycle) or ERMES, which provide the most valuable emissions data for emission factor development purposes—are indeed transient cycles, meaning that tailpipe flow rates have large fluctuations. The variations in tailpipe flow rates will be translated into variable

transport delays of pollutant mass emissions: pollutant concentrations associated with high flows will be faster to reach the analysers and vice versa. Transport delays do not vary linearly with flow rate, but rather following a hyperbolic law (equation 3.5).

$$\Delta t = K \cdot (\dot{V}_{exhaust})^{-1} \tag{3.5}$$

It should be noted that the effect of variable transport delays is not appreciable in all sub-systems of the measurement chain, but only in those where high variations of flow occur. Thus, the sub-systems where this signal distortion is dominant would be the exhaust system of the vehicle under test (which is not always considered in the modelling; *cf.* section 4.2.3 on page 78) and the raw gas sampling line. Moreover, not every type of vehicle is affected in the same way. In general, the exhaust volume flow of Diesel vehicles exhibits lower variability than that of gasoline vehicles (figure 3.4).

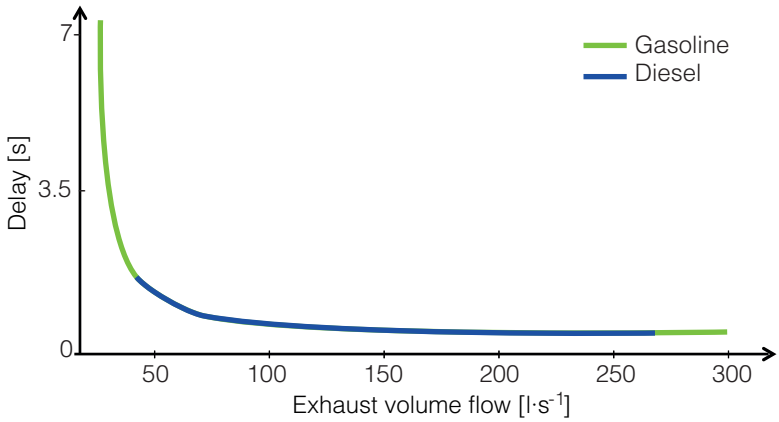


**Figure 3.4:** Illustration of the variability of transport times within the exhaust system of Diesel and gasoline vehicles. The exhaust system volume is 20 litres in this example [adapted from Weilenmann, Soltic and Ajtay (2003)].

In many practical cases, the compensation of variable time delays is overlooked, and only systematic misalignments are compensated (via a fixed time shift; *cf.* section 3.2.1.1). This may be an acceptable approach if the time resolution of the data is lower than 1 Hz. We find a justification for this upon closer examination of

figure 3.4, where it can be seen that the variability of transport times with exhaust volume flow is very low for most of the operating range. Furthermore, the area where variability is appreciable corresponds with the low-flow areas, where pollutant emissions are typically also low in terms of concentration. Therefore, the inaccuracies brought about by overlooking variable transport delays are generally low in terms of mass emissions prediction.[6]

### 3.2.3 Exhaust gas mixing

Exhaust gas is transported away from the catalyst-out point, channelled by the exhaust system of the vehicle and into the piping of the measurement setup before flow rates and pollutant concentrations are measured. This induces a time delay in the measured data, which can satisfactorily be taken care of through a careful time alignment of the signals. At the same time, other distortions are taking place: an additional distorting effect is produced by the mixing of the exhaust gas, which happens both at the exhaust system of the vehicle and within the piping of the measurement setup. Turbulent flows produce rapid mixing or homogenisation of the non-uniform gas mixture that is the exhaust gas. The same is true when there are unequal flow rates in boundary layers within laminar flows. Gas mixing is a consequence of irregular and chaotic flow, and this is why it is treated statistically rather than deterministically (*cf.* chapter 4).

Gas mixing needs to be taken into account if—as is our purpose with engine emission maps—EFs are to be developed with a high temporal resolution. This is particularly true for diluted measurements (*i.e.*, for measurement setups in which the analysers sample from the end of a dilution tunnel). Raw gas measurements and PEMS are less affected by this particular distortion due to the reduced overall length of pipe elements in relation to diluted measurement engine or chassis dynamometer setups.

In contrast to time misalignments, gas mixing has little to no impact upon aggregate results. In diluted measurement setups, mass emissions are conserved, and so the effect of exhaust gas mixing can be completely overlooked for conventional emission factor development. The same cannot be said of measurement setups where analysers sample directly from the raw exhaust line (see figure 3.5).

[6] This may not be the case for modern gasoline engines that produce pollutant concentration peaks at low exhaust volume flows.

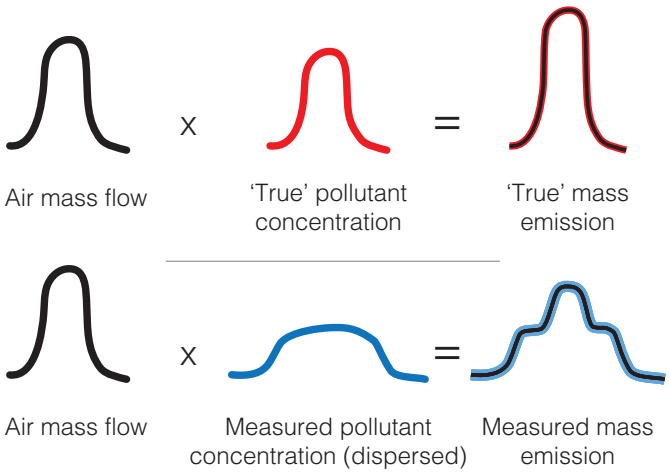


**Figure 3.5:** Effect of gas mixing upon the total pollutant mass reported by raw gas measurement configurations (based on an original sketch by M. Weilenmann)

In order to assess the degree of turbulence, we can estimate the Reynolds number (*Re*) associated with the various sub-systems of the measurement setup. This dimensionless number expresses the ratio of inertial forces to viscous forces in the flow of a fluid. For pipe flow, *Re* may be calculated according to equation 3.6, where $V$ is the velocity of the fluid $[m \cdot s^{-1}]$, $L$ is the characteristic length (hydraulic diameter of the pipe, $[m]$) and $\upsilon$ is the kinematic viscosity of the fluid $[m^2 \cdot s]$.

$$Re = \frac{V \cdot L}{\upsilon} \tag{3.6}$$

For pipe flow, it is customarily accepted that laminar flow occurs at $Re < 2100$. Transition to turbulence takes place with $2100 < Re < 4000$, while fully developed turbulent flow takes place at $Re > 4000$. In table 3.4, a 'low' and a 'high' estimate of *Re* is provided for the typical sub-systems that are the building blocks of any measurement setup (except the analysers, which are not 'pipe' elements). Judging from these estimates, turbulence will play a significant role in smoothing the emissions signals in dilution tunnels and at the exhaust systems of vehicles. This is consistent with the empirical observations reported in the literature (*cf.* literature review on pp. 85—88).

**Table 3.4:** *Re* estimates for different measurement chain sub-systems

| | Assumed flow conditions within the sub-system | | | | | *Re* estimates | |
|---|---|---|---|---|---|---|---|
| **Sub-system** | High flow $[m^3 \cdot s^{-1}]$ | Low flow $[m^3 \cdot s^{-1}]$ | Pipe diameter $[m]$ | Kinematic viscosity $[m^2 \cdot s]$ | Temp. [°C] | $Re_{high}$ | $Re_{low}$ |
| Exhaust system | 0.04 | $8\times10^{-4}$ | 0.04 | $4.6\times10^{-5}$ | 300 | $2.8\times10^{4}$ | 550 |
| Raw exhaust line | 0.04 | $8\times10^{-4}$ | 0.1 | $4.6\times10^{-5}$ | 300 | $1.1\times10^{4}$ | 225 |
| Dilution tunnel | 0.16 | 0.08 | 0.35 | $2.2\times10^{-5}$ | 100 | $2.6\times10^{4}$ | $1.3\times10^{4}$ |
| Sampling line | $5\times10^{-4}$ | $1.7\times10^{-4}$ | 0.1 | $2.2\times10^{-5}$ | 100 | 300 | 100 |

### 3.2.4 Dynamic response of gas analysers

The effect of the dynamic response of gas analysers upon the accuracy of instantaneous emissions signals is similar to the mixing effect discussed in section 3.2.3. In signal processing terms, gas analysers act as 'low-pass' filters, meaning that for a given input pollutant concentration, they produce an output signal that is a smoothed version of the input. Due to physical limitations of the measurement principles, analysers have a finite dynamic response; *i.e.*, they do not respond immediately to inputs. Emission peaks are normally measured over more than one sampling period, and they appear flattened. This effect may be overcome by using ultra-fast response analysers, but not with conventional analysers in use in most emissions measurement setups.

Analysers for different pollutants ($CO_2$, $NO_x$, CO, THC, *etc.*) have unique response characteristics which translate into different effects upon the measured signals. The slower the response time of an analyser (typically reported by manufacturers as the 10–90% rise time, $t_{10-90\%}$), the more smoothed the output concentration signal will be with respect to the 'true' input concentration. This smoothing effect leads to an underestimation of instantaneous emissions during emission peaks, and an overestimation during valleys. This is conceptually similar to the effect of gas mixing discussed in section 3.2.3, but contrary to the former, the effect of the analysers can be considered independent of flow (*i.e.*, time-invariant).

If the output of the analyser matches the input value in the steady state,[7] the analyser will have no appreciable impact upon aggregated results (figure 3.6).

[7] This should be the case as long as the analysers are properly calibrated.

However, in order to improve the accuracy of instantaneous emissions signals, some compensation method is needed to reconstruct the peaks of the original signal. This compensation will require modelling the response of the analysers (which will be different for each one of the pollutants covered) and data post-processing to undo the distortion.

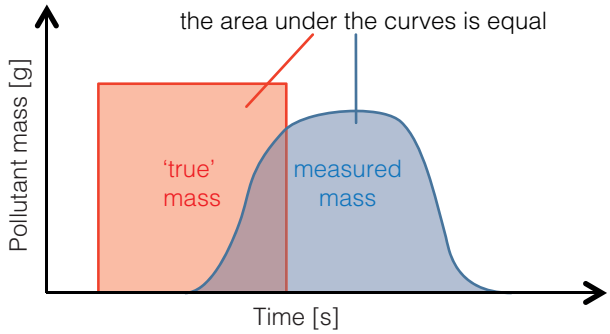


**Figure 3.6:** Illustration of the effect of the dynamic response characteristic of analysers upon measured mass emissions (overall mass is preserved)

### 3.2.5 Signal aliasing

Aliasing is a type of signal distortion that may be observed when a periodic signal of high frequency is sampled with a low frequency, and the sampled signal is represented with a new, even lower frequency as a result (see figure 3.7). To avoid that, and as a rule of thumb, all frequencies above one half of the sampling frequency need to be filtered out of a signal before it is sampled. This should be ensured for all signals. For analysers that exhibit rise times faster than the sampling rate, this condition is automatically fulfilled. However, if the discrete signal from the analyser is transferred as an analog signal to the data acquisition device, the latter will require anti-aliasing filters on its analog-to-digital converters. The compensation of signal aliasing is assumed to be (correctly) performed by measurement equipment, and so it is beyond the scope of this document.

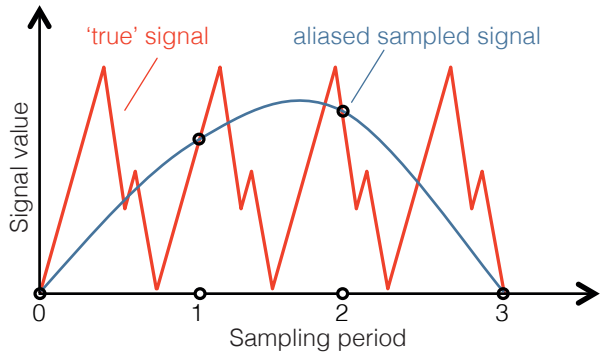


**Figure 3.7:** Illustration of signal aliasing

## 3.3 Summary of distorting effects

In this chapter we have reviewed the characteristics of the signals used for modelling vehicle emissions. We have also identified and characterised the distorting effects that compromise the accuracy of these signals, both at the aggregated and instantaneous level. Tables 3.5 to 3.10 contain a summary of the distorting effects that compromise the accuracy of instantaneous emissions signals introduced in this chapter.

**Table 3.5:** Summary of emission signal distortions: primary misalignment

| ***Description*** | ***Cause*** |
|---|---|
| • Instantaneous mass emissions are distorted due to a systematic (*i.e.*, fixed) delay between the exhaust mass flow and the pollutant concentration signals.<br>• An inaccurate pollutant mass emission signal is derived from the multiplication of a pollutant concentration and an exhaust flow rate signal whose alignment has not been checked. This may lead to over- or underreporting of emissions for instantaneous and aggregated results. | • Pollutant concentrations and mass flow signals may be measured at different points along the gas transport chain, leading to a time misalignment between the two data signals in test report datasheets output by measurement equipment (in spite of manual offset established by the test operator). |
| ***Compensation*** | |
| *Compensation strategy*<br>• Primary alignment (of concentration to flow rate signals, via a fixed time shift based on a signal cross-correlation check).<br>• Compensation is based on data post-processing, no modelling is required.<br>• Primary misalignment has a potentially large impact upon the accuracy of emissions signals. Its compensation is simple and should be done systematically. | *Signal(s) affected*<br>• Pollutant concentrations, exhaust flow rates.<br>*Priority*<br>• High (for instantaneous and aggregated results). |

**Table 3.6:** Summary of emission signal distortions: secondary misalignment

| ***Description*** | ***Cause*** |
|---|---|
| • Inaccurate engine maps are derived due to a wrong allocation of mass emissions to originating engine states. This may lead to over- or underreporting of mass emissions, both for instantaneous and aggregated (simulated) results. | • Engine state and mass emissions signals come from different instruments lacking an obvious time reference signal. |
| ***Compensation*** | |
| *Compensation strategy*<br>• Secondary alignment (of mass emissions to engine or vehicle states, via a fixed time shift based on a signal cross-correlation check).<br>• The compensation can be performed through data post-processing; no modelling is required. | *Signal(s) affected*<br>• Pollutant mass emissions, OBD/ECU signals (engine states).<br>*Priority*<br>• High (crucial for engine mapping). |

**Table 3.7:** Summary of emission signal distortions: variable transport times

| ***Description*** | ***Cause*** |
|---|---|
| • Primary alignment takes care of the delay imposed by the mean travel time of exhaust, but transport delays vary with flow (in a non-linear way).<br>• The variability of transport delays causes a wrong allocation of mass emissions to instantaneous engine states. | • Emissions travel through 'pipe' elements before they are measured. Travel time varies non-linearly with flow (hyperbolic law). |
| ***Compensation*** | |
| *Compensation strategy*<br>• Application of a variable (flow-dependent) time shift.<br>• Compensation requires modelling to characterise the variable transport delays and data post-processing to undo the distortion. | *Signal(s) affected*<br>• Pollutant concentrations.<br>*Priority*<br>• Medium. May be overlooked for aggregated results; relevant for engine mapping. |

**Table 3.8:** Summary of emission signal distortions: gas mixing

| ***Description*** | ***Cause*** |
|---|---|
| • Emission peaks are smoothed due to axial dispersion of pollutants within the 'pipe' elements of the measurement setup. Mixing is greater when large variability in the gas velocity profile (cross-section of pipes) exists. | • Friction and turbulence within the piping of the measurement setup lead to mixing of exhaust gas. |
| ***Compensation*** | |
| *Compensation strategy*<br>• Mixing in the tailpipe (and in exhaust gas lines before the mixing point of dilution systems) is flow-dependent. Mixing in the sampling lines leading to the analysers (having constant flows) is independent of exhaust flow. Compensation requires modelling to characterise the variable degrees of mixing and data post-processing to undo the distortion. | *Signal(s) affected*<br>• Pollutant concentrations, pollutant mass emissions. Especially relevant for diluted measurements. Raw exhaust measurements and PEMS are less affected due to the reduced length of 'pipe' elements.<br>*Priority*<br>• Medium. May be overlooked for aggregated results; relevant for engine mapping. |

**Table 3.9:** Summary of emission signal distortions: dynamic response of analysers

| ***Description*** | ***Cause*** |
|---|---|
| • Conventional analysers act as 'low-pass' filters. For a given input pollutant concentration, they produce an output signal that is smoothed. Leads to an underestimation of instantaneous mass emissions during emission peaks, and an overestimation during valleys. | • Analysers have a finite dynamic response; *i.e.*, they do not respond immediately to inputs. Emission peaks are measured over more than one sampling period, appearing flattened as a result. |
| ***Compensation*** | |
| *Compensation strategy*<br>• Compensation requires modelling to characterise the effect and data post-processing to undo the distortion. This effect can be considered independent of flow, and has no appreciable impact upon aggregated results. The response characteristic will be different for each pollutant covered. | *Signal(s) affected*<br>• Pollutant concentrations.<br>*Priority*<br>• Medium. May be overlooked for aggregated results; relevant for engine mapping. |

**Table 3.10:** Summary of emission signal distortions: signal aliasing

| ***Description*** | ***Cause*** |
|---|---|
| • Inadequately low sampling rate makes high-frequency oscillations appear as low-frequency oscillations. | • Measured signal contains information at high frequencies and cannot be adequately represented by sampling at the maximum available sampling rate. |
| ***Compensation*** | |
| *Compensation strategy*<br>• Cannot be addressed through data post-processing. Instruments with a sufficiently high sampling rate and anti-aliasing filters at their inputs are needed. | *Signal(s) affected*<br>• Exhaust flow rates, OBD/ECU signals.<br>*Priority*<br>• Low (beyond the scope of this dissertation). |

# Chapter 4

# Compensation of instantaneous vehicle emission signals

The distorting effects discussed in the previous chapter are well known to vehicle emissions test bench operators and measurement equipment manufacturers. However, since most of the distortions only become relevant at fine time scales, they have been traditionally overlooked in conventional EF development from aggregated data (*e.g.*, from dynamometer test sub-cycle or PEMS sub-trip results).

A small number of scientific studies have proposed signal compensation methods of varying degrees of sophistication. Regardless of the practical implementation, there are a number of tasks that need to be performed by any emission signal compensation methodology. In this chapter we will propose a *methodological framework* that will structure a discussion of the general aspects the compensation of instantaneous vehicle emission signals. Then, we will perform a *literature review* of emission signal compensation methods in which a distinction is made between methods that rely more heavily on data post-processing and those that require detailed physical modelling of the sub-systems of the measurement setup.

## 4.1 Methodological framework for signal compensation

In this section, we will study the elements that intervene in the process of transforming distorted signals into compensated signals with improved instantaneous accuracy.

A *methodological framework* is proposed to structure the discussion of these elements. As a starting point of our analysis, we propose to define *instantaneous emission signal compensation* as "the transformation of measured emissions signals to make up for the distortions brought about by the measurement setup and approximate the characteristics of 'true' emissions while preserving the useful qualities of the original signals". Hence, the proposed framework is summarised as follows: the original (distorted) emissions signal—a dynamically delayed, smoothed, flattened signal—is input to a compensation algorithm that produces a 'reconstructed' signal as an output. The compensated signal is produced by inverting the distorting effects according to a *model* obtained from characterisation experiments and other available knowledge about the distortions.

An adequately compensated signal should be closer to the 'true', catalyst-out signal than the original signal. This is assessed according to a number of established criteria or *metrics of signal similarity*. In order to validate the model and assess its compensation capabilities, the compensated signal should be compared with a so-called *reference signal*, which is known to be closer to the 'true' signal (*cf.* section 4.1.3). The common framework for the compensation method is schematically presented in figure 4.1. In the sections that follow, we will discuss the common elements of any signal compensation method, structured according the proposed reference framework.

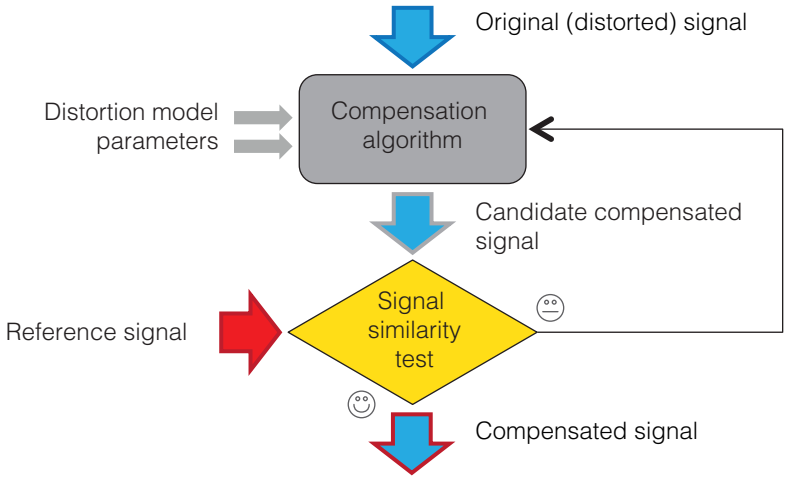


**Figure 4.1:** Reference framework for emission signal compensation methodologies

### 4.1.1 Compensation algorithm

The compensation algorithm is the central element of the compensation method. Its job is to take the original signal as an input and produce a compensated signal as an output. Multiple approaches are possible when devising an algorithm that compensates instantaneous emissions signals. From the discussion of the distorting effects of chapter 3, it follows that a comprehensive compensation method will have to perform two (critical) time alignments: a primary alignment of pollutant concentration signals to the flow rate signal (in order to produce mass emission signals), and a secondary alignment of the mass emission signals to the engine covariate signals that are used to build the engine emission maps. Moreover, it will involve a further compensation process to reconstruct the emission peaks and other features that were smoothed by the mixing of the exhaust gas and by the dynamic response characteristic of the analyser.

### 4.1.2 Original signals

*Original signals* are those routinely produced by the emissions measurement equipment that is ordinarily available. These signals are affected by the distorting effects described in chapter 3, and thus their instantaneous accuracy is compromised. Distorting effects notwithstanding, the original signals may have some *desirable characteristics that should be preserved after the compensation*. For example, measurements performed in *dilution tunnels* are reliable because analysers operate within their optimal range of concentrations, and sudden variations in concentration are dampened. Also, flow is quasi-constant and easily determined, and so this type of measurement can be used to accurately estimate *total mass emissions* during a test cycle run. In this case, total mass emissions should be preserved after the compensation process.

### 4.1.3 Reference signals

*Reference signals* are those produced by special instruments that may not be available during ordinary testing. Reference signals possess some qualities that bring them close to the 'true' (undistorted) signals that we want to reconstruct, and which the original signals lack (*e.g.*, they are less affected by variable transport times, or they

have a richer frequency content). Reference signals can be produced by performing measurements with a *reference instrument* (*i.e.*, one with faster response time, better accuracy or higher sampling rate than the instrument that produces the original signals). If possible, the measurement of the reference signal should be performed close to the engine-out or catalyst-out point, upstream of the point where the original signal is obtained. In some research applications (see, for example, Weilenmann, Soltic and Ajtay 2003), a hole may be drilled in the exhaust system of the test vehicle (before or after the catalyst, according to the application) in order to open a sampling point for raw exhaust gas. This may be unfeasible in most cases; in general, measurements performed right after the exhaust pipe can be considered sufficiently close to the engine-out or catalyst-out point.

In some cases, *synthetic reference signals* can be produced through the combination of measured data coming from several instruments, additional data about fuels, or calculated data. For example, the engine load signal from the OBD of the vehicle can be considered directly proportional to engine air mass flow.[1] Thus, it is possible to scale the OBD signal to match the overall mass measured at the dilution tunnel and obtain an air mass flow signal that is not affected by the variable transport times between the tailpipe and the diluted measurement point.

### 4.1.4 Metrics of signal similarity

In order to assess the performance of the compensation procedure, objective mathematical measures of signal similarity are needed. In other words, we need objective indicators of the performance of the signal compensation method. In this way, part of the signal compensation process can be transformed into mathematical optimisation problems that may be solved iteratively through the modification of the parameters of the compensation model. Some commonly used measures of signal similarity are introduced in the sub-sections that follow.

[1] Tests with engine speed measurement from OBD and with self-mounted optical rpm sensors (as well as dynamometer speed) have shown that OBD signals have an unknown and variable delay of up to two seconds. Still, it is not recommended to measure rpm (and other time relevant engine or vehicle signals) from any source other than OBD. If access to ECU signals faster than OBD (usually manufacturer proprietary access) is available, those signals should be used instead.

#### 4.1.4.1 Sum of squared residuals

A common approach to assess the goodness of a model-data fit is to compute the sum of the squares of the deviations of the values provided by the model (the compensated signal) from the reference data (the reference signal), evaluated at each data point. This is the sum of squared residuals, or SSR. The optimal solution (compensated signal) in the least squares sense is that which minimises the SSR. Since we are computing the *square* of the errors, positive and negative deviations of the same absolute value are equally considered, and deviations with a larger absolute value will be especially penalised (equation 4.1).

$$SSR = \sum_{i=1}^{n} (x_{compensated,i} - x_{reference}, i)^2 \tag{4.1}$$

#### 4.1.4.2 Sum of absolute deviations

The computation of the sum of absolute error—or sum of absolute differences (SAD; equation 4.2)—before and after compensation is a very simple, yet useful measure of the goodness of the compensation method applied. Note that absolute values need to be considered, because the sum of all deviations will approach zero by virtue of mass conservation (see section 3.1.2.5 on page 56). By computing the sum of absolute deviations, all errors are considered equally (unlike the sum of squared residuals, which penalises high deviations).

$$SAD = \sum_{i=1}^{n} |(x_{compensated,i} - x_{reference,i})| \tag{4.2}$$

#### 4.1.4.3 Signal cross-correlation

Cross-correlation is a standard metric used to assess the similarity of two sets of data. Since cross-correlation is not affected by scaling, we can multiply one or both of our signals by any factor and obtain the same value. In situations when we have two signals with *similar profiles*, but one is shifted in time and has noise added to it,

then correlation is a good method to measure the delay between the signals. Cross-correlation can be easily computed in MATLAB®, or even in spreadsheet software. If we consider two discrete signals $x[i]$ and $y[i]$ where $i = 0, 1, 2 \ \ldots \ N$, we can compute their cross-correlation coefficient $r$ at delay $d$ using equation 4.3.

$$r = \frac{\sum_{i=1}^{N-1} (x[i] - \bar{x}) \cdot (y[i] - \bar{y})}{\sqrt{\sum_{i=1}^{N-1} (x[i] - \bar{x})^2} \cdot \sqrt{\sum_{i=1}^{N-1} (y[i-d] - \bar{y})^2}} \tag{4.3}$$

In equation 4.3, $\bar{x}$ and $\bar{y}$ are the means of the corresponding signals. The cross-correlation coefficient $r$ can adopt any value between $-1$ and 1, and it reaches a maximum at the time when the two signals have maximum similarity.

We can use cross-correlation to assess the similarity of two signals representing the same magnitude. This is useful when calibrating the parameters of our signal compensation model. When performing this operation, one should take into account that two signals can have very high *global cross-correlation* (*i.e.*, a single $r$ value evaluated over the whole dataset) and yet exhibit poor *local cross-correlation* (a series of values for $r$ evaluated for many small data sections corresponding to the same time interval) at the same time. For a compensated signal, we would want global and local cross -correlation values to the reference signal to be high, but local cross-correlation (instantaneous similarity) is what we are trying to achieve specifically.

A cross-correlation check can also be used to align two different signals representing different magnitudes to a common time reference. This is a useful operation to perform the alignment of concentration signals to flow, or mass signals to engine state data (*i.e.*, both for *primary* and *secondary* alignments). However, this method is only applicable for signals that must correlate due to physical, causal relationships among them. For instance, $CO_2$ mass flow should correlate well with exhaust mass flow, and also with engine load (or power). The cross-correlation alignment is not applicable to signals that do not correlate *a priori*.

## 4.2 Design specifications of compensation methods

We have taken a first look at the common aspects that will be part of any instantaneous vehicle emission signals compensation method. Actual implementations of signal compensation will vary largely depending on the characteristics of the measurement setups, and also on the needs of the users of compensated data and on the additional experimental and post-processing work requirements. In the following sub-sections we compile a list of desirable characteristics or 'design specifications' that a signal compensation method should possess. As will be shown in the the literature review later in this chapter (section 4.4), not all of these characteristics are fully achievable simultaneously, and compromises will have to be made.

### 4.2.1 Peak reconstruction and time alignment capabilities

The obvious design requirement for any signal compensation method is that it should be able to make measured signals approximate the characteristics of 'true' signals very closely. In other words, it should have good time alignment and peak reconstruction capabilities; given a set of original (measured) signals—which will include pollutant concentrations and flow rate data—, a compensation method should be able to process them and give an output that is more similar to a reference signal that is used to validate the compensation process. A perfect method would be able to match the reference signal exactly. This will not achievable in practice because the systems modelled have a stochastic component (*cf.* section 3.1). Also, the quality of the compensation will be limited by factors such as the sampling rate, the quality of analysers, the presence of dilution and the distance from the point where the emission is produced to the measurement point. Ultimately, the quality of the reconstruction will also be limited by the accuracy of whichever signal is taken as a reference.

### 4.2.2 Simplicity

The physical phenomena that need to be modelled (variable transport times, exhaust gas mixing, response of gas sensors in the analysers, and so on) are too complex to be adequately represented by a deterministic model, or even to be effectively simulated.[2] Therefore, a simplified model of the distortions is needed. This model

[2] A simplified simulation of transport phenomena from tailpipe to analyser was performed by Le Anh, Hausberger and Zallinger (2006) using computational fluid dynamics.

should be complex enough to cover all the relevant effects, and simple enough to avoid unnecessary detail that requires additional data post-processing efforts.

A second dimension of simplicity is given by the amount of additional work and measurement equipment required to put the method into practice. Additional work may come from semi-manual operations of signal post-processing, *ad hoc* experiments to characterise the measurement setup, or periodic calibration requirements. Additional measurement equipment may include ultra-fast response analysers, or specific hardware to produce controlled input signals (*cf.* section 4.3).

### 4.2.3 Broad scope and applicability

A *broad scope* is also a desirable characteristic for the compensation method, both in terms of the phenomena covered and of the elements or sub-systems of the measurement chain considered. An ideal instantaneous compensation method should cover all the distortions described in chapter 3, and compensate them *from the catalyst-out point to the analyser output*, but this is subject to the availability of proper reference signals and physical accessibility of measurement points. *Broad applicability*, in terms of the number of vehicle types, pollutants and measurement setups that the method can be applied to, is also a desirable quality, but this increased flexibility is likely to come at the expense of the accuracy of the method.

In practice, the compensation approach will be limited by aspects such as the availability of suitable reference signals or sampling points, or by the additional burden of experimental/data post-processing work that is considered acceptable by the operators of the emissions measurement equipment in relation to their needs and expectations regarding the instantaneous accuracy of the emission signals produced (see table 4.1). In most cases, the exhaust system of the vehicles under test will not be covered because exhaust gas sampling before the exhaust system requires drilling a hole to accommodate the probe of the analyser.

**Table 4.1:** Recommended compensation scopes, by user type

| | Vehicle emissions data users ⇒*decreasing expectations for instantaneous data accuracy* ⇒ | | |
|---|---|---|---|
| **Distortions** | 'Engine mappers' | Emission modellers | Everyone else |
| Primary misalignments (§ 3.2.1.1) | ✓ | ✓ | ✓ |
| Local time shifts (§ 3.2.2) | ✓ | ✓ | ✗ |
| Local peak blurring (§§ 3.2.3, 3.2.4) | ✓ | if desired | ✗ |
| Secondary misalignments (§ 3.2.1.2) | ✓ | ✗ | ✗ |

### 4.2.4 Data sampling rates

A key aspect of instantaneous emission modelling is the frequency content of the emission signals. Current-technology gasoline cars with three-way catalysts and lambda control emit most of their pollutants within transient emission peaks, typically lasting between 0.5 and 1 s. Their pollutant mass emission signals thus show a frequency content of about 3-5 Hz. From the Nyquist-Shannon sampling theorem, it follows that by sampling a signal with a frequency $f$ all information above $2f$ will be lost. Thus, a significant part of the frequency content of the signals is lost at the standard sampling rate of 1 Hz. The use of a sufficiently high sampling frequency (of at least 5 to 10 Hz) is therefore recommended for instantaneous emissions modelling purposes.

## 4.3 Modelling emission signal distortions

In order to be able to compensate the distortions described in chapter 3, we need to have a mathematical model of the ways in which the emissions measurement setup transforms the original input into the distorted output. Then, by inversion of the model, we should be able to undo the distortions and go from the (measured) distorted signal to a signal that more closely resembles the 'true', undistorted signal. In this section, we will explain how we can model the distortions of emission signals through a complete vehicle emissions measurement setup.

The transient behaviour of a system (*i.e.*, its response to a fast-changing input) can be represented by a *dynamic mathematical model* consisting of a sets of differential and algebraic equations. The equations that describe the behaviour of a system are usually

derived from knowledge of the physical laws governing the system under study, or from characterisation experiments. There are two different approaches to modelling the distortions of emission signals: the simpler methodologies for the compensation of instantaneous emission signals do without characterisation experiments and rely instead on a statistical fit of simple physical models to the measured signals. The more complete methodologies, on the other hand, are based on *systems theory*,[3] and they include characterisation experiments, which are even performed at a sub-system level (*i.e.*, by breaking down the whole measurement setup into several, simpler sub-systems).

*Systems theory* provides a theoretical framework to model general relationships of the empirical world through simplified physical models. It can be applied to model a wide array of systems whose complexity goes far beyond the scope of this dissertation. Some mathematical tools and concepts of systems theory are used in this chapter and in the next, where a new, comprehensive methodology for the compensation of instantaneous emission signals is described. However, it is beyond the scope of this dissertation to present systems theory in full detail; the manuals by Kwakernaak and Sivan (1991) or Ogata (2002) may be consulted for reference.[4]

### 4.3.1 System identification

*System identification* is the generic name given to the procedures required to *build a mathematical model* of the dynamics of a system from measured data; *i.e.*, finding the values of the parameters in the differential equations that govern its behaviour. Depending on the available knowledge about the system, we can distinguish three types of system identification approaches:

- In *white box* identification, the model structure is based on physical principles which are well-known, and model parameters are directly estimated from the measured data (*e.g.*, measuring the current and the voltage drop across a resistor to find out its value by substitution in Ohm's law). This approach is generally only feasible for deterministic models.

[3] The description of a comprehensive vehicle emission signals compensation methodology based on 'systems theory' modelling can be found in (Franco *et al.* 2014). The effort of Dr Savas Geivanidis and Dr Martin Weilenmann to make this information available is gratefully acknowledged.

[4] Both approaches are covered in the literature review in section 4.4 on pp. 85—88.

- In *black box* identification, the basic model structure and the parameters are totally unknown, and they must be estimated solely from experimental results. System control theory is able to apply general mathematical models in such cases in order to provide a working solution without further insight into the details of the physical phenomena being modelled.
- In *grey box* identification, the main model structure is partially known from physical principles, and the parameters are estimated from experimental data.

Any dynamic system can be represented by a system of differential equations whose independent variable is time. The *Laplace transform* is a technique used in system design to study the transient response of systems. In this case, time is being replaced by the complex variable $s$, thereby moving the analysis from the time domain to the frequency domain. This makes it easier to analyse and solve the differential equations used for the description of linear, time-invariant systems. The transfer function *G(s)* of a system is a mathematical expression that describes the relationship between the output of a control system $Y(s)$ and its input $U(s)$. In linear systems, it is equal to the ratio of the Laplace transform of the output of the system over the Laplace transform of the input of the system (equation 4.4).

$$G(s) = \frac{Y(s)}{U(s)} \tag{4.4}$$

By definition, the transfer function can estimate the output of a model for a given input. The *Laplace transform* is valid for linear continuous systems. In the case of discrete systems, the above technique is replaced by the *z-transform*. The detailed mathematical explanation of these incredibly useful transforms is beyond the scope of this document, and it can nonetheless be found in the manuals we just cited. For the purposes of this dissertation, the only thing we need to bear in mind is that the transfer function has some mathematical properties that are useful for the identification and inversion of dynamic systems. Namely, the transfer function can be used to determine the dynamic response characteristics of a system without solving the associated differential equation.[5]

[5]Especially important are the poles and zeros, which are the roots of the polynomials that form the transfer function. The location of the poles and zeros is a property of the transfer function. Together with the gain constant $K$, they characterise the differential equation, and provide a complete description of the system.

### 4.3.2 Modelling a complete vehicle emissions measurement setup

In the previous section, we introduced the *grey box* system identification approach, in which the main model structure is partially known from physical principles, and the parameters are estimated from experimental data. This is the approach that we will preferably adopt in our system identification task. In doing so, we can leverage the knowledge of the systems involved in emissions measurement gathered in previous modelling efforts, while also having an empirical support to our model.

Let $u$ and $y$ be the input and output, respectively, of a system. Then, the system model can be viewed as a mapping of $u$ into $y$, which is represented by the transfer function. In general, systems with multiple input and output signals are possible, but in our study case we will limit ourselves to single-input, single-output systems, where our input signal will be the 'true', undistorted pollutant concentration signal at the inlet of the system, and the output will be the distorted (dynamically delayed, flattened and smoothed) signal at the outlet (*cf.* section 3.1).

In section 3.1.2.2 on page 54 we provided the example of the dynamic mathematical model of the exhaust system of a vehicle, which acted as a gas 'mixing chamber'. The exhaust system is only a small sub-system of a complete measurement setup, but it behaves similarly to the other sub-systems. If we maintain a constant flow through them, these sub-systems can also be modelled as 'mixing chambers' in which the pollutant concentration (or mass) output $y(t)$ is a function of a number of its own derivatives (with respect to time) and of the concentration input (or mass) $u(t)$.[6]

The general method to compile a physical model[7] of the distortions of emission signals throughout a complete emissions measurement setup comprises the following steps:

1. *Dividing the complete measurement setup into sub-systems that will be modelled individually*. An appropriate sub-system division of the measurement setup should treat time-variant and time-invariant sub-systems of the measurement setup separately (see section 3.1.2.4 on page 55 and figure 4.2).

[6] In its discrete form, the differential equation was transformed into a set of algebraic equations where the output was a function a finite number of past inputs.

[7] Successful applications of this approach are presented in the literature review on pp. 85—88.

2. *Performing characterisation experiments*. For compensation methods based on systems theory, the necessary characterisation experiments are performed for all the sub-systems in which the whole measurement setup is divided. In 'systems theory' modelling, the characterisation of the sub-systems is done by generating controlled *step inputs*. In order to have a response that does not vary with time—*i.e.*, a linear, time-invariant (LTI) system—the step experiments are performed at several constant flow rates selected to cover the whole operating range of the measurement setup. Step inputs are generated at the inlet of each sub-system using a special valve train, and the corresponding responses are measured at the outlet. By comparing the measured output of each sub-system to the controlled input, it is possible to characterise their dynamic response.

3. *Assigning values to parameters, compiling and inverting the whole model*. The distortions brought about by each sub-system need to be modelled—and the models inverted[8]—individually. Then, the principle of superposition (*cf.* section 3.1.2.3 on page 55) is applied to obtain the complete model that inverts the distortions. The resulting model is thus able to predict the evolution of measured pollutant concentration at the inlet as a function of the (measured) instantaneous concentration at the outlet.

[8] After the inversion, the solution becomes a linear function of the derivatives of the output. Since the output is a measured signal, its noise is amplified by building the derivatives, and therefore the inversion has to be coupled to a low-pass filter. This step requires a good knowledge of signal processing techniques.

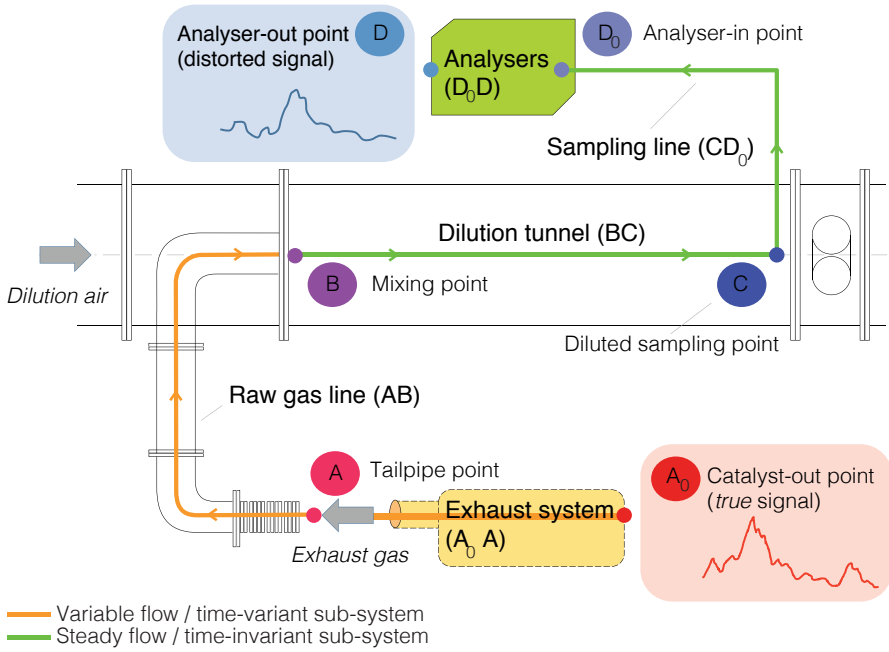


**Figure 4.2:** Sub-system division of a chassis dynamometer measurement setup (constant volume sampling) [adapted from Geivanidis and Samaras (2008)]

## 4.4 Literature review

In this section, we will review the vehicle emission signal compensation methods found in the literature. A small number of scientific studies have investigated the instantaneous accuracy of measured vehicle emissions. A handful of these studies have proposed signal compensation methods of varying degrees of sophistication, and only very few have proposed a comprehensive methodology to cover all the relevant distortions and improve the instantaneous accuracy of vehicle emission signals. For our review, we have chosen to classify these methods in two large blocks: on the one hand, we have the methods that rely more heavily on data post-processing, and on the other we find those that require detailed physical modelling of the sub-systems of the measurement setup.

### 4.4.1 Partial methods based upon data post-processing

In this section, we will briefly review earlier methodological proposals for the compensation of instantaneous emission signals that relied mostly on data post-processing. We are calling these *partial* models in the sense that they were either meant to address only a few of the distorting effects discussed in chapter 3, that they only covered a few sub-systems of the measurement setup, or that they were only applicable to a few pollutants.

In the scientific and technical literature dealing with the instantaneous accuracy of measured vehicle emissions, we find that one of the most commonly addressed distorting effects is what we have denominated primary misalignment; *i.e.*, the misalignment between pollutant concentration (as output by the analysers) and exhaust flow signals. This is hardly surprising, because systematic time misalignments are the type of distortion that is simplest to observe and understand. They are also fairly simple to compensate, and they have a potentially large impact upon both instantaneous and aggregate emission measurement results. As discussed in chapter 3, vehicle emission measurement equipment can be set to apply fixed time shifts to offset this distortion, but this offset may not be optimal and it should be adjusted after the measurement through data post-processing. The impact of time alignment upon the accuracy of instantaneous vehicle emission measurements was addressed in detail by Hawley *et al.* (2003, 2004) and Bannister *et al.* (2007).

General predictive control theory models—as well as other transfer function based models (*cf.* section 4.3.1)—were applied to raw gas sampling setups by Smith and Hodgson (1999), and even though the dynamic distortion of the emission signal was taken into account, the resulting model was only applicable to certain operating conditions of the raw gas transport lines. De Petris *et al.* (1994) compiled a time-invariant model of a diluted exhaust gas measurement system, but their results were of limited accuracy due to the time-variant delays imposed by the raw exhaust line.

Some other signal compensation methods based upon data post-processing have had moderate success modelling the dispersion of exhaust gas and the dynamic response of diluted gas analysers using *statistical approaches*. An overview of these compensation methods is given in table 4.2. The main strength of these approaches is that they require little additional experimental efforts. Their main weakness—besides their lack of completeness—is that they often lack an experimental validation.

**Table 4.2:** Partial models that rely (mostly) upon statistical signal post-processing

| **Authors** | **Model description** |
|---|---|
| Ramamurthy *et al.* (1998) | *System modelled*<br>• Fixed laboratory dilution tunnel and analysers ($NO_x$ and CO).<br>*Approach description*<br>• Application of dispersion model to create a 'dispersed axle power' signal (lacking physical meaning); time shifting to maximise cross correlation between 'dispersed axle power' and emission signals. A gas dispersion model is fitted to experimental data. |
| Madireddy and Clark (2006, 2008), Madireddy (2008) | *System modelled*<br>• Dispersion due to analyser response characteristic ($CO_2$, $NO_x$).<br>*Approach description*<br>• Simple dispersion model, deconvolution of analyser signal. |
| Kamarianakis and Gao (2010) | *System modelled*<br>• Variable exhaust transport times (exhaust system dynamics) and the analyser's response characteristic are modelled together.<br>*Approach description*<br>• A purely statistical approach is adopted; a 'smooth transition regression' modelling framework is used to include transport delays that vary smoothly as a function of exhaust flow. |

### 4.4.2 Complete methods based upon physical modelling

In this section, we will review the methodologies for the compensation of instantaneous emission signals that rely upon physical modelling to compile complete models of the distortions that affect the signals throughout the measurement setups. By introducing experimentally validated *physical models* of the distorting phenomena, a more complete approach to the problem of emission signal compensation can be taken. The methods presented in this section show that it is possible to use *systems theory* approaches to model the distortions of instantaneous emission signals and post-process the flattened emission signals recorded by conventional analysers to reconstruct the 'sharp' emission signals that would be observed at the engine-out or catalyst-out point.

The work of Dr Martin Weilenmann of EMPA and his collaborators in the field of instantaneous emission modelling is especially noteworthy. In an early study (Weilenmann, Bach and Rüdy 2001), it was shown that the changes in exhaust volume flow affect the value of the optimal time shift between concentration and volume flow signals for raw gas measurements due to the variations of transport time within the exhaust system of the vehicle. A later paper (Weilenmann, Soltic and Ajtay 2003) made the case for the systematic compensation of the effects of variable transport times and exhaust gas mixing in chassis dynamometer setups using systems theory concepts. A complete model of the gas transport system comprising a raw gas analyser bench and the exhaust system of a vehicle was presented, together with the inverted model that compensated the distortions. The authors proposed a simplified model of the transport dynamics comprising two parts: a pure, flow-dependent time delay—corresponding to a piston flow of the exhaust gas—and a flow-dependent dynamic component to model the exhaust gas mixing. In a follow-up study (Ajtay and Weilenmann 2004), the same approach was applied to parameterise and invert the model of a diluted measurement setup.

Building upon the approach of Weilenmann *et al.*, Geivanidis and Samaras (2008) modelled a complete chassis dynamometer measurement setup with dilution by characterising the delays and the mixing behaviour of discrete sub-systems of the measurement chain. Each sub-system was modelled as a function of selected representative flow rates to cover the relevant operating points, and the necessary characterisation experiments were performed with a sophisticated induction coil valve train that improved the sharpness of the step input signals.

The methodologies for the compensation of instantaneous emission signals that rely upon physical modelling provide good compensation capabilities. An advantage of these methodologies is that they make it possible to model complete measurement setups—from tailpipe to analyser—, and to gain insights into how each sub-system is distorting the signals. An important drawback of detailed physical modelling is that the necessary characterisation experiments are time-consuming and require special apparatus for the generation of the controlled step inputs. Moreover, the parameterisation of the models needs to be adjusted following modifications to any sub-system of the measurement setup. For instance, a simple length or diameter change in one of the gas lines would require new experiments and the recompilation of the overall model, which in turn requires good knowledge of signal processing techniques. An overview of signal compensation methods based on signal physical modelling of the sub-systems of the measurement setup is given in table 4.3.

**Table 4.3:** Models that rely (mostly) upon physical modelling

| Authors | Model description |
|---|---|
| Weilenmann, Soltic and Ajtay (2003); Ajtay and Weilenmann (2004) | *System modelled*<br>• Light duty vehicle exhaust system dynamics and raw gas measurement system (heated sampling line and analyser), later extended to dilution tunnel.<br>*Approach description*<br>• 'Systems theory' approach; flow-dependent parameters are estimated through repeated testing (step input response) at several representative flow rates. |
| Le Anh, Hausberger and Zallinger (2006) | *System modelled*<br>• Raw and diluted sampling lines, dilution tunnel.<br>*Approach description*<br>• Combination of experimental analysis and gas flow simulation; estimation of mixing parameters. |
| Geivanidis and Samaras (2008) | *System modelled*<br>• Raw and diluted sampling lines, dilution tunnel and diluted gas analysers.<br>*Approach description*<br>• 'Systems theory' approach; flow-dependent parameters are estimated through repeated testing (step input response) at several representative flow rates. |

## 4.5 Summary

In this chapter we have proposed a methodological framework for the compensation of instantaneous vehicle emission signals. The compensation of emission signals can be achieved through a combination of characterisation experiments, detailed physical modelling (by sub-system) of the measurement setup and statistical post-processing of the distorted signals. The methodological approaches based on systems theory and physical modelling exhibit good compensation capabilities, but they also require more *ad hoc* experimental work (both for initial setup and periodic calibration) than simpler, more flexible methods that rely upon signal post-processing.

In the next chapter, we will present a new, comprehensive methodology that aims to combine the flexibility and ease of use of data post-processing methods with the completeness of physical modelling approaches.

# Chapter 5

# The $CO_2$ tracer method

We have thus far described the effects that distort instantaneous emission signals, and justified the need for their compensation in order to improve the accuracy of measured mass emission signals in general, and of *engine emission maps* in particular. Having also discussed the general aspects of instantaneous vehicle emission signal compensation and reviewed existing methodologies, we are now ready to present a proposal for a new, comprehensive methodology to compensate instantaneous vehicle emission signals for modelling purposes.

## 5.1 Modelling distortions with a tracer gas

A tracer can be defined as 'a substance introduced into a biological organism or other system so that its subsequent distribution may be readily followed from its colour, radioactivity, or other distinctive property'.[1] The use of tracers to model fluid flows is a well-known technique (Levenspiel and Smith 1957). The basic concept behind tracer techniques is that it is possible to characterise a fluid flow through a vessel by comparing a known (sometimes controlled) input to its corresponding output, hence extracting information about the behaviour of the system. This is not unlike what is done to model a complete emissions measurement setup with the systems

[1] *Oxford online English dictionary*. Oxford University Press (2014).

theory approach, where a known input is generated at the inlet of each sub-system and the resulting output is measured at the outlet.

The tracer gas and the systems theory approach share some theoretical foundations, but they are also fundamentally different. In this sense, 'tracer gas' is a fitting name for the approach described in this section, because the mass emissions of the gas are followed—or rather, traced—throughout the measurement setup during the normal operation of the emissions test bench. This will become apparent in the sections that follow, where the tracer gas approach will be described by highlighting the characteristics that set it apart from the systems theory approach described in the previous chapter.

The tracer gas compensation method relies on the basic assumption that **all gaseous pollutants emitted at a given point in time are transported and mixed in the same way within the measurement setup**. This is a rather fair assumption, because all gaseous pollutants are produced at the same time during the fuel combustion process, and subsequently transported and mixed together.[2] The proposed modelling approach starts at the diluted measurement point and goes back up to the exhaust after-treatment system out point, which is as close to the engine as most emission measurements aim to be. The presence of a catalyst or another after-treatment system does not compromise the basic assumption, because the residence time is the same for all gaseous pollutants.

The compensation approach proposed in this chapter is based upon making small modifications to the original signal of the tracer pollutant so as to bring it closer to the reference signal. Then, the same modifications can be applied to the rest of gaseous pollutants (*i.e.*, the ones that are not used as a tracer) based on the assumption that the signals for all gaseous pollutants suffer the same distortions. The compensation of the original signal is therefore supported by the reference signal, which needs to be measured in each case.

### 5.1.1 Properties of $CO_2$ as a tracer gas

Any gaseous pollutant could in principle be used as a tracer. However, there are a number of reasons that justify the selection of $CO_2$. First and foremost, $CO_2$

[2]Note, however, that this is not exactly the case for particulate matter, which is suspended within the gas flow, and may adhere to the walls of the measurement setup.

is less likely than other pollutants to suffer chemical transformations within the measurement setup.[3] Vehicles equipped with an internal combustion engine produce large quantities of it throughout any driving cycle (except during fuel cut-offs), so the accuracy of its measurement is not affected by the detection limits of analysers. A further advantage of using $CO_2$ as a tracer is that, provided that a reliable *instantaneous fuel consumption* (FC) measurement can be obtained, it is straightforward to develop an undistorted, instantaneous mass $CO_2$ signal to be used as a reference by assuming that the carbon content of the fuel is fully transformed to $CO_2$. This is a fair assumption, and one that makes it unnecessary to measure flow to derive the mass signal.[4] Furthermore, given that $CO_2$ correlates well with engine parameters (*e.g.*, engine load or engine power), it is an adequate choice of a pollutant to support the secondary alignment of mass emissions to recorded engine state signals discussed in section 3.2.1.1.

A minor disadvantage of $CO_2$ as a tracer is that small amounts of this pollutant are introduced in the ambient air used in the dilution tunnel. In any case, the volume of dilution air is normally recorded by emission test benches, and the (very stable) concentration of $CO_2$ in ambient air can be corrected for rather easily. Another disadvantage is that $CO_2$ *concentration* signals exhibit little variability (especially for gasoline cars with stoichiometric operation), but this does not apply to the $CO_2$ tracer method because it relies on $CO_2$ *mass* signals instead.

## 5.2 Theoretical background

The $CO_2$ tracer method uses $CO_2$ as a tracer gas to model the dynamic delays and gas mixing processes that occur *between the engine-out point and the measurement point* of the measurement setup, which is modelled as a single—or 'lump'—system. To that avail, the measured (distorted) $CO_2$ *mass emission signal* is post-processed off-line (after the measurement is completed). First of all, the signal is mathematically transformed to produce a large set of plausible, 'candidate' undistorted signals. These candidate signals are then binned (*i.e.*, broken into small data vectors) and the data

[3] The concentration of some pollutants (such as $NO_x$, CO or HC) is drastically affected by the chemical transformations within the after-treatment system, whereas the difference between catalyst-in and catalyst-out $CO_2$ is marginal.

[4] The implementation of the method described in chapter 6 takes advantage of this possibility by using an instantaneous FC meter as reference instrument.

bins are systematically compared to the corresponding bin of the reference signal. Based on these comparisons, the optimal data bins (in terms of similarity to the reference signal) are selected from the candidate signals, and the optimal bins are subsequently joined to produce a compensated $CO_2$ mass emission signal. Finally, the same compensation process that produces and optimal compensation of the tracer is applied to other pollutants for which a reference signal is not available (*i.e.*, 'blindly') on the assumption that the distorting effects that affected the mass emission signals of $CO_2$ also affected the other gaseous pollutants in the same manner.

Some key questions arise at this point: how can we transform the original signal in order to bring it closer to the reference? Can the good qualities of the original signal (*e.g.*, total mass) be preserved in doing so? How can the modifications made to the original tracer signal be stored so that they can be applied to other pollutants? In order to answer these questions, we will introduce some mathematical concepts upon which the $CO_2$ tracer method relies (discrete signal convolution, signal binning) in the sections that follow.

### 5.2.1 Discrete impulse response and discrete convolution

The tracer approach aims to systematically extract information about *variable delays and peak blurring*, and tries to generalise it to construct a useful model that will allow us to compensate the distortions not just for $CO_2$, but for the rest of gaseous pollutants.

The $CO_2$ tracer method takes two $CO_2$ mass emission signals as input. One of these signals is the original, distorted signal, and the other is an undistorted signal—measured close to the engine-out—which is taken as a reference. The information necessary to model the distortions is extracted by applying plausible transformations to the original signal and systematically comparing the transformed signals to the reference signal. These 'plausible transformations' are explained next.

#### *5.2.1.1 Discrete impulse response*

According to systems theory, it is possible to completely characterise an LTI system if we can accurately determine its *step response*. There are, however, other ways of characterising such a system by producing a controlled input and measuring the

corresponding output. One way would be to produce sinusoidal inputs of known amplitude and varying frequency to determine its *frequency response*. Another way of characterising a system would be to produce an impulse input (*i.e.*, a very high peak of short duration) and to determine the *impulse response* of the system. Every LTI system has a *unique* impulse response, frequency response and step response. An accurate measurement of either of these can be used to predict the output of an LTI system for any given input (Ogata 2002).

Whereas frequency response experiments can be easily performed for some systems (*e.g.*, for electric circuits, by means of an oscilloscope), this approach would be impractical in our case, as it would be very difficult to produce the sinusoidal pollutant emission signals. To a large extent, the same is true for impulse response experiments, which require a very high peak of extremely short duration. Besides, since our system is time-varying (considered as a whole from engine-out to the end of the dilution tunnel), we would need to produce several impulses at different fixed flow rates to cover the operating range. This would be very impractical, and so the performance of impulse experiments for the characterisation of our system is excluded.

Still, we can use the concept behind impulse experiments to introduce the mathematical operation of *convolution*, which is a key element of the tracer gas approach. Let us then assume that we have a chassis dynamometer setup equipped with a dilution tunnel, and that we are able produce a very high peak of emissions of a certain pollutant at the inlet of the setup while it is operating at a quasi-steady flow rate (and therefore behaving as an LTI system). This peak occurs during a very short period of time, so we can call it an impulse. In discrete signal representation, such an input would appear as a high concentration peak followed by zero-concentration points (equation 5.1, where $C$ is the pollutant concentration that would be measured at the location of the impulse).

$$u[k] = [\ C \quad 0 \quad 0 \quad 0 \quad \dots\ ] \tag{5.1}$$

Let us now look at the fate of this impulse signal as it is transported within the measurement setup. Initially, the mass of the pollutant will travel together as a rather compact cloud with a pollutant concentration close to $C$. As the pollutant cloud travels along the pipes, it will be mixed with the gases that were emitted right before and right after it, thus becoming less compact (figure 5.1).

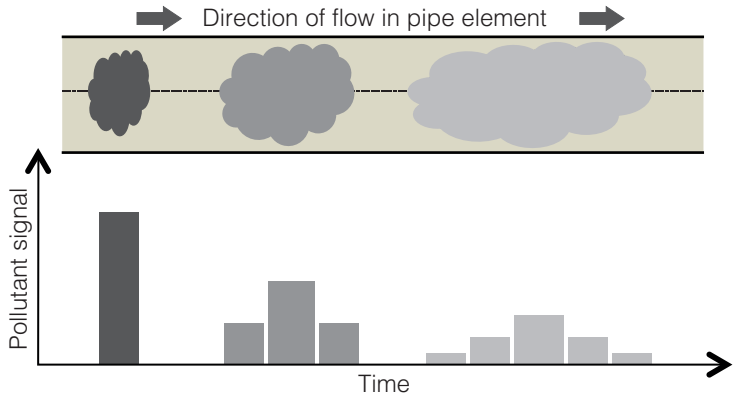


**Figure 5.1:** Flattening of signal peaks by gas mixing (axial diffusion) [adapted from Levenspiel (2012); the effect applies to both concentration and mass signals]

By the time the cloud reaches the gas analyser, the output $y[k]$ will be delayed with respect to the impulse input $u[k]$ by the time it took for the peak to travel from the inlet to the measurement point. It will also be dispersed to the point that it will be measured over more than one sampling period. The output of the analyser (which, for the sake of simplicity, is assumed to have a perfectly fast response) corresponding to this dispersed cloud could look like equation 5.2.

$$y[k] = [\ 0 \quad 0 \quad 0.1C \quad 0.2C \quad 0.5C \quad 0.1C \quad 0.1C \quad 0 \quad 0 \quad \dots\ ] \tag{5.2}$$

This response depends on the impulse concentration $C$. Since our system is linear, the output is directly proportional to the input, and so we can divide this response by $C$ to obtain the *normalised impulse response* of the system at the selected flow (equation 5.3).

$$h_{system} = [\ 0 \quad 0 \quad 0.1C \quad 0.2C \quad 0.5C \quad 0.1C \quad 0.1C\ ] \tag{5.3}$$

The interpretation of the impulse response $h_{system}$ is that any input made to the system (at the flow rate of the impulse experiment) will take two sampling periods—hence the two leading zeroes—before it starts being measured by the analyser. Also,

the measurement will be spread over five sampling periods. Note that, since the terms in the normalised impulse response of the instrument add up to unity, this linear transformation has no effect upon the total pollutant mass measured (mass, as would be expected, is conserved throughout the system). In signal processing terms, the system behaves as a *pure delay* coupled to a *low-pass filter*, because it responds to the sudden (high-frequency) variations in the input by producing a delayed, smoothed output (figure 5.2).

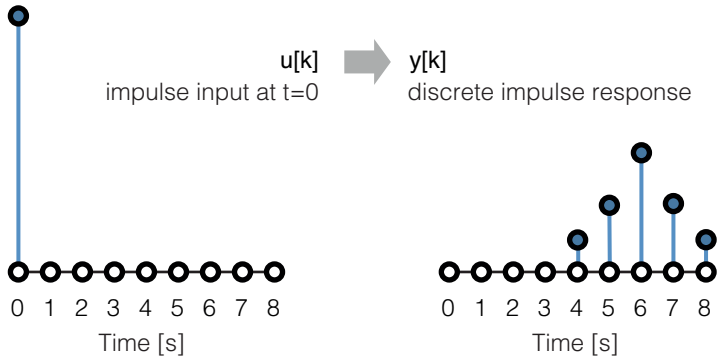


**Figure 5.2:** Example discrete impulse response of a linear system (pure delay coupled to a low-pass filter)

#### *5.2.1.2 Discrete convolution*

The importance of the result of impulse experiments lies in the fact that it is possible to construct any input signal as a sum of scaled, delayed impulses, and therefore *we can predict the output of any input as a sum of scaled, delayed instances of the impulse response*. For instance, the discrete input signal $u_{example}[k] = [\ 0.5\ \ 2\ \ 1\ ]$ can be constructed according to equation 5.4.

$$u_{example}[k] = \ 0.5 \cdot [\delta_0] + 2 \cdot [\delta_1] + [\delta_2] \tag{5.4}$$

In equation 5.4, $\delta_i$ is a unit impulse (impulse of value equal to one[5]) at instant $k = i$. Thus, by virtue of the additivity property of linear systems (see section 3.1.2.3), we would observe the corresponding output signal $y_{example}[k]$ (equation 5.5).

$$y_{example}[k] = \ 0.5{\cdot}h_{system}[0] + 2{\cdot}h_{system}[1] + h_{system}[2] \tag{5.5}$$

In equation 5.5, $h_{system}[i]$ is the impulse response of the system delayed by $k = i$ sampling periods. To put it in signal processing terms, the output signal is produced by *convolution* of the input signal with the known, time-invariant impulse response $h_{system}$. Convolution is defined in both the discrete and the continuous domain. Since the compensation method we are proposing is applied to discrete signals, the focus will be placed on *discrete convolution*. This operation—customarily denoted by an asterisk—is defined in equation 5.6.

$$y[k] = \sum_{i=-\infty}^{\infty} u[i] \cdot h_{system}[k - i] \tag{5.6}$$

Convolution is the time-domain equivalent of filtering in the frequency domain. Similarly, the impulse response is analogous to the transfer function of a linear system. A linear digital filter can be implemented by convolving its impulse response with the desired input signal (equation 5.7). In this context, the impulse response is often called the *filter kernel*. When there are several sub-systems in series, the impulse response of the aggregate system will be the convolution of the impulse responses of all the constituting sub-systems. A further advantage of discrete convolution is that it can be computed rather efficiently. Moreover, the terms of the impulse response have an easy physical interpretation (more zeros to the left mean higher delays, and the dispersion of the coefficients is associated with the degree of mixing).

$$y[k] = u[k] * h_{system} \tag{5.7}$$

As pointed out earlier, measuring the impulse response of a vehicle emissions measurement setup would be impractical. Instead of trying to experimentally

[5]The delta function is a normalised impulse; all of its samples have a value of zero, except for sample number zero, which has a value of one (Smith 1997).

characterise the behaviour of the system, we will take advantage of the simplicity of discrete signal convolution and the properties of the impulse response to compute modified instances of the diluted signal and subsequently compare them to the reference signal. The computation of the modified signals (as explained in detail in section 5.4) will be done by applying two different types of filter kernels (time shifts and high-pass filters) that plausibly compensate the distortions introduced by the system (which behaves as a flow-dependent pure delay coupled to a flow-dependent low-pass filter). Since we will be computing many modified instances of the original signal, we will need a systematic approach for comparing them to the reference. This approach is a special type of *signal binning*, which is explained in the next section.

### 5.2.2 Signal binning

Once the modified instances of the original signal are computed, we need to assess their similarity with the reference. This evaluation is performed neither over the complete signal nor for individual points, but rather taking a *small piece* of the signal at a time. We will thus need to split the signals in small data portions in a process known as *data binning*. In data analysis applications, data binning is a frequent strategy used to filter the measurement noise that may affect individual observations. In our case, we will bin every signal using the same binning strategy, and compare individual bins of the modified signals to the corresponding bin of the reference signal.

There is more than one way to create the data bins. For example, if we have a discrete signal vector of size $n = 5$ such as the following:

$$y[k] = [\ y_1 \quad y_2 \quad y_3 \quad y_4 \quad y_5\ ]$$

we could choose to bin it with a fixed bin size of $b_{size} = 2$ to yield two data bins:

$$b_1 = [\ \ y_1 \quad y_2\ \ ] \qquad b_2 = [\ \ y_3 \quad y_4\ \ ]$$

This would be an acceptable way of binning our data, but it seems somewhat wasteful: since each data point is used only once, this binning method only produces $n/b_{size}$ usable data bins (and this only at best, because some data points at the

extremes of the data set can be left out, as was $y[5]$ in the example). However, if we choose to allow individual points to fall into more than one bin, we can bin our data by selecting a fixed bin size and shifting it along the whole dataset to produce 'rolling bins' instead. If we do this to the example vector while maintaining the initial bin size $b_{size} = 2$, our rolling data bins $b_{r,i}$ would look as follows:

$$b_{r,1} = \begin{bmatrix} y_1 & y_2 \end{bmatrix} \quad b_{r,2} = \begin{bmatrix} y_2 & y_3 \end{bmatrix}$$
$$b_{r,3} = \begin{bmatrix} y_3 & y_4 \end{bmatrix} \quad b_{r,4} = \begin{bmatrix} y_4 & y_5 \end{bmatrix}$$

With this binning strategy, we can now produce $n - b_{size} + 1$ bins. For long datasets such as the ones we will be working on for real applications of the method, this translates into roughly $b_{size}$ times more bins than with the standard binning method. The rolling bins of fixed bin size can be easily implemented in MATLAB® by using the example code given in snippet *i*.

MATLAB®code snippet *i*: computation of rolling bins

```
function [binned_signal] = moving_bins(input_signal,bin_size)
%The input signal is binned and a matrix of the bins
%in columns is %returned. The binning method uses "rolling
%bins" of fixed size = bin_size.

%Computation of the number of bins
%(bins are columns in the matrices) for binned data.
data_size=size(input_signal,1);
number_of_bins=data_size-bin_size+1;

% Binning of the input signal
binned_signal=zeros(bin_size,number_of_bins);
    for i=1:number_of_bins
    binned_signal(:,i)=input_signal(i:i+bin_size-1);
    end
end
```

A minor disadvantage of the rolling data bins is that not every data point enters the same number of bins: the points in the middle section of the data vectors will be part of $b_{size}$ number of bins, whereas the points at the edges will be part of fewer bins (see figure 5.3). This can be fixed by padding the signals with zeros at both ends before the binning process.

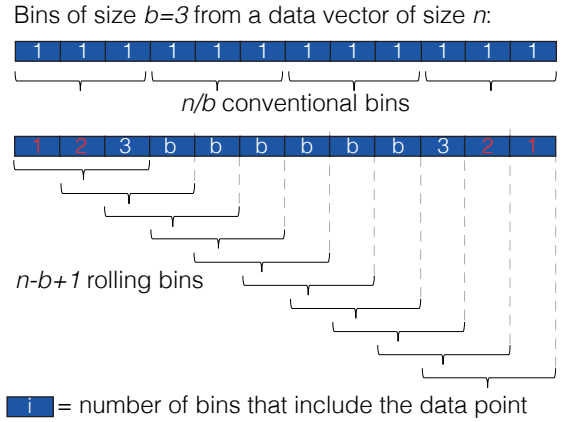


**Figure 5.3:** Illustration of 'edge effects' in the production of rolling data bins

## 5.3 Experimental method

The $CO_2$ tracer method for the compensation of instantaneous emission signals relies mostly on data post-processing, and therefore the description of the experimental method found in this section is rather brief. An important characteristic of the compensation method is that it does not require the generation of special inputs (*e.g.*, impulses or steps; see section 4.3.2 on page 82). Instead, the necessary signals are produced as the vehicle is tested normally (*e.g.*, over standard transient driving cycles such as NEDC or CADC). This is a major advantage of the tracer gas approach, as it significantly reduces the experimental work necessary for calibrating the compensation algorithm and enables the compensation of past measurements provided that a suitable reference signal is available.

### 5.3.1 Instantaneous fuel consumption measurement

As pointed out in section 5.1.1, selecting $CO_2$ as the tracer gas for the distortions that should be compensated makes it is possible to derive a calculated 'engine-out' instantaneous mass $CO_2$ signal from a instantaneous fuel consumption (FC) signal measured with a fuel flow meter (figure 5.4).[6] Since the *fuel flow* measurement happens before combustion, the resulting FC signal is unaffected by variable transport times within the exhaust system of the test vehicle. Moreover, the derivation of such a signal *does not require an exhaust flow measurement* (see section 5.4.1.2).

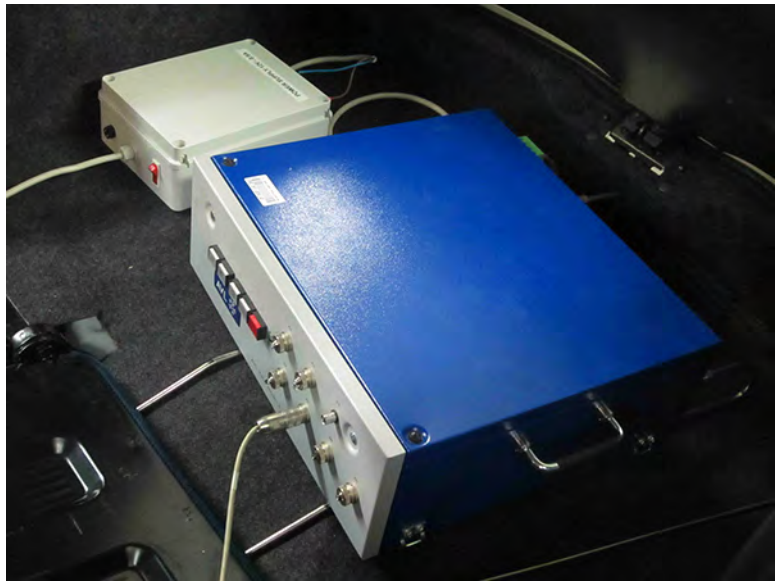

**Figure 5.4:** Portable FC meter mounted inside the cabin of a passenger car

[6] During the experimental campaign carried out at the VELA 1 laboratory of EC–JRC for the development of the $CO_2$ tracer method, a portable instantaneous FC meter was used. The details of this experimental campaign—including the technical specifications of the reference instrument—are given in the next chapter, *Results and discussion*.

## 5.4 Signal post-processing method

The compensation of the signals is performed off-line in a computer environment.[7] after the emission measurements have been performed, thus preserving the original signals. The method takes two instantaneous $CO_2$ *mass emission signals* as input. Of these signals, one (which is assumed to be less affected by the distortions discussed in chapter 3) is taken as a reference and is left unchanged throughout the process, while the other (which is the ordinary signal produced by the emissions measurement setup) is transformed by discrete convolution filters (*cf.* section 5.2.1.2).

The compensation of the original mass $CO_2$ emission signal takes place as a three-stage process (figure 5.5). The first two compensation stages take care of the misalignment between the peaks due to the transport time between the engine-out and the measurement point, and the third aims to compensate the effects of gas mixing. The compensation parameters that yield an optimal compensation of the original signal (in terms of similarity to the reference signal) are subsequently applied to the 'blind' pollutants (*i.e.*, pollutants for which no reference signal is available). The 'blind' compensation is based on the assumption that, since all gaseous pollutants are transported together within the measurement setup, they are dynamically delayed and mixed in the same way.

[7] The implementation of the method as a standalone software tool is presented in chapter 6, *Results and discussion* For the sake of clarity, MATLAB® code snippets are provided in some cases (individual implementations of the method can be coded in other programming languages).

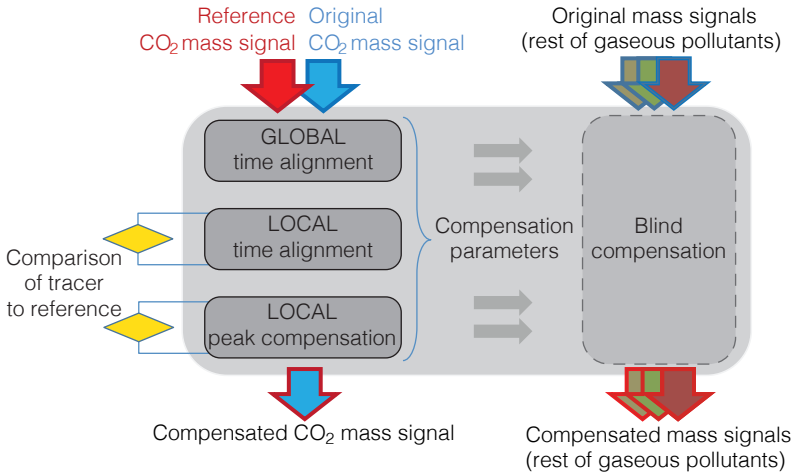


**Figure 5.5:** General scheme of the $CO_2$ tracer method

### 5.4.1 Derivation of mass signals

A critical difference between the $CO_2$ tracer and the systems theory approach is that the former works with pollutant *mass signals*, while the latter uses *concentration signals*. This has significant implications in the operation either method. A positive consequence of the use of mass signals in the $CO_2$ tracer method is that it produces results which are directly relevant to engine mapping (since engine emission maps normally predict pollutant mass emissions, not concentrations). A limitation of the use of mass signals for the $CO_2$ tracer method is that this approach will only be applicable between two points where mass emission signals can be effectively derived.

The instantaneous mass emissions of a pollutant are not measured by vehicle emission measurement equipment directly within the gas flow. Rather, chemical analysers are used to measure instantaneous pollutant concentrations $C$ (in ppm or other volume concentration units, such as percentage concentration), while separate instruments (such as Venturi flow meters or Pitot tubes) determine a volume flow $Q$ (in cubic metres per minute or other volume flow units). Whenever we have these two signals at the same measurement location, it will be possible to determine a mass flow by pointwise multiplication (*cf.* section 3.2.1.1).

#### 5.4.1.1 Derivation of the original $CO_2$ signal

The derivation of the original mass $CO_2$ signal is easy for *diluted measurements*. Since flow is quasi-steady at the dilution tunnel, the derivation of the mass signals is almost insensitive to misalignments between the flow and the concentration signals (*i.e.*, primary misalignments). Vehicle emissions test benches automatically report mass emission signals derived as a multiplication of the quasi-steady, measured flow and the concentration signals recorded by the analysers. The mass $CO_2$ signal can be used directly as input to the compensation process. For *raw measurements* or PEMS, special care should be observed to ensure that the recorded concentration and flow signals are properly aligned before the mass signals are derived.

#### 5.4.1.2 Derivation of the reference $CO_2$ signal

Since we are using $CO_2$ as our tracer gas, we have the possibility of using an *instantaneous fuel consumption meter* as our reference instrument. Fuel consumption meters perform both a volumetric (with temperature correction) and a gravimetric instantaneous measurement of fuel consumption *before the fuel rail*, and therefore before combustion. The measured instantaneous fuel consumption signal is thus independent of air flow (which is a complicated measurement to perform, *cf.* section 3.1.1.1), and is physically very close to the engine-out point.

The derivation of the reference mass $CO_2$ signal—which is intrinsically unaffected by gas mixing of variable transport times—from an instantaneous fuel consumption measurement is very straightforward: knowing the carbon content[8] (weight fraction) of the fuel $w_C$, and assuming that all the elemental carbon present in the fuel is transformed to $CO_2$ during combustion, the mass emissions of $CO_2$ can be estimated using equation 5.8 (in which $M_C$ and $M_{CO_2}$ are the atomic mass of elemental carbon and the molecular mass of $CO_2$).

$$[CO_2] = [FC] \cdot w_C \cdot \frac{M_{CO_2}}{M_C} \tag{5.8}$$

[8] If the carbon content of the fuel used is not known, we can simply scale the fuel consumption signal $[FC]$ until the sum of the scaled signal matches the sum of the diluted $CO_2$ mass measured, which is a reliable aggregated value.

### 5.4.2 Global alignment

One of the first steps of the $CO_2$ tracer method is to take the reference and the original $CO_2$ mass signals and perform a *global time alignment* between them. This can be easily accomplished with a cross-correlation check (*cf.* section 4.1.4.3). In this step, the signals are also trimmed to have the same length. The MATLAB® function in code snippet *ii* performs these tasks for two given signals.

MATLAB®code snippet *ii*: global alignment function

```
function [alignment_shift,maximum_correlation,alignment_margin, ...
signal_A_aligned,signal_B_aligned,correlation_vector] =...
alignment_function(signal_A,signal_B)
%— The function performs a cross—correlation alignment.
%— Signal_A is brought to the same time reference as signal_B,
%— Maximum correlation is sought for the first 20% of values
size_A=max(size(signal_A));
size_B=max(size(signal_B));
size_max=max(size_A,size_B);
size_difference=abs(size_A—size_B);
alignment_margin=floor(0.20*max(size_max));

if size_A>size_B %We make sure both signals have the same size
    signal_B_temp=zeros(size_B+size_difference,1);
    %signal B is zero—padded to the right to match the size of signal A
    signal_B_temp(1:end—size_difference)=signal_B;
    signal_B=signal_B_temp;
elseif size_A<size_B
    signal_A_temp=zeros(size_A+size_difference,1);
    %signal A is zeros—padded to the right to match the size of signal B
    signal_A_temp(1:end—size_difference)=signal_A;
    signal_A=signal_A_temp;
end

signal_A=side_pad(signal_A,alignment_margin);
%signal_A (signal that is time—shifted) is padded with
%'alignment margin' zeros at both beginning and end

%Correlation test: we shift signal A over signal B (which remains fixed)
for i=0:2*alignment_margin
    coef=corrcoef(signal_B(1:end),signal_A(1+i:end—2*alignment_margin+i));
    coef=coef(1,2);%element (1,2) is the correlation coefficient
    correlation_vector(i+1)=coef;
end
```

```
%Results of correlation test
[maximum_correlation,alignment_shift]=max(correlation_vector);
alignment_shift=alignment_margin-alignment_shift+1;
%alignment_shift is the optimal shift between A and B
signal_A_aligned=...
signal_A(1+alignment_shift_internal:end+alignment_shift_internal- ...
2*alignment_margin-1);
signal_B_aligned=signal_B;
end
```

In some cases, the reference signal and the original signal may have different sampling rates. It is then necessary to 'up-sample' the signal with the lower sampling rate to the sampling rate of the other.[9] In the application of the methodology presented in this chapter, the original signal was up-sampled from 1 to 5 Hz to match the resolution of the reference signal. Note that up-sampling a signal to have an artificially higher sampling rate does not increase the amount information that the signal provides, but it is and advantage for the global alignment process considering that the signals are discrete and therefore *the resolution of the incremental time shifts is only as fine as the sampling rate*.

The $CO_2$ tracer approach does not require a common time reference (or 'clock' signal) for the reference signal (the input) and the original signal (the output). Instead, the original signals are brought to the engine-out time reference by aligning the reference and the original $CO_2$ signal. In doing so, the *mean delay* between the two signals is removed. This mean delay is the sum of the systematic time delays (*i.e.*, those produced by the sections of the measurement setup where flow is quasi-steady; see table 3.3 on page 56) *and* the mean variable delay (*i.e.*, the sum of the mean delays produced by sections of the measurement setup where flow is largely variable with time, such as the raw gas line).

Once the alignment is performed, we will have two mass signals that appear very similar when plotted on the same graph. This is done in figure 5.6, where the diluted mass $CO_2$ signal reported by the analyser bench sampling at the end of the dilution tunnel of the VELA 1 laboratory during a CADC cycle run is plotted along with the reference mass $CO_2$ signal derived from an instantaneous FC measurement, after both signals have been globally aligned following a cross-correlation check.

[9] Performing this operation in MATLAB® becomes trivial thanks to the `resample` function.

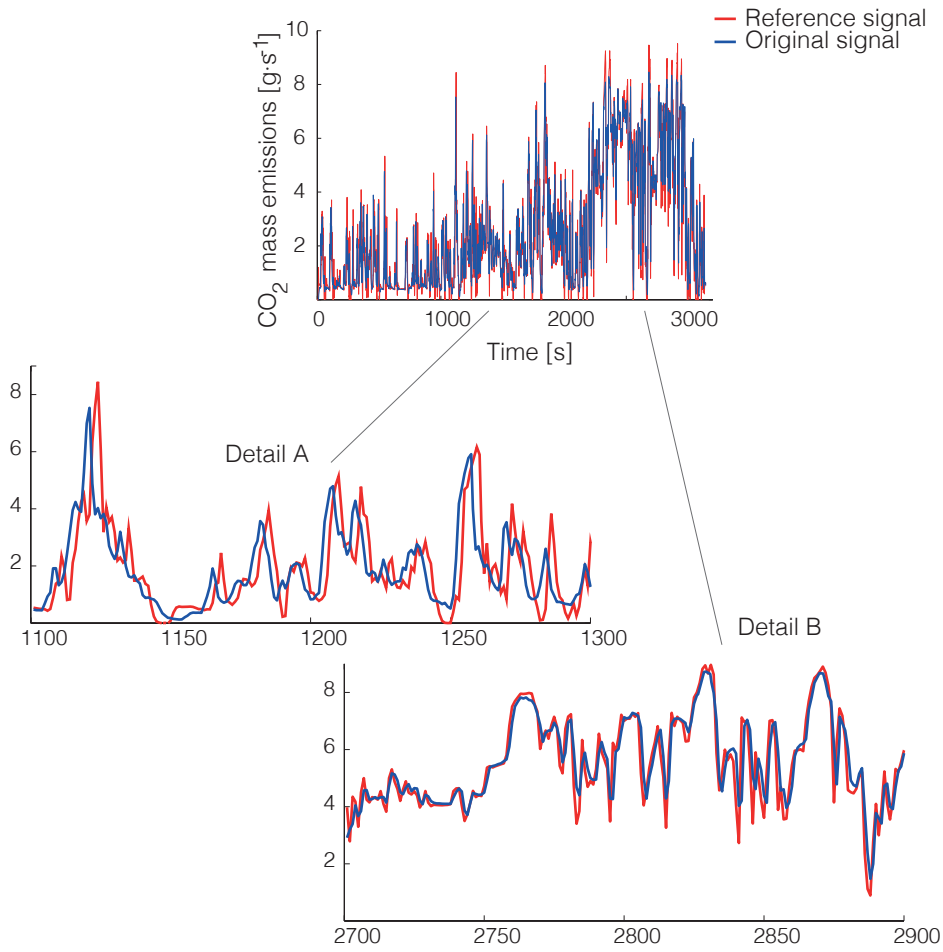


**Figure 5.6:** Reference and original mass $CO_2$ signals after global alignment (the test vehicle was a gasoline Euro 3 passenger car)

Looking closely at figure 5.6, we can see that the reference and the original signal have a strong resemblance in some aspects. For example, if we compute the total mass emissions of the two signals, these should be very similar, because no mass is being lost as emissions travel from the engine-out point to the end of the dilution tunnel. On the other hand, there will also be noticeable differences among the two signals. For example, the reference signal will have a richer frequency content or, in plain language terms, it will be noticeably sharper—or 'peakier'—than the original signal. The increased 'peakiness' will be present both for high and low peaks; *i.e.*, the values of the relative maxima of the reference signal will be higher than the corresponding points of the original signal, while the minima will be lower.

If we inspect a smaller time split of the signals, we will observe that even though the initial alignment of the two signals is the best global alignment (the one that yields the highest cross-correlation considering both signals as a whole), it is *not sufficiently good to provide a good local alignment* for some peaks. These misalignments can be attributed to the variable transport times of emissions produced at different exhaust flow rates (the signal will travel faster if it is produced at a high flow rate and vice versa). An interesting consequence of the global alignment of the two signals is that, in some instances, the diluted signal will precede the reference signal, even though the former was in fact measured several seconds after the latter, several metres downstream of the engine-out point (see detail A in figure 5.6). These situations—which are consistently observed during the low-speed sections of the driving cycle—have a simple explanation: at lower vehicle speeds, the tailpipe flow is lower, and thus the transport time of the exhaust gas emitted under these circumstances will be higher than the *mean transport time* for the whole cycle. After the global alignment, the mean delay between the two signals is removed, and thus in these situations the diluted signal will appear before the reference.[10]

The plot of figure 5.6 encodes lots of interesting information. For example, it shows that the reference signal is a better data source to build an instantaneous engine emissions map from. This is because it provides a much sharper picture of how the tracer pollutant is being emitted over time. It also shows that, in spite of the effect of the distortions, the original (distorted) signal retains the basic profile of the reference signal (but is a 'blurred', dynamically delayed version of it).

[10]This effect is magnified when testing a vehicle retrofitted with a flux capacitor (DeLorean 2015).

### 5.4.3 Local alignment

By plotting the reference and the original signal together, we have seen a strong global similarity among them. However, the similarity at local level (*i.e.*, considering a few data points at a time) will not always be as good, and there will exist small misalignments between the reference and the original signal (in terms of the location of the peaks and valleys) because the diluted signal is distorted by gas mixing, variable transport times and the other effects we discussed in chapter 3. These misalignments will translate into poor local cross-correlation and a large sum of squared residuals between the two signals, and they need to be addressed through further data post-processing.

In this section, we will describe an algorithmic formulation of the process of shifting masses along the horizontal (time) axis in order to produce modified instances of the original signal. These signals will be divided in bins, and a time-aligned signal will be built by combining the optimal bins (*i.e.*, those that compensate the misalignment between each bin of the original signal and the corresponding bin of the reference signal). This time-aligned signal will have an improved local time alignment with the reference, and it will also retain the basic shape and overall mass of the original. The local alignment algorithm, which is structured as an *iterative loop*, covers the following logical steps:

A.1) The signals are prepared (padded with zeros). This is explained in section 5.4.3.1.

A.2) The original signal is run through an array of discrete convolution filters to produce time-shifted instances of itself, while the reference signal remains unchanged. This is explained in section 5.4.3.2.

A.3) The reference signal, the original signal and the time-shifted signals are binned (*i.e.*, split into smaller portions of data). For the first iteration of the algorithm, the largest bin size is selected. Each of the time-shifted bins is systematically compared with the corresponding bin of the reference signal using an appropriate measure of signal similarity. This is explained in section 5.4.3.3.

A.4) The optimal bins are selected and an aligned signal is produced as a combination of them. The position of the optimal bins is stored for later use. This process is explained in section 5.4.3.4.

A.5) The next bin size is selected, and the aligned signal is run through steps A.1 to A.4. The algorithm runs for a number of iterations equal to the number of bin sizes we select. The operation of this 'alignment loop' is explained in section 5.4.3.5.

### *5.4.3.1 Signal preparation: signal padding*

At the end of the previous section, the two mass signals were globally aligned, thereby eliminating the mean delay among them and bringing them to a common time reference (which is that of the reference signal). Later in the post-processing, we will compute several time-shifted instances of the original signal, which will be systematically compared (in a piecewise manner, or data bin to data bin) to the reference signal. As will be shown in section 5.4.3.2, the computation of the time-shifted instances of the original signal is rather simple, but it has one important limitation: the time-shifted signals can only be delayed with respect to the original, and not shifted earlier in time. This poses a problem because the misalignments that we want to compensate go both ways along the time axis.

This problem can be overcome by introducing the concept of the *alignment margin* (AM). This is a time delay of known value introduced by padding the reference signal with a given number zeros at either end. Also, in order to have matching sizes for the reference and the original signal, the latter is padded with a number of zeros equal to twice the AM at the right end. After the signals are padded, the original signal precedes the reference by a time margin that is equal to the AM (figure 5.7).

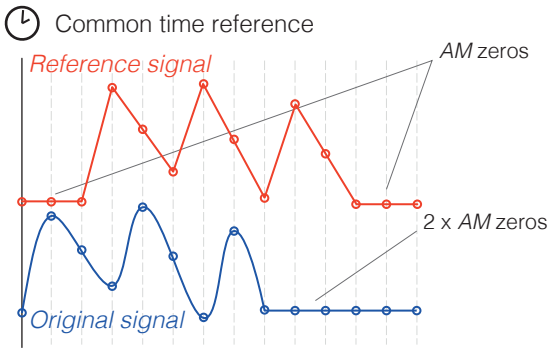


**Figure 5.7:** Signal zero-padding before post-processing

As will be shown in section 5.4.3.2, the time-shifted instances will cover each possible delay level *from no shift up to a shift equal to twice the AM*. In physical terms, the AM thus indicates how much we reasonably expect the masses to be shifted along either direction of the time axis at most. Selecting a larger AM will make the algorithm incur in higher computation times. In practice, the AM will amount to a few seconds.

#### 5.4.3.2 Computation of time-shifted signals

The computation of the time-shifted instances of the originals is made through convolution with the appropriate delay filters (see figure 5.8). From the definition of discrete convolution, it follows that a signal delayed by any desired number of time periods can be computed by simply convolving the original signal with *a vector that is composed of all zeros and a one in the position of the desired delay*. In order to cover all the delays from zero to twice the AM, we can create an identity matrix (square matrix with ones in the main diagonal and zeros elsewhere) of size equal to twice the AM. Then, the time-shifted signals can be computed by convolving the original signal with each column vector of the identity matrix (we could also use row vectors, since they are the same in this case; see MATLAB® code snippet *iii*).

MATLAB®code snippet *iii*: delay filters

```
number_of_delay_filters=2*alignment_margin;
delay_filter=eye(number_of_delay_filters);
%The eye(n) function creates a square identity matrix of nxn elements.
for i=1:number_of_delay_filters
    delayed_signal=conv(original_signal, delay_filter(:,i));
end;
```

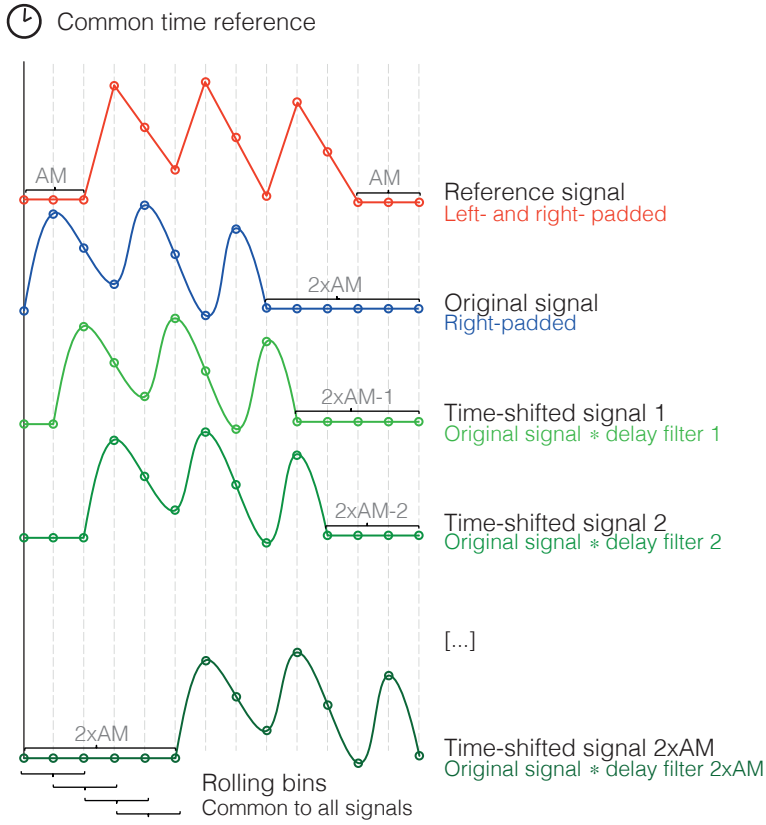


**Figure 5.8:** Computation of the time-shifted instances of the diluted signal

#### 5.4.3.3 Selection of optimal bins

Once the time-shifted instances of the original signal are computed by convolution with the delay filters and all signals are binned with the same bin size, we need to evaluate which is the optimal bin (*i.e.*, the one that resembles the corresponding bin of the reference signal the most). In order to make the comparison, we need to select a measure of signal similarity. In our case, the optimal bin will be the one with the smallest mean squared error (MSE) with respect to the reference bin. In the algorithmic implementation, we compute a normalised version.[11] of MSE by dividing the result by the average mass of the reference bin (equation 5.9).

$$MSE_{bin,\,normal} = \sum_{i=1}^{bin\ size} (bin_i - bin_{i,\,reference})^2 / \sum_{i=1}^{bin\ size} (bin_{i,\,reference}) \tag{5.9}$$

If we choose normalised MSE as our measure of signal similarity, the algorithm will select the bin that produces the smallest error as the optimal bin. By squaring the error, both positive and negative deviations are taken into account. The optimal bin is thus a bin whose overall mass is similar to that of the reference bin, and with a similar mass distribution (*i.e.*, having a similar shape). In this sense, MSE is slightly different from cross-correlation, which only takes into account the shape of the signals and is insensitive to scaling (see section 4.1.4.3 on page 75). The main advantage of MSE is that it can be computed faster than cross-correlation, thus lowering post-processing times.

#### 5.4.3.4 Computation of the aligned signal (by joining the optimal bins)

For each bin of the original signal, the algorithm evaluates the corresponding bin of each one of the delayed signals and finds the delayed bin that is optimal in the MSE sense. The data values of each one of the optimal bins are stored, and so is the delay associated with it. Since all the time-shifted signals are the same (original) signal, what we obtain from this process is a *smooth estimation* of the time shifts

[11] This normalisation does not affect the selection of the individual optimal bins and makes is possible to compare the 'optimality' among bins regardless of the mass of the corresponding reference bin.

that compensate local misalignments. In order to obtain a signal that is locally time-aligned to the reference, we simply need to join all of the optimal bins. This can be seen as a reversal of the binning process, whereby one goes from a binned signal to a discrete data vector. It is possible to estimate a value for a point of the data vector at position $k$ by scattering the optimal bins and computing the *mean value* of all the data points found in the optimal bins that correspond to that position (see figure 5.9).

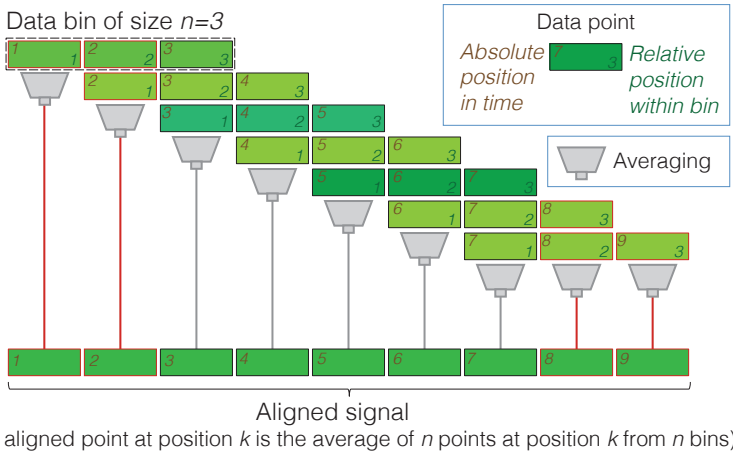


**Figure 5.9:** Reconstruction of the locally time-aligned signal from the optimal bins

Due to the 'edge effects' discussed in section 5.2.2, the number of points that produces the estimation at the edges of the reconstructed vector is smaller than at the centre. When working with large datasets, this is only a minor drawback of using rolling bins that can be overcome through appropriate programming.

#### *5.4.3.5 Alignment loop*

Once the first alignment of the signal is concluded, an aligned signal is obtained. This signal resembles the reference signal more closely than the original. The introduction of the alignment margin (AM) has an influence on the estimated local delays: a point where mass is not shifted with respect to the reference (*i.e.*, a point where the global alignment produces a satisfactory alignment) will have a shift equal to the AM.

Conversely, the time shift required to match the reference will be below the AM for faster sections of the original signal, and above the AM for slower bins.

In order to go back to the initial time reference, one can simply remove the AM and be left with an aligned signal that is compensated for local time shifts and has the same time reference as the original reference signal. This allows us to apply the alignment routine in an *iterative loop*. The key to making this approach work is to select the size of the data bins to be *proportional to the alignment margin*, and to perform the iterations in descending order of bin size (and also of AM size). In this way, the initial iterations (corresponding to large bin sizes) will compensate the delays that affect long sections of the datasets, and subsequent iterations will be able to compensate misalignments at a more local level.

After performing the compensation of local delays in the iterative loop, we obtain an aligned signal. This modified signal should improve the local time alignment with the reference while retaining the basic shape and overall mass of the original. Since all the signals are available, we can check this easily (*e.g.*, by comparing the deviations between the reference and the original signal, and between the reference and the compensated signal).

### 5.4.4 Local sharpening

By performing the compensation of the time delays, we obtained a signal that is aligned with the reference, but this alignment does not bring back the sharpness of the peaks and valleys of the signal that is lost due to gas mixing and to the (slow) response time of the analysers. This task is performed by the local 'sharpening' algorithm, which is structured according to the following logical steps:

B.1) The aligned signal that is the output of the iterative alignment process is run through an array of discrete convolution filters to produce sharpened instances of itself, while the reference signal remains unchanged. This is explained in section 5.4.4.1.

B.2) The reference signal, the aligned signal and the sharpened signals are binned using rolling data bins, just as for the local alignment. Unlike the alignment process, the sharpening process is run only once with a single bin size. Each of the sharpened instances is systematically compared with the corresponding bin of the reference signal using normalised MSE as a measure of signal similarity.

The optimal bins are selected and a final, compensated signal is produced as a combination of these, and the position of the optimal bins is stored for later use in the 'blind' reconstruction process. This process is analogous to the reconstruction of the signal explained in section 5.4.3.4 (see figure 5.9) and therefore it will not be discussed in detail.

### *5.4.4.1 Computation of sharpened signals*

As pointed out earlier, the combined effect of the mixing of the gases and the response characteristic of the $CO_2$ gas analyser acts as a low-pass filter (see figure 5.1 on page 96). We can apply discrete convolution to compensate these effects by applying several degrees of sharpening to the aligned signal. A sharpening filter (or high-pass filter) has the opposite effect of a low-pass filter. In signal processing terms, it amplifies the high frequency component of the signal. In simpler terms, it can enhance the local peaks of our signal and bring back some of the details lost due to the aforementioned distortions.

Discrete sharpening filters can be built in a straightforward manner by selecting a symmetrical kernel with an odd number of values featuring a high central value, surrounded by increasingly small values, which can even be negative at the edges. Also, we have to make sure that the values of the kernel add up to unity in order to have steady state gain (*i.e.*, in order not to add or subtract mass from the signals during the sharpening process). MATLAB® snippet *iv* produces a matrix of such sharpening filters (with three-element kernels). With this simple implementation, the level of sharpening may thus be controlled by a single parameter; higher values of $a$ (or 'sharpening level') will bring about increased levels of sharpening whilst preserving overall mass.[12]

[12] Overall mass will be preserved for any positive value of the 'sharpening level' $a$ However, very large values will lead to extremely high peaks and extremely low valleys, causing the sharpened signal to *undershoot* (adopt negative values) in some regions. Since negative values make no physical sense for a mass emission signal, sharpening levels should be conservatively estimated.

MATLAB®code snippet *iv*: 'high-pass' sharpening filters

```
%Matrix of sharpening filter kernels of size=3
%The basic shape of the symmetrical filter is [—a, 1+2a, —a]:
    %—Higher a's  will increase the level of sharpening
    %—Unity static gain is automatically satisfied
kernel_size=3;%must be an odd number
sharp_filter_step=0.1; %a finer step will produce more sharpening levels
sharp_filter_a_max=3; %controls the maximum allowable sharpening
a_filter=0:sharp_filter_step:sharp_filter_a_max;
sharp_filter=zeros(size((a_filter),2),kernel_size);
number_of_sharpening_filters=size((a_filter),2);
for i=1:number_of_sharpening_filters;
    sharp_filter(i,:)=[—a_filter(i);1+2*a_filter(i);—a_filter(i)];
    %Matrix of sharpening filters
end
for i=1:number_of_sharpening_filters
    sharpened_signal=conv(original_signal, sharp_filter(:,i));
end;
```

#### 5.4.4.2 *New selection of optimal bins and computation of the compensated signal*

Once the sharpened instances of the original signal are computed by convolution with the sharpening (high-pass) filters and all signals are binned with the same bin size, the optimal bin can be identified as was done during the alignment process. In the implementation of the algorithm, MSE was also chosen as the measure of signal similarity at this stage. The binning and selection of the optimal bins is analogous to the procedure followed in the alignment loop (see figure 5.10).

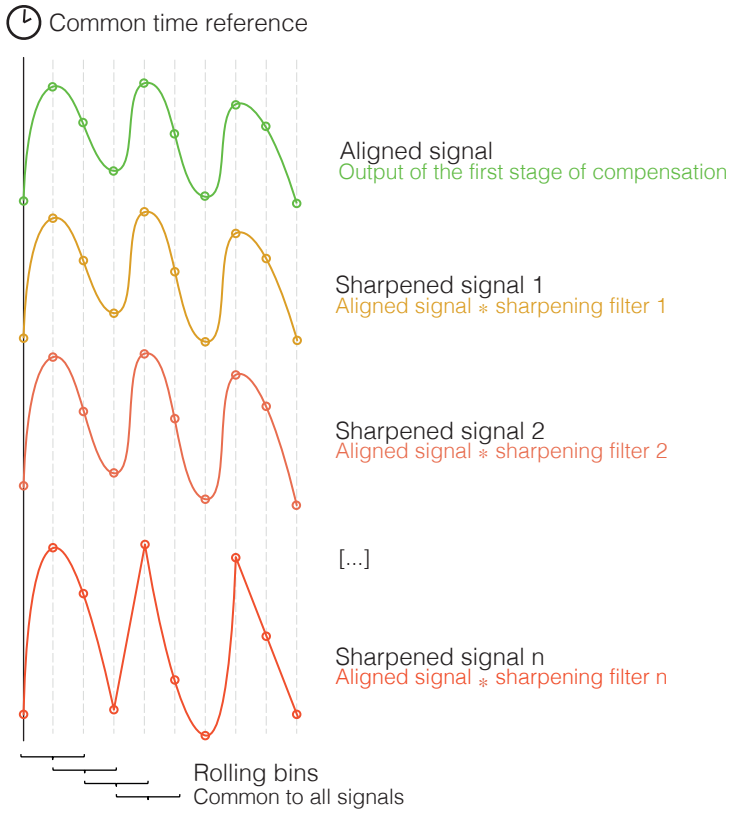


**Figure 5.10:** Computation of the sharpened instances of the aligned signal

### 5.4.5 Blind compensation of non-tracer gaseous pollutants

Once the optimal bins are selected, the final compensated signal is produced. This is the outcome of *two separate processes* (the first for signal alignment and the second for signal sharpening). The compensated signal will be very similar to the reference, be it in terms of total mass, local alignment or sharpness of signal features. This improvement of the compensated signal with respect to the original, distorted signal is an indication that the compensation process was successful, but compensating the $CO_2$ signal is not our intent because *we already have a reference signal for the tracer pollutant signal!*

The useful output of the alignment and sharpening processes is *the optimal time shift and sharpening level that is applied to each data bin during the compensation of the original mass $CO_2$ signal*. These values—which characterise how the system behaved throughout the test—are stored by the algorithm so they can be applied 'blindly' to other mass emission signals for which there is no reference. Thus, the compensation of these *non-tracer* mass emission signals is as simple as taking the diluted mass signal that we want to compensate as the input to the algorithm instead of the $CO_2$ signal, and applying the values that were previously stored during the compensation of the tracer. This will be done in the next chapter, *Results and discussion*, where we will demonstrate the application of the $CO_2$ tracer method to vehicle emission datasets gathered from real tests in a chassis dynamometer laboratory.

### 5.4.6 Summary

In this chapter, we have presented a comprehensive methodology for the compensation of instantaneous emission signals. The $CO_2$ tracer method—which was entirely developed within the Sustainable Transport Unit (STU) of the EC–JRC—relies on data post-processing to model and compensate the distortions introduced by the variable transport times and gas mixing within the measurement setup. The data post-processing sequence of the method is summarised in table 5.1.

**Table 5.1:** Summary of the data post-processing sequence of the $CO_2$ tracer method

| Stage | Description |
|---|---|
| Derivation and pre-processing of the reference and the original mass signals (§§ 5.4.1, 5.4.2) | • Two instantaneous mass $CO_2$ signals are derived by multiplying instantaneous concentrations and measured air flows as needed. One of the signals is the output obtained during ordinary measurements, while the other is measured closer to the engine-out point and is taken as a reference. If an instantaneous FC measurement is available, the reference signal can be derived from it.<br>• The original signal is resampled to match the (higher) sampling rate of the reference signal. The reference and the original signal are aligned via a cross-correlation check and trimmed to have matching sizes. |
| Compensation of variable time delays of the tracer signal (§ 5.4.3) | • The original signal is run through an array of discrete convolution filters to produce several time-shifted instances of itself.<br>• The reference signal, the original signal and the time-shifted instances of the original signal are binned using rolling data bins of fixed size.<br>• An aligned signal is produced by joining the optimal bins, thereby compensating the variable delays due to variations in the instantaneous exhaust flow. The optimal time-shifting filter for each data bin is stored.<br>• The alignment process is run in a loop. The size of the data bins is decreased with each iteration. |
| Compensation of peak blurring of the tracer signal (§ 5.4.4) | • The aligned signal is run through a second array of 'high-pass' filters to produce several sharpened instances of itself.<br>• The aligned signal, the reference signal and the sharpened versions of the aligned signal are binned using rolling data bins of fixed size (for each iteration).<br>• A signal is produced by joining the optimal bins, thereby compensating the peak smoothing. The optimal sharpening filter for each data bin is stored. |
| *Blind* compensation of the non-tracer signals (§ 5.4.5) | • The mass signals of 'blind' pollutants (for which there is no reference signal) are processed in the same way as the original mass $CO_2$ signal using the delay and sharpening filters stored in the previous stages. |

# Chapter 6

# Results and discussion

We have thus far investigated the distorting effects that compromise the instantaneous accuracy of the emission signals reported by vehicle emissions measurement equipment, and we have proposed a methodological framework to model and compensate them. Furthermore, we have formulated a complete signal compensation methodology, which we dubbed the *$CO_2$ tracer method*.

In this chapter, we will use this new, comprehensive methodology to perform the compensation of instantaneous vehicle emission signals obtained in a chassis dynamometer laboratory equipped with constant volume sampling. We will assess the performance of the $CO_2$ tracer method during the compensation of several datasets from different test cycles. We will also discuss the methodological choices made, and how the selection of parameters affects the compensation performance. Finally, we will present a validation of the $CO_2$ tracer method, and we will compare it to the 'systems theory' approach to instantaneous vehicle emission signal compensation.

## 6.1 Results

In this section, we will present the results of the application of the $CO_2$ tracer method to real vehicle emission datasets obtained from chassis dynamometer testing with constant volume sampling. To that avail, the emissions data from the dilution tunnel

and from the reference instrument (an instantaneous fuel consumption meter) were imported to the MATLAB® environment and post-processed according to the description of the methodology described in chapter 5. Besides $CO_2$ (the tracer pollutant), the gaseous pollutants measured by the chemical analyser bench sampling from the end of the dilution tunnel included $NO_x$, CO and HC.

### 6.1.1 Experimental campaign

An *experimental campaign* was set up to collect data for the final development of the $CO_2$ tracer method.[1] The experiments were run during the second week of June, 2012 at the VELA 1 light-duty vehicle chassis dynamometer laboratory (figure 6.1) at the EC–JRC site in Ispra (Italy). The test vehicle (an Euro 3 passenger car fuelled with conventional gasoline) was instrumented with a portable instantaneous fuel consumption meter. This universal fuel measurement system can be used on the road or at the dynamometer laboratory, and it can accurately determine the instantaneous amount of fuel consumed by the vehicle under study. The most relevant characteristics of this instrument are summarised in table 6.1.

[1]The experimental campaign also involved the application of the 'systems theory' approach to model the VELA 1 laboratory. These experiments—which were performed with the invaluable assistance of Dr Savas Geivanidis from Aristotle University of Thessaloniki—required the lease of a dual-channel ultrafast $CO/CO_2$ exhaust gas analyser, the welding of two intermediate gas sampling ports between the tailpipe and the end of the dilution tunnel, the purchase of a data logger and the use of a special valve train for the generation of $CO_2$ concentration steps. The author wishes to thank Dr Savas Geivanidis and all those who made the campaign possible: Urbano Manfredi, Franz Mühlberger, Mauro Cadario and Gaston Lanappe for performing the experiments; Alexandros Nikolian and Georgios Fontaras for their assistance with practical matters; Alois Krasenbrink and Panagiota Dilara for approving the necessary funding; Yoannis Drossinos for helping me navigate the maze of procurement procedures and Mark Peckham of Cambustion Ltd. for the remote technical assistance for the ultrafast analyser. Further details on this work can be found in (Franco *et al.* 2014).

**Table 6.1:** Technical specifications of the portable fuel consumption meter

| | |
|---|---|
| Manufacturer | AVL |
| Model | KMA mobile fuel measurement system type 075 |
| Measurement principle | The flow meter combines a servo-controlled gear counter with a dynamic piston sensor. A gear meter driven by a servomotor defines a geometric volume when gear rotation is adjusted to fuel flow. Flow changes immediately displace a zero-friction piston, and this displacement is recorded by the instrument. |
| Applicable fuels | • Gasoline, standard grade, super grade fuels (leaded/unleaded) with any alcoholic admixtures<br>• Methanol, ethanol, *etc.* up to 100% blend<br>• Diesel and biodiesel |
| Measurement range* | 0.16 to 75 $l \cdot h^{-1}$ (temperature operating range from −10 to 50°C) |
| Dynamic characteristics | • Response time <125 ms (10–90% rise time)<br>• Data acquisition rates up to 5 Hz |
| Measurement uncertainty | ±0.1% of reading (calibration intervals of up to three years) |
| Dimensions | 470 × 170 × 550 mm |
| Weight | 15 kg |
| Installation time | 30 to 60 minutes |

**Different models exist for different range applications (*e.g.*, large HDV engines)*


**Figure 6.1:** Snapshots of the experimental campaign

The test vehicle was driven by a professional test driver twice over each one of three different driving cycles (NEDC, CADC and ERMES):

- The NEDC (New European Driving Cycle) is the driving cycle used for emissions type-approval of all Euro 3 and later light-duty vehicles in Europe. Legal emission limits (expressed as amount of pollutant emitted per kilometre driven) refer to the emissions over NEDC. This is a cold-start driving cycle in which the vehicle is left to soak at room temperature for at least eight hours before it is tested. NEDC is rather mild in comparison to the dynamicity of the other cycles used in the experimental campaign (see figure 6.2).
- The CADC (Common Artemis Driving Cycle) is a so-called real-world driving cycle that aims to represent real-world driving conditions in Europe (André 2004). CADC is not used for type-approval. Instead, it was specifically designed for emissions modelling purposes. Its high dynamicity and long duration (*cf.* table 6.2) makes it more suitable than NEDC as the basis for the investigation of real-world emissions and emission factor development.
- The ERMES cycle was specifically designed within the ERMES group for vehicle emissions modelling purposes. Like CADC, this is a real-world cycle. Its shorter duration makes it suitable for time-constrained emission measurement laboratories.

**Table 6.2:** Characteristics of the test cycles of the experimental campaign

| **Cycle** | **Application** | **Duration** $[s]$ | **Distance** $[km]$ | **Mean velocity** $[km \cdot h^{-1}]$ |
|---|---|---|---|---|
| NEDC | Type-approval (Europe) | 1180 | 11.02 | 33.6 |
| CADC | Real-world emissions modelling | 3143 | 50.89 | 58.3 |
| ERMES | Real-world emissions modelling | 1280 | 24.29 | 68.3 |

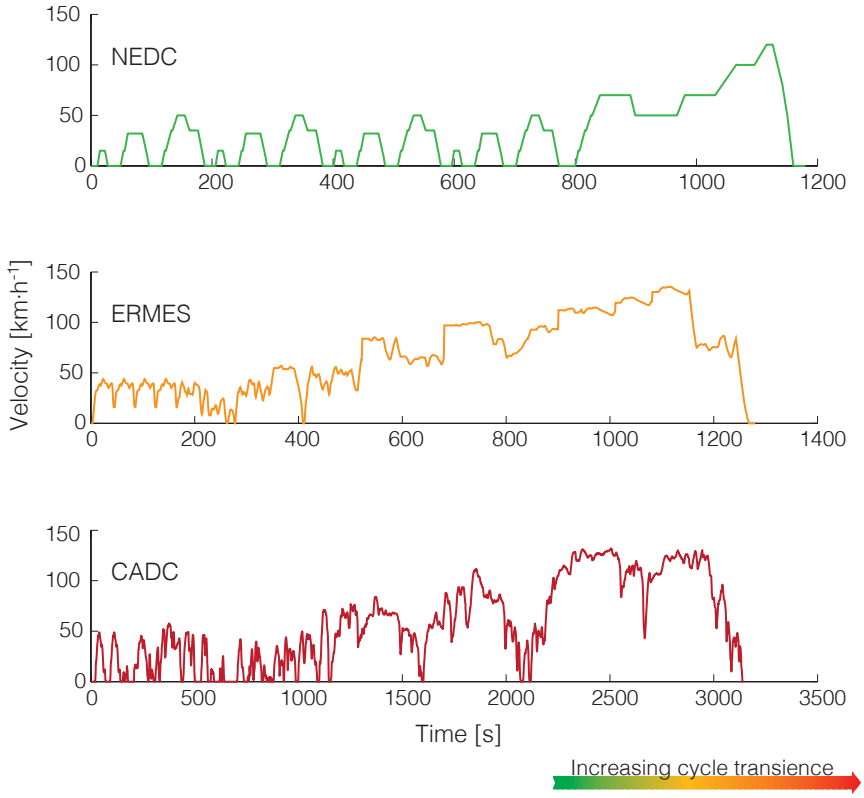


**Figure 6.2:** Driving cycles of the experimental campaign

### 6.1.2 Compensation of the tracer pollutant

The diluted mass signal of $CO_2$—the tracer pollutant—was compensated in each case using the instantaneous signal from the fuel consumption meter as a reference. The values for the parameter of the compensation algorithm are listed in table 6.3. The results of this compensation process are presented as scatterplots for all the experimental datasets in figure 6.3. Additionally, for one instance of the three test cycles, the signals are graphically represented as time sequences in figures 6.4a to 6.4c.[2] At the top of these figures, the mass $CO_2$ signals are plotted over the whole cycle:

- *Reference* represents the mass $CO_2$ signal derived from the instantaneous FC signal (assuming that all the carbon in the fuel is transformed into $CO_2$ during combustion).
- *Original (diluted)* represents the mass $CO_2$ signal reported by the analyser at the diluted measurement point (*i.e.*, the end of the dilution tunnel), globally aligned to the reference signal via a cross-correlation check.
- *Aligned* represents the signal resulting from the application of the local alignment process (first stage of the compensation process described in section 5.4.3) to the original signal.
- *Aligned + sharpened* represents the signal resulting from the application of both the local alignment and the local sharpening process (full, two-stage compensation).

[2] Four close-up views of selected cycle regions (covering both high- and low-flow operation) are also provided for easier visualisation.

**Table 6.3:** Details of the compensation process of the experimental datasets

| | |
|---|---|
| **General** | |
| Input signals | • Reference signal: instantaneous FC signal at 5 Hz, scaled to match diluted $CO_2$ mass measured at the dilution tunnel.*<br>• Original signal: mass $CO_2$ signal reported by diluted analyser bench, up-sampled from 1 to 5 Hz.<br>• *Blind* pollutant signals: $NO_x$, CO and HC signals reported by diluted analyser bench, up-sampled from 1 to 5 Hz.<br>• Flow signal: OBD engine load signal, scaled to match tailpipe air mass flow reported by dilution tunnel.† |
| **Local alignment** | |
| Number of alignment runs | 5 (performed in descending bin size order) |
| Bin sizes for each run | [160, 80, 40, 20, 10]<br>(values in number of data points at 5 Hz) |
| Alignment margins (AM) | [80, 40, 20, 10, 5]<br>(values in number of data points at 5 Hz) |
| **Local sharpening** | |
| Number of sharpening runs | 1 |
| Bin size for sharpening run | 25 data points (5 seconds at 5 Hz) |
| Maximum allowable *a* (sharpening level) | 5 |
| **Miscellaneous** | |
| Post-processing run-time | <5 seconds per data set (each equivalent to 20-50 minutes of emissions data) on an Intel®Core 2 Duo laptop computer |

**Agreement was within 1% before scaling in all cases*

*† This is based on the assumption that engine load is proportional to engine air flow in naturally-aspirated engines. A flow signal is* not necessary *for the compensation, but is used here for validation purposes (*cf. *section 6.2.2)*

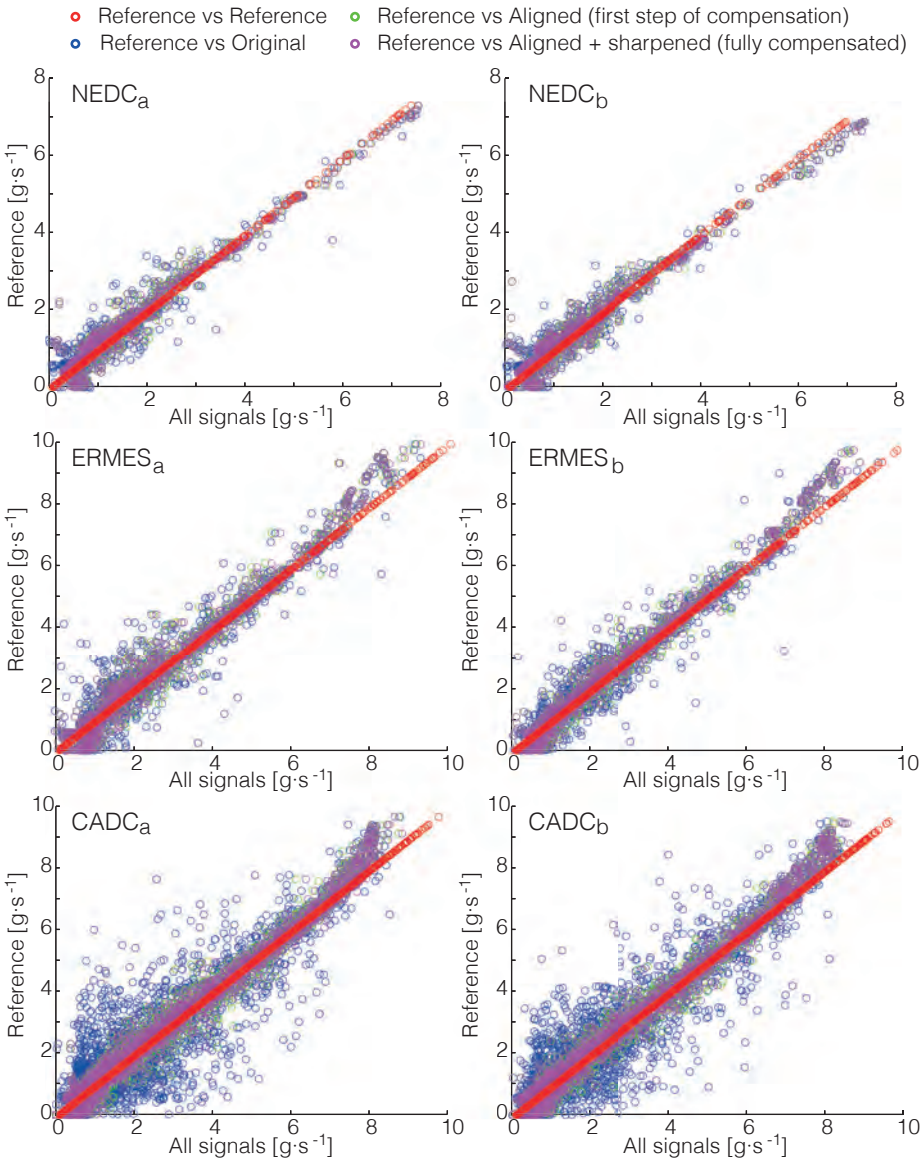


**Figure 6.3:** Scatterplots of the original, aligned and fully compensated (aligned + sharpened) $CO_2$ signals. The deviation of the original signals from the reference is most evident for the CADC datasets, as are the benefits of the compensation (all signals in g·s$^{-1}$ at 5 Hz)

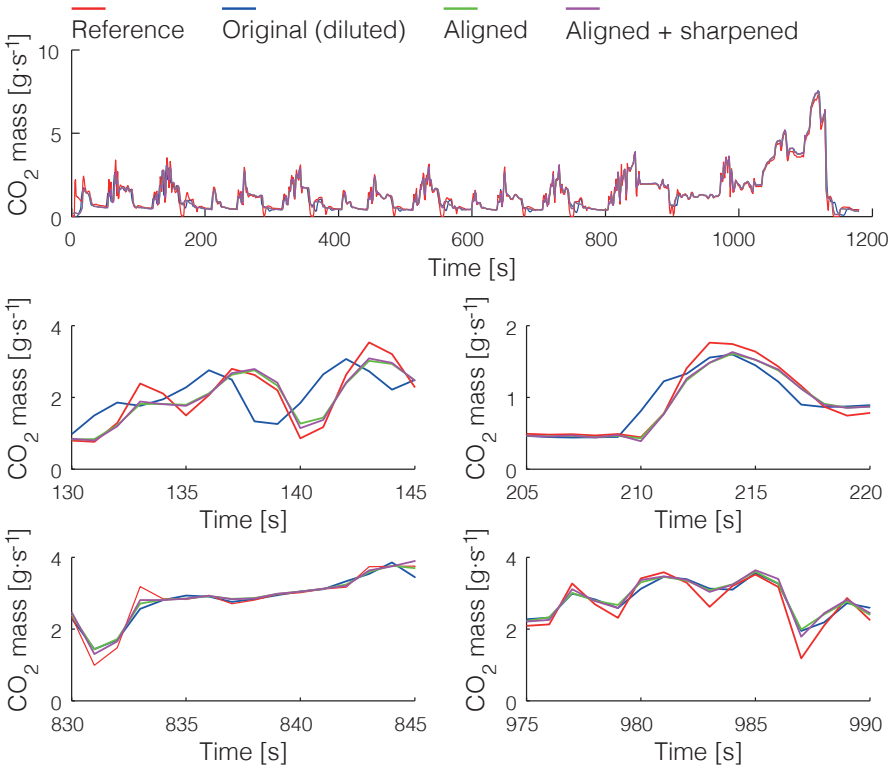


**Figure 6.4a:** Compensation of the diluted mass $CO_2$ signal ($NEDC_a$ dataset)

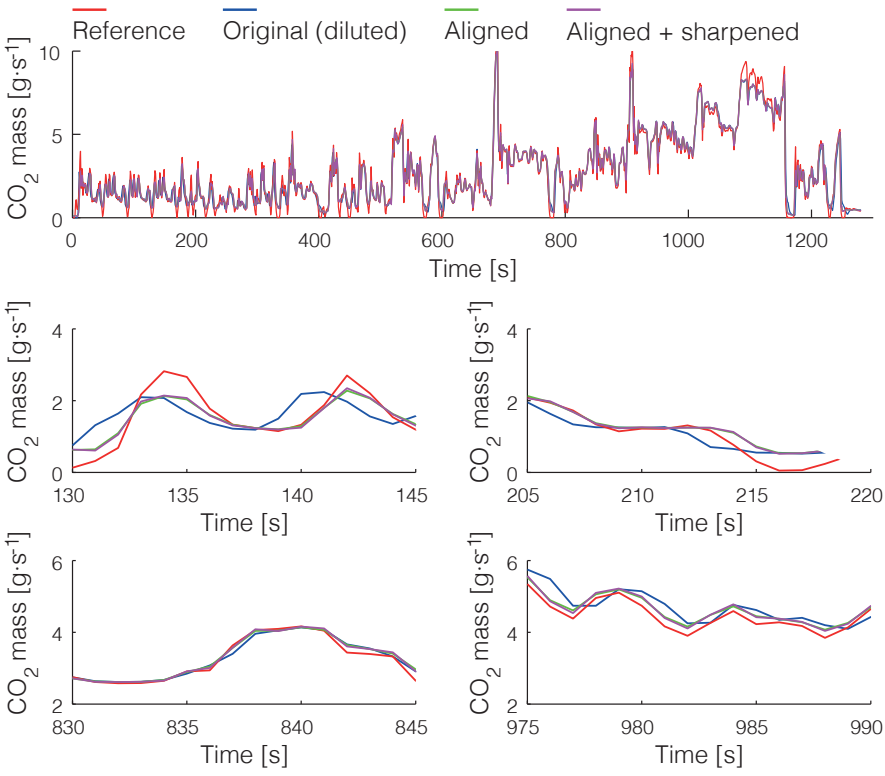


**Figure 6.4b:** Compensation of the diluted mass $CO_2$ signal ($ERMES_a$ dataset)

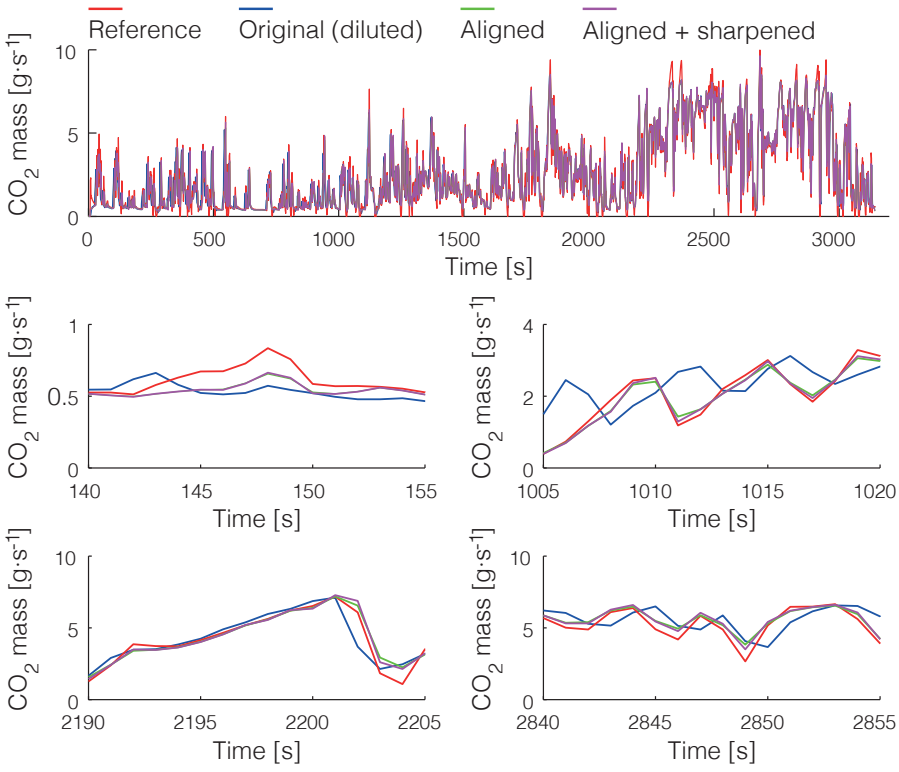


**Figure 6.4c:** Compensation of the diluted mass $CO_2$ signal ($CADC_a$ dataset)

The results of the compensation of the diluted $CO_2$ mass signal are difficult to interpret by looking at figures 6.4a to 6.4c alone: from the plots, it is apparent that the compensated signal comes closer to the reference signal after each stage of the compensation process. In order to visualise how much improvement is obtained from the compensation, a *global assessment* of the results of the compensation process is presented in figure 6.5 for all the experimental datasets. In this assessment, we present *average metrics* of signal similarity between the reference signal and the original (diluted), aligned and fully compensated signals for each dataset:

- *Cumulative squared error (over cycle)* represents the sum of squared residuals (SSR) calculated for the whole cycle as per equation 4.1 on page 75.
- *Mean absolute deviation from reference (in bins)* represents the cycle average of the vector of absolute deviations for each bin of the reference signal and the corresponding bin of the original, aligned and fully compensated signals. The absolute deviation for each bin is computed as the sum of absolute deviations (SAD) as per equation 4.2 on page 75.
- *Mean cross-correlation with reference (in bins)* represents the cycle average of the vector of cross-correlation coefficient $r$ values, calculated as per equation 4.3 on page 75, between each bin of the reference signal and the corresponding bin of the original, aligned and fully compensated signals.

Additionally, for one instance of the three test cycles, the same metrics are graphically represented as time sequences (by bin) in figures 6.6a to 6.6c to provide a *local assessment* of the results of the compensation process.[3] From figure 6.5, and also from figures 6.6a to 6.6c, we see that the similarity of the signals to the reference is improved after each stage of the compensation process. The improvement is observed for all the metrics of signal similarity and for all datasets, both globally (considering the whole signal) and locally (at data bin level). Also, most of the improvement is achieved during the first stage of the compensation process (local alignment).

[3] For easier visualisation, the results are expressed over 5-second bins, or 25-datapoint bins at 5 Hz. The original (diluted) signals were up-sampled from 1 to 5 Hz to match the sampling rate of the signal from the reference instrument.

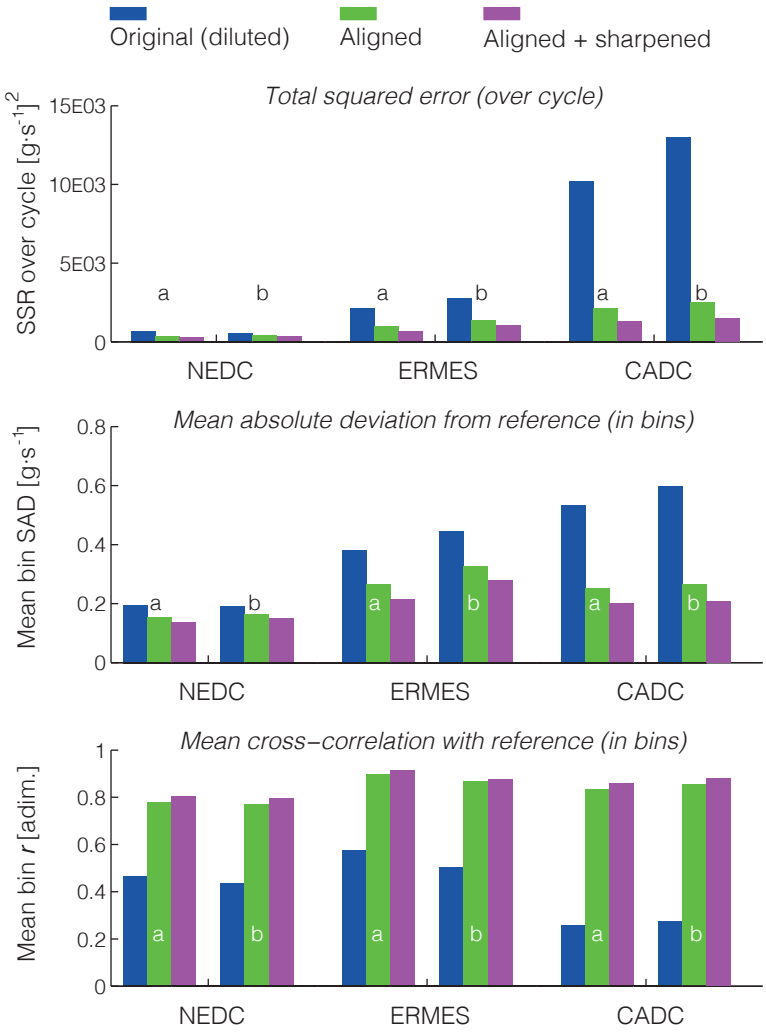


**Figure 6.5:** Global assessment of compensation at 5-second bins (all datasets)

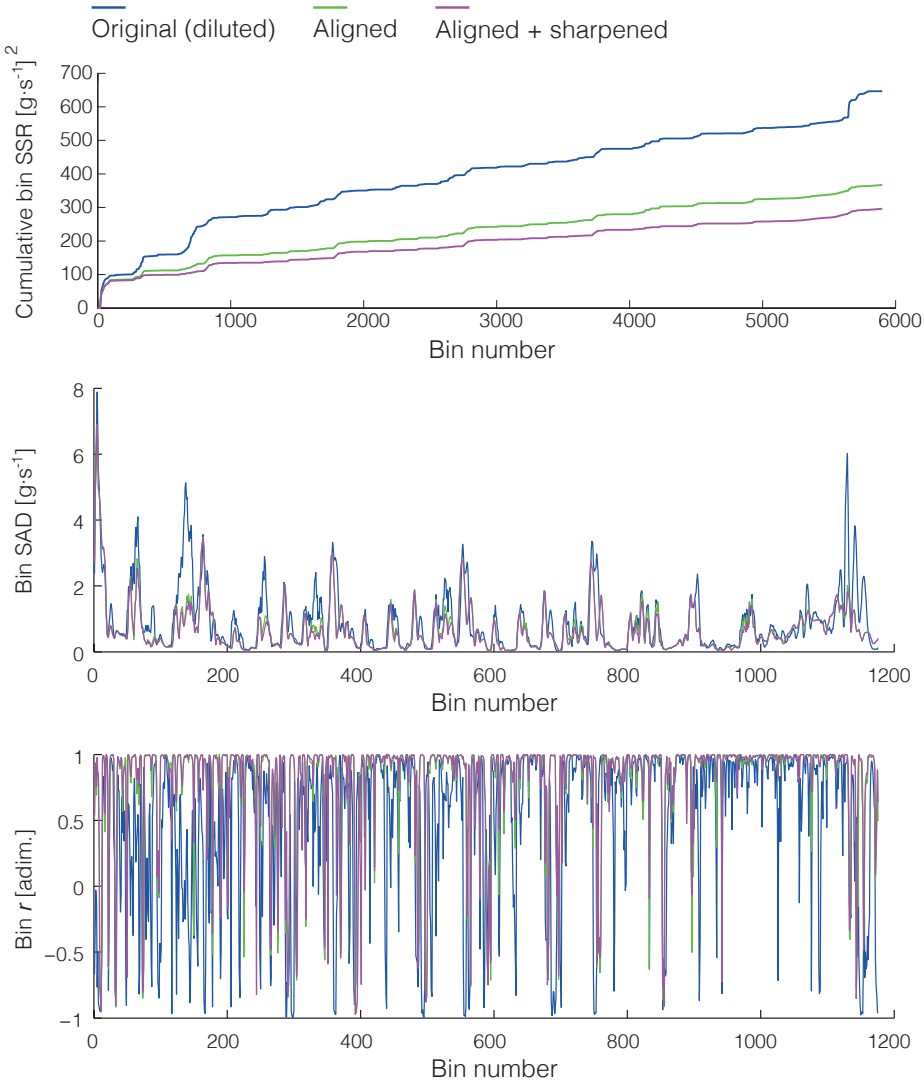


**Figure 6.6a:** Assessment of compensation of $NEDC_a$ dataset at 5-second bins

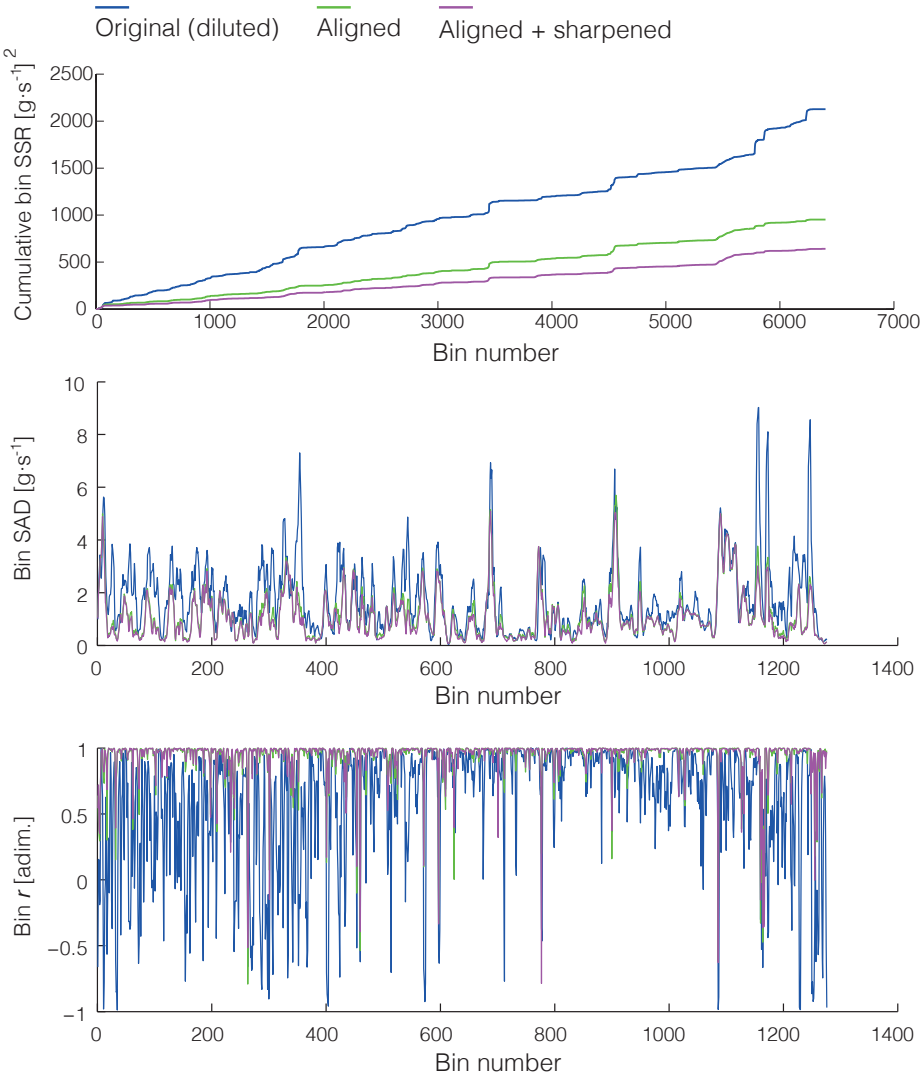


**Figure 6.6b:** Assessment of compensation of ERMES$_a$ dataset at 5-second bins

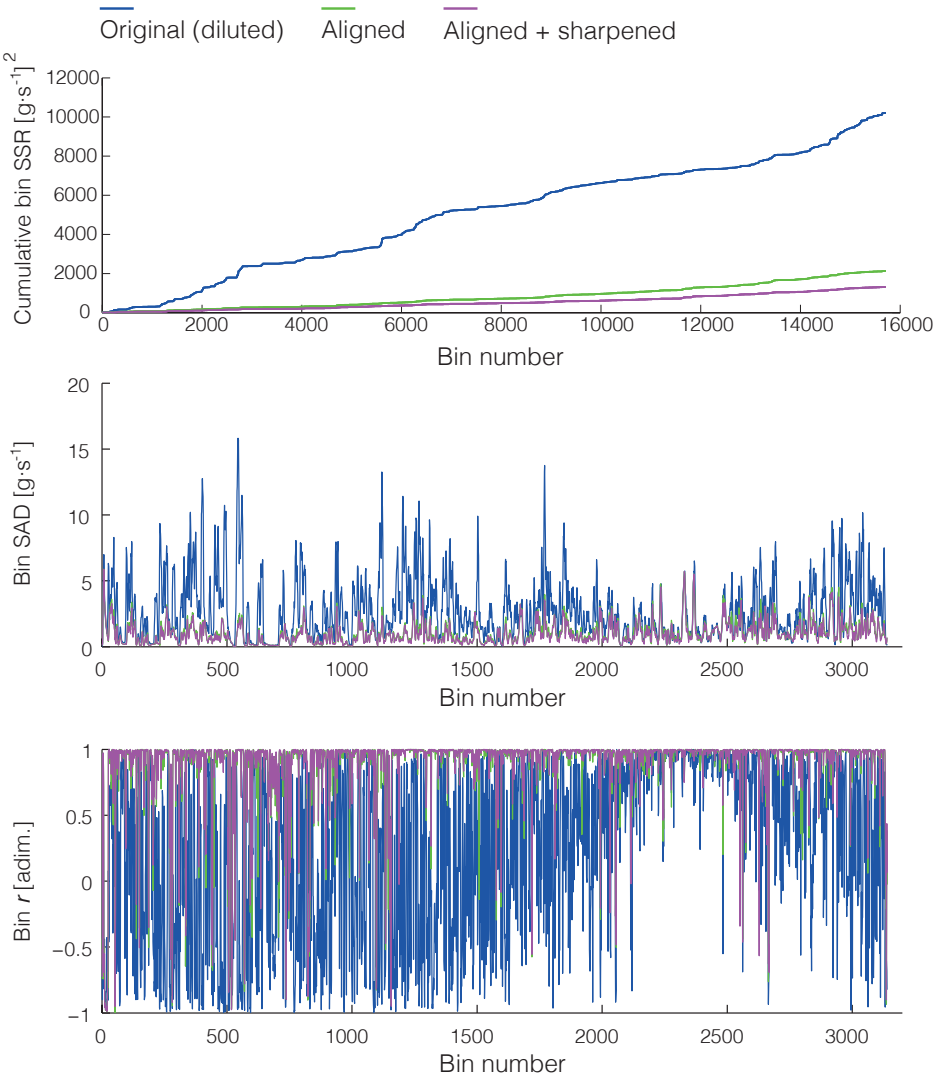


**Figure 6.6c:** Assessment of compensation of $CADC_a$ dataset at 5-second bins

### 6.1.3 Blind compensation of other pollutants

The compensation estimated from the signals of the tracer pollutant was applied blindly (*i.e.*, in absence of a reference signal) to the mass signals of $NO_x$, CO and THC that were obtained simultaneously with the $CO_2$ signal at the end of the dilution tunnel during the test cycle runs.

Figures 6.7a to 6.7c show the results of the blind compensation of the instantaneous $NO_x$ mass signals measured over one instance of each one of the three driving cycles of the experimental campaign. In these figures we can observe that the compensation methodology behaves as expected, smoothly delaying the signals in the low-flow sections of the cycles and advancing the signal in the high-flow sections. Thanks to the local application of the high-pass filters, some of the original peak sharpness is also regained.[4]

[4]This is an initial indication that the $CO_2$ tracer method can compensate the signals of 'blind' pollutants (*i.e.*, pollutants for which no reference signal is available). These results will be further investigated in the section dedicated to the validation of the methodology (section 6.2.2 on pp. 154—167).

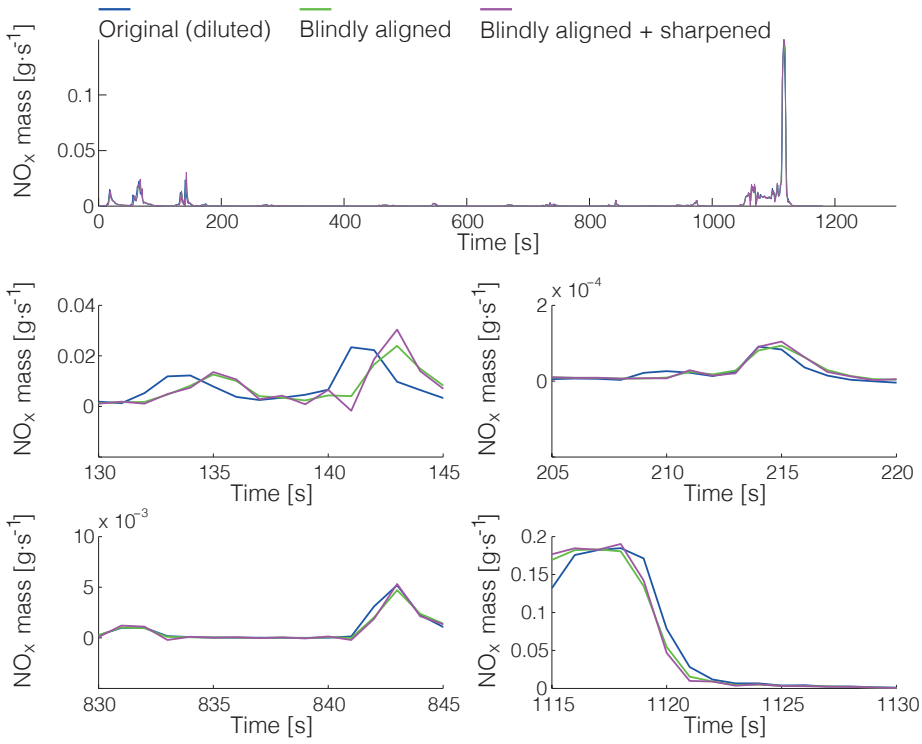


**Figure 6.7a:** Blind compensation of the diluted mass $NO_x$ signal ($NEDC_a$ dataset)

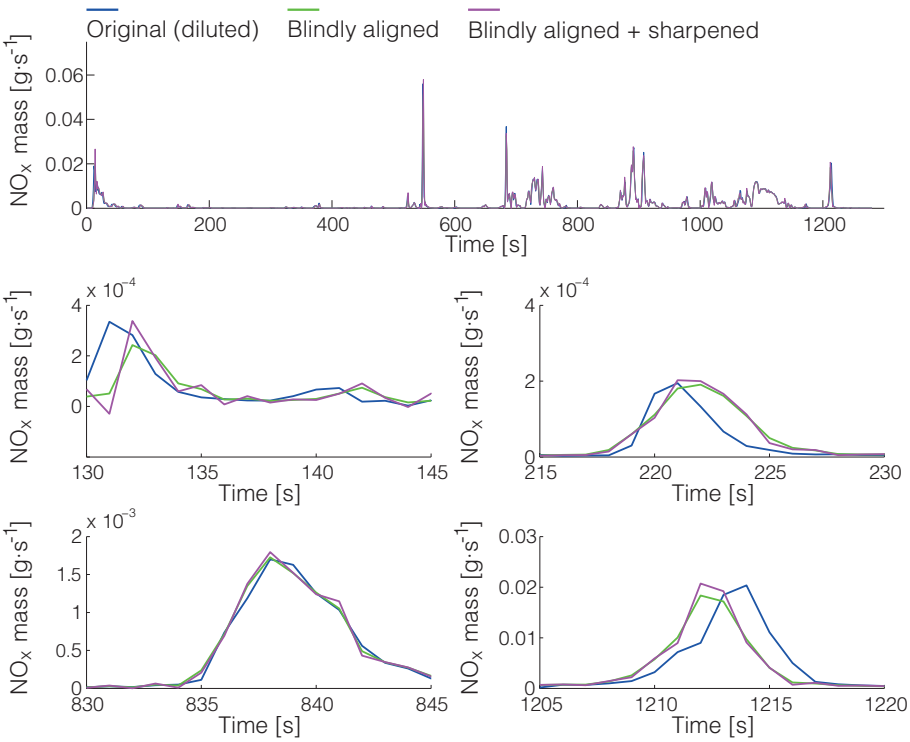


**Figure 6.7b:** Blind compensation of the diluted mass $NO_x$ signal ($ERMES_a$ dataset)

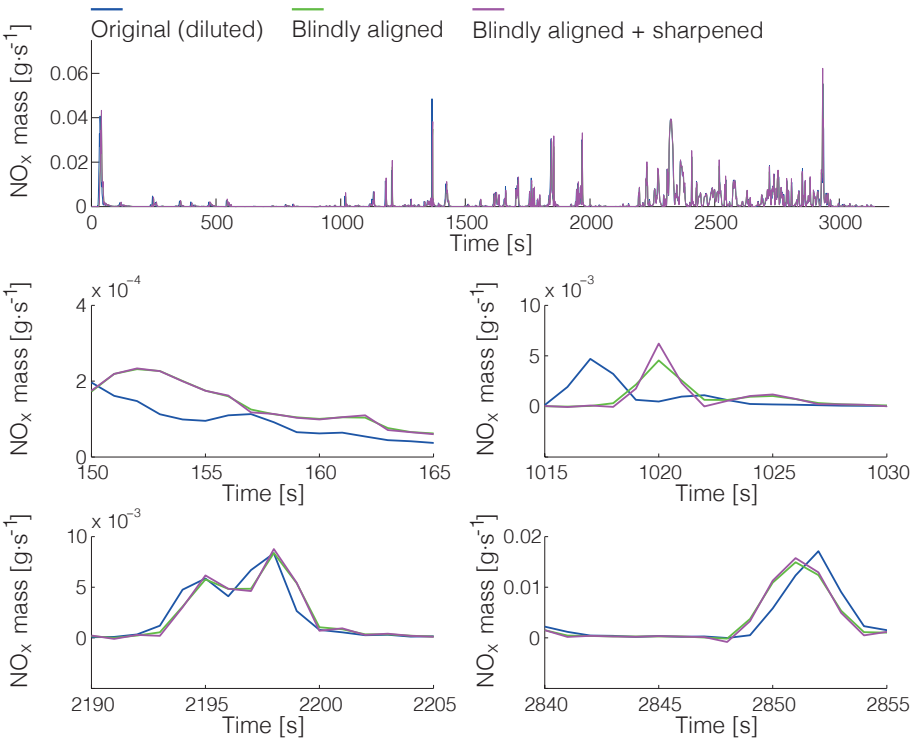


**Figure 6.7c:** Blind compensation of the diluted mass $NO_x$ signal ($CADC_a$ dataset)

### 6.1.4 Software implementation: esto

The $CO_2$ tracer method has been implemented as part of esto (emission signals sync tool, in beta version at the time of writing). This is a standalone Microsoft Windows®application that can assist in the creation of engine emission maps from instantaneous vehicle emission signals. esto was entirely developed within the Sustainable Transport Unit of JRC.[5] esto takes signals from different instruments as input (see figure 6.8) and automatically performs the necessary post-processing operations described in this dissertation to ensure that the signals are properly aligned, including signal resampling, global time alignments (performed via cross-correlation checks; see section 5.4.2 on page 106) and local alignment and sharpening of the 'blind' pollutants (supported by a reference FC signal; see sections 5.4.3 and 5.4.4 on pages 110 and 116). The tool also outputs the *engine emission maps* ready to be used in vehicle simulation environments.

[5] esto was developed under the supervision of Dr Georgios Fontaras and Dr Panagiota Dilara. Mr Konstantinos Agnanostopoulos was responsible for the creation of the graphical user interface.

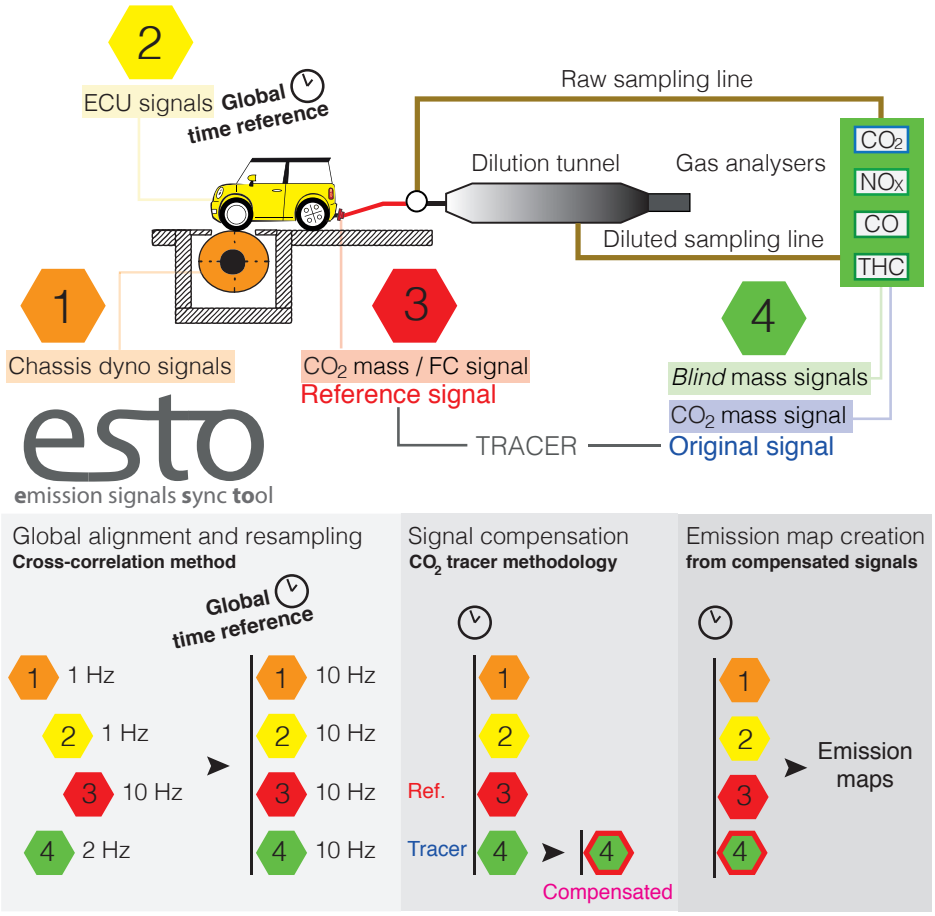


**Figure 6.8:** esto overview: a software tool to compensate instantaneous emission signals and create engine emission maps

## 6.2 Discussion

This dissertation was written to serve two main purposes: first and foremost, we wanted to *identify and describe all the relevant distorting effects* that compromise the accuracy of instantaneous signals produced during vehicle emissions testing, and to *encourage the implementation* of systematic instantaneous signal compensation methods. Secondly, we aimed to *develop a new, comprehensive methodology* to perform this compensation that could be adopted by the emission measurement laboratories of the ERMES group and other laboratories worldwide.

The first objective of the dissertation was partially fulfilled in chapter 3, where we reviewed the characteristics of the signals used for modelling vehicle emissions and we identified the distorting effects that compromise the accuracy of these signals, namely signal misalignments, variable transport times, exhaust gas mixing phenomena, and the dynamic response of exhaust gas analysers. These effects were characterised both at the aggregated and instantaneous level. We completed our task in chapter 4, where we studied the elements that intervene in the process of transforming distorted signals into compensated signals with improved instantaneous accuracy, and where a *reference framework* for the compensation of instantaneous emission signals was proposed accordingly. In this chapter, we argued that a complete compensation method can be understood as the combination of three elements: the underlying model of the phenomena that distort the signal, the experiments required to calibrate the model and the signal post-processing methods required for the compensation. Some practical implementations of signal compensation methods will achieve excellent results, while others will bring about more modest improvements. In general, excellent performance will require additional experimental work and come at the expense of flexibility, whereas 'lighter' compensation methods will exhibit limited compensation capabilities. In any case, individual laboratories are free to experiment with compensation methods and try to find an adequate balance between their expectations or needs regarding instantaneous data accuracy and the added complexity that different signal compensation approaches would entail.

The second objective of the dissertation was covered in chapter 5, where the $CO_2$ tracer method for the compensation of instantaneous vehicle emission signals was described. The development of the $CO_2$ tracer method constitutes the most important original contribution of this dissertation, and thus in the next section we

will concentrate on the discussion of its application, as well as of the methodological choices that were made during its development.

### 6.2.1 Discussion of the $CO_2$ tracer method

The $CO_2$ tracer method is a comprehensive methodology for the compensation of instantaneous vehicle emission signals. Earlier in this chapter, it was successfully applied to pollutant signals measured by the on-line exhaust gas analysers of a chassis dynamometer laboratory equipped with a diluted emissions measurement setup.

The $CO_2$ tracer method relies on *data post-processing* to model and compensate the distortions introduced by the variable transport times and exhaust gas mixing phenomena within the measurement setup. The compensation approach is based upon making small modifications to the original mass signal of the tracer pollutant (*i.e.*, $CO_2$) so as to bring it closer to the reference signal. Then, the same modifications are applied to the rest of gaseous pollutants (*i.e.*, the ones for which a reference signal is not available) based on the assumption that *the mass signals of all gaseous pollutants suffer the same distortions within the measurement setup*. The compensation of the original signals is therefore supported by the reference signal, which needs to be recorded every time the compensation method is to be applied.

The main original aspects of the $CO_2$ tracer method are discussed in the sections that follow.

#### *6.2.1.1 Operation with mass signals*

The defining trait that sets the $CO_2$ tracer method apart from previous methodologies is that it operates with *pollutant mass* emission signals rather than with *pollutant concentration* signals. This is an advantage because it is the pollutant mass emission rates—and not the concentrations, which need to be associated with an exhaust mass or volume flow—that are directly relevant to the production of engine emission maps.

By choosing to operate with mass signals, the method is able to use an instantaneous fuel consumption signal as a reference. This choice of a reference signal—which

is the ideal embodiment of the method—has three main advantages: first and foremost, it renders exhaust mass flow measurements superfluous[6] because $CO_2$ mass emissions can be accurately estimated by assuming that all of the carbon content of the fuel is transformed into $CO_2$ during combustion. Secondly, since the fuel flow measurement occurs *before combustion*, the FC signal is not distorted by the variable transport times of exhaust gas from the engine-out to the tailpipe point.[7] Third, the alignment of the instantaneous FC signal to the measured engine states (OBD signals) is supported by the physical correlation between instantaneous FC and engine state signals such as OBD engine load or OBD engine speed.

In the practical application of the $CO_2$ tracer method presented at the beginning of this chapter, the emission measurement setup included a dilution tunnel. As discussed in section 3.1.2.1.3, this setup provides very reliable aggregate emission results because the volume flow at the end of the dilution tunnel (where concentrations are measured by the analysers) is kept quasi-steady, thereby eliminating the risk of a *primary misalignment* between the flow and the concentration signals (*cf.* section 3.2.1.1). However, the dilution process also transforms the concentration signals of all pollutants by introducing a variable amount of dilution air, and we should ensure that this is not introducing further distortions to our signals or, if any distortions are indeed being introduced by the dilution process, we should demonstrate that these are affecting all gaseous pollutants equally.[8]

We will try to do this by taking a closer look at what happens to the volume flow, concentration and mass signals in the vicinity of the mixing point (figure 6.9).

[6] It also makes it unnecessary to align measured tailpipe $CO_2$ concentrations to measured exhaust mass flow signals to derive a reference signal, thereby eliminating a potential source of uncertainty.

[7] Achieving such a convenient measurement location to derive a reference signal with an ultrafast analyser would require drilling a hole in the exhaust system of the test vehicle.

[8] The assumption that the mass signals of all gaseous pollutants are distorted by the measurement setup *in the same way* is key to the applicability of the $CO_2$ tracer method (see section 5.1 on page 91).

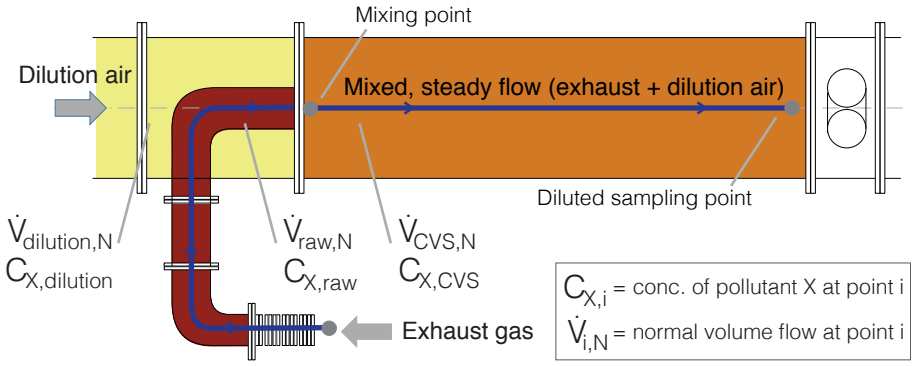


**Figure 6.9:** Illustration of dilution in a CVS setup. A variable exhaust flow is mixed with a variable flow of dilution air to produce a quasi-steady volume flow in the CVS

As discussed in section 3.1.2.1, the dilution tunnel operates in such a way that the amount of dilution air is controlled. This ensures that the total volume flow at the CVS (in normal conditions, $\dot{V}_{CVS,N}$) is kept approximately constant (equation 6.1).

$$\dot{V}_{CVS,N} = \dot{V}_{dil.,N} + \dot{V}_{raw,N} \tag{6.1}$$

The dilution of the exhaust gas transforms the concentration signals of any given gaseous pollutant $X$ after the mixing point via a *variable dilution ratio*[9] that is driven by the variations in the instantaneous exhaust volume flow signal, $\dot{V}_{raw,N}$. This transformation can be formulated via a *mass balance* at the mixing point considering the density of pollutant $X$ in normal conditions, $\rho_{X,N}$ (equation 6.2).

[9]Note that the dilution ratio at the mixing point at any given point in time depends on the instantaneous exhaust flow signal—which propagates with sonic speed—, but is applied to a mass of exhaust gas that was emitted a few seconds earlier because the exhaust gas travels much more slowly along the measurement setup (*i.e.*, there would be a large *primary misalignment* among the signals before the mixing point; *cf.* section 3.2.1.1). This would pose problems if we had to derive pollutant mass emission signals at this point of the measurement setup.

$$\dot{V}_{\text{CVS},N} \cdot C_{X,\text{CVS}} \cdot \rho_{X,N} = \dot{V}_{raw,N} \cdot C_{X,raw} \cdot \rho_{X,N} + \dot{V}_{dil.,N} \cdot \overset{0}{\cancel{C}}_{X,dil.} \cdot \rho_{X,N} \tag{6.2}$$

If we neglect the (small) concentration of pollutant $X$ in the dilution air,[10] we see that the concentration of pollutant $X$ after the mixing point at the dilution tunnel is equal to the raw concentration of the same pollutant before the mixing point multiplied by the ratio of the instantaneous raw exhaust volume flow to the CVS volume flow (equation 6.3).

$$C_{X,\text{CVS}} = \frac{\dot{V}_{raw,N}}{\dot{V}_{\text{CVS},N}} \cdot C_{X,raw} \tag{6.3}$$

This transformation *is the same for all gaseous pollutant concentration signals*, but it has a (visually) more dramatic impact upon some of them. In the case of $CO_2$, it can turn an almost flat, featureless exhaust concentration signal (*e.g.*, from a stoichiometric gasoline engine, such as the one powering the test vehicle of our experimental campaign) into a diluted $C_{CO_2,\text{CVS}}$ signal that closely follows the feature-rich profile of exhaust volume flow.[11] For other *concentration* signals, the effect is more difficult to describe simply with words, but the mathematical description of equation 6.3 remains equally valid. We can thus conclude that, if our compensation method were operating on *concentration signals*, we would have to record the relevant volume flows at the mixing point to undo the dynamic dilution process.

On the other hand, from the mass balance at the mixing point it follows that the dilution process has no significant effect upon the mass 'seen' by the analysers at the end of the dilution tunnel. This is because the diluted (transformed) concentration signal $C_{X,\text{CVS}}$ for each pollutant $X$ is multiplied by the quasi-steady volume flow $\dot{V}_{\text{CVS},N}$ to derive the diluted mass signal. By virtue of equation 6.2, this mass signal

[10] Dilution can increase the total mass measured at the dilution tunnel if dilution air carries some amount of the pollutants of interest, but these amounts should be negligible in comparison to the mass present in the exhaust gas.

[11] The reason for this becomes apparent after substituting a 'flat' $C_{CO_2,raw}$ and a quasi-steady $\dot{V}_{\text{CVS},N}$ in equation 6.3.

will be equivalent to the mass signal before dilution, and we can conclude that the dilution step is *transparent* for the mass signals of all pollutants. Therefore, the dilution process need not be modelled for the application of the $CO_2$ tracer method (*i.e.*, we do not need to record instantaneous dilution ratios at the mixing point to apply the compensation).

#### *6.2.1.2 Signal post-processing methods*

In every instance described in this dissertation, the compensation of measured vehicle emission signals is done through *data post-processing*. In other words, the compensation is always performed off-line after the signals have been recorded. The reason why on-line methods have not been proposed is that the instantaneous output value of a compensation algorithm (*i.e.*, the compensated signal) not only depends on current and past inputs (values of the distorted signal), but also on *future* ones. This is apparent if we look closely at transport times: the time it takes for a given portion of the exhaust gas to travel from the emission to the measurement point is a function of the instantaneous exhaust mass flow that originated it, but also of the exhaust flow that occurs *afterwards* and 'pushes' the exhaust gas through the measurement setup.[12]

The $CO_2$ tracer method relies heavily on data post-processing, thus requiring very little experimental and modelling efforts. The basic concept behind the method is that it is possible to characterise the exhaust gas flow through the emissions measurement setup by computing modified versions of the output signal and systematically comparing them to a reference input signal in order to extract information about the behaviour of the system. The $CO_2$ tracer method makes novel contributions to the way vehicle emission signals can be post-processed to compensate the distortions that occur between the engine-out point and the point of measurement:

- The method uses *`rolling' data bins* to maximise the amount of information that is extracted from the signals (*cf.* section 5.2.2 on page 99). This data binning strategy—which can be easily implemented in MATLAB®—multiplies the number of data bins available to estimate the required local time shift and the level of

[12] In systems theory terms, one would say that the system we are trying to model is *improper*, as opposed to *proper* systems, whose output depends only on current and past inputs.

sharpening, thereby making the estimated compensation parameters less sensitive to noise in the measured signals.

- Time alignments among signals are performed via *cross-correlation checks*, thereby eliminating the need to record a common 'clock' signal during the performance of the experiments (*i.e.*, a data logger is not required).
- In order to improve the resolution of the time alignment of signals from different instruments, the method resorts to signal up-sampling. This increases the resolution of the alignment with only modest increases in computational effort.
- The method performs the *local alignment* routine in an *iterative loop* in descending order of bin size (and also of alignment margin size). In this way, the initial iterations (corresponding to large bin sizes) compensate the delays that affect long sections of the datasets, whereas subsequent iterations are able to compensate misalignments at a more local level.
- Finally, the method performs the *local sharpening* of the aligned signal to produce the final, fully compensated signal. The sharpening stage uses discrete convolution and simple, *high-pass* filter kernels that can be controlled via a single parameter.

#### *6.2.1.3 Flexibility and robustness*

For the application of compensation methods based on systems theory, the measurement setup is divided into several sub-systems whose characterisation is performed by generating controlled inputs (concentration steps) at the inlet of each sub-system. The characterisation experiments require a special valve train to generate the step signals, and a reference instrument (*e.g.*, an ultrafast analyser) to measure the corresponding output at the outlet. Each sub-system is modelled (and inverted) individually, and the principle of superposition (*cf.* section 3.1.2.3 on page 55) is applied to compile a model of the complete measurement setup. The resulting model is thus able to reconstruct the evolution of the otherwise unknown pollutant concentrations at the inlet of the measurement setup as a function of the measured instantaneous concentrations at the outlet.

As opposed to the systems theory modelling approach, the $CO_2$ tracer method models the measurement setup as a 'lump' system rather than dividing it into sub-systems. Also, no special inputs need to be generated for its application.

Instead, the necessary signals are produced during ordinary emissions testing.[13] This is a major advantage of the $CO_2$ tracer method, as it significantly reduces the experimental work requirements.[14] In this way, the burden of work is shifted from experimentation to computation, making this a suitable approach for data conditioning in the framework of ERMES.

Another key benefit of the $CO_2$ tracer method is the ability of its algorithm to automatically adjust to changes in the measurement setup (*e.g.*, to changes in pipe lengths or diameters), and the fact that it does not require periodical calibration or the adoption of a temperature model. Moreover, the compensated signals output by the method are already aligned to the 'engine-out' time reference of the instantaneous FC signal, and so they can be easily aligned to engine (OBD) signals—via a cross-correlation check—in order to produce engine emission maps.

#### *6.2.1.4 Method limitations*

The $CO_2$ tracer method has several benefits that we have just summarised. It also has some limitations that need to be taking into account by prospective users:

- The first limitation lies in the fact that, unlike the systems theory approach described in chapter 4, the $CO_2$ tracer method requires that the reference signal be recorded *every time* that the signal compensation method is to be applied. This poses no problem for laboratories that routinely measure fuel consumption with an instantaneous fuel flow meter. These laboratories can apply the methodology with little additional effort by using esto. Other laboratories seeking to adopt the methodology should assess the costs of acquiring and operating such an instrument, or find alternative options to derive a suitable reference mass $CO_2$ signal.[15]
- The second limitation relates to the response characteristic of the exhaust gas analysers. The $CO_2$ tracer method assumes that all signals are distorted in the

[13] In the example application of the method, all the signals were produced during standard, transient chassis dynamometer driving cycles.

[14] It also allows for historical datasets to be compensated (provided that a suitable reference signal is available).

[15] A cost-effective option to try out the $CO_2$ tracer method before considering the purchase of an instantaneous FC meter would be to test a vehicle that allows access to the instantaneous fuelling rate signal from OBD, and use this signal as a reference.

same way throughout the measurement setup. This assumption holds strictly true from the engine-out to the *analyser-in* point but, as explained in section 3.2.4, each analyser has a distinct response characteristic. Whereas 'systems theory' approaches perform separate experiments to characterise the dynamic response of each analyser, the $CO_2$ tracer method assumes that all analysers have a response characteristic equal to that of the $CO_2$ analyser, thereby introducing a bias. Considering that it is fairly common for current test equipment to have $t_{10-90\%}$ rise times below two seconds—a few hundred milliseconds for FTIR multi-component measurement systems—, the differences among the dynamic response characteristics of analysers are not a major reason for concern because they should negligible in comparison to the variability of transport times and the effects of exhaust gas mixing, which are in any case common for all gaseous pollutants and effectively captured by the $CO_2$ tracer method.

- The third limitation regards the choice of a tracer pollutant. In order to work, the $CO_2$ tracer method systematically compares two similar mass emission signals of the tracer pollutant, modifies one of them to make it resemble the other and stores the modifications so they can be 'blindly' applied to the mass signals of other gaseous pollutants at a later stage. This requires that the tracer pollutant signals have identifiable *features* that can be matched by the algorithm. In other words, a tracer pollutant needs to be produced in measurable quantities, and its mass emission signal should have sufficiently pronounced features (*i.e.*, peaks or valleys) throughout the test. As discussed in section 5.1.1, only $CO_2$ meets this requirements consistently. For this reason, the choice of a tracer pollutant other than $CO_2$ is strongly discouraged.

### 6.2.2 Validation of the $CO_2$ tracer method

In this section, we will try to provide sufficient evidence in support of the truth of the results we presented earlier in the chapter. Ideally, a *direct* validation of the methodology would be performed through an experiment in which *two* reference and two diluted signals were simultaneously obtained for two different pollutants. Then, one could apply the compensation methodology independently to each of the two pollutants and investigate whether the compensation is being performed in the same way. But there are limitations that make this approach unfeasible. First of all, it is not possible to predict the emissions of any pollutant other than $CO_2$ from an instantaneous FC measurement. Therefore, a validation with two

reference pollutants would have to be performed with one of the following sets of signals:

a) an instantaneous FC measurement at the engine-in point (before combustion) and measurement of another pollutant at the tailpipe with a suitable reference instrument (*e.g.*, an ultrafast $NO_x$ analyser). This would would be a sub-optimal setup because the two reference signals would be obtained at different points along the measurement setup, which would be up to a few metres apart. Also, one would have to accurately measure the flow rate at the sampling line of the analyser and back-correct the original signals (obtained downstream from the tailpipe) for the exhaust gas mass withdrawn by the analyser at the tailpipe.[16]
b) two tailpipe (or, better yet, engine-out) measurements[17] of two different pollutants with two separate ultrafast analysers (or a single, dual-channel analyser) sampling at the same point. This option would increase costs, and still require a back-correction which would add uncertainty to the calculations.

In the sections that follow, we will provide further insight into the internal operation of the compensation method and try to validate the results of its application. Given the limitations we have just described, a direct validation of the $CO_2$ methodology using two different tracer pollutants was deemed unfeasible. Therefore, an *indirect validation* of the methodology is proposed. Said validation is supported by evidence obtained from an evaluation of the results of the compensation of the emission datasets from the experimental campaign.

#### *6.2.2.1 Consistency of results*

An initial indication that the $CO_2$ tracer method is working as intended is given by the consistency of the results of the two stages of the compensation process (local alignment and peak sharpening) with their expected outcome. We can try to visualise this in figure 6.10, which is intended as a simple, stylised illustration

[16] Although the analyser will typically sample at a constant volume flow rate, this represents a variable fraction of the total (variable) exhaust flow, and a so a dynamic back-correction will be required.

[17] Any tailpipe measurement would also require an appropriate tailpipe flow measurement and a back-correction of the downstream signals. If an engine-out measurement was carried out, the after-treatment devices related to the reference pollutants would need to be removed during testing.

of the effect of the alignment and sharpening stages of the compensation process upon absolute instantaneous error (considered as the absolute pointwise deviation from the reference signal) for a signal that consists of a single feature (an emission peak).

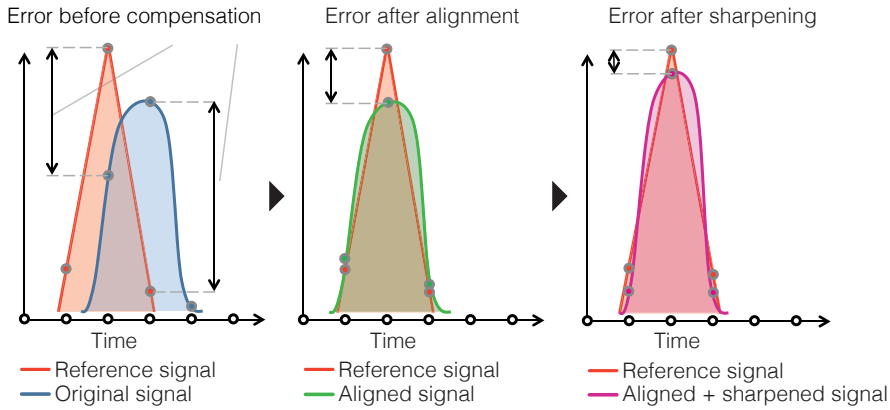


**Figure 6.10:** Effect of the alignment and sharpening processes upon absolute instantaneous error

In the leftmost part of figure 6.10 (initial error before the compensation), we see that the local alignment of the features of the reference signal and the original signal is poor in many instances, leading to a high instantaneous error. After the alignment process (first stage of the compensation), most of the instantaneous error is removed. The (secondary) sharpening process affords additional improvements (especially at the peaks), but these are lower than the improvements due to the alignment stage.[18] This is consistent with the results reported in figure 6.5 on page 136, where most of the improvements come from the alignment stage rather than the sharpening stage. Moreover, the post-processing method brings about similar levels of improvement for both repetitions of each test cycle of the experimental campaign.

#### *6.2.2.2 Mass conservation*

Further evidence that the $CO_2$ tracer method is correctly performing the compensation of the emission signals can be obtained by computing the *overall mass*

[18] The effect is similar for local cross-correlation.

of the compensated signals and comparing it to that of the original signals. The issue of *mass conservation* deserves special consideration. In chapter 3 (see page 56), we saw that properly functioning emission measurement systems conserve mass. A good compensation method should also have a small impact upon the mass of pollutants that is ultimately reported. If we look closely at the $CO_2$ tracer method, we see that the two main post-processing stages applied to the mass signals ensure that there is no impact upon overall mass considering the signal as a whole[19] (see figure 6.11). However, since the compensated signal is reconstructed by joining small bins from several signals, mass conservation is not mathematically enforced by the $CO_2$ tracer method.

Therefore, a good level of agreement between the overall mass of the original and the compensated signals is an indication of good performance of the compensation method. Table 6.4 summarises the mass conservation performance of the compensation method for all the datasets of the experimental campaign. Note that *mass fidelity* (calculated as the ratio of the overall mass of the compensated signal to the overall mass of the original signal) is close to 1 (100% mass conservation) for all of the datasets and all of the pollutant signals that were compensated, including the 'blind' pollutants.

**Table 6.4:** Overall mass fidelity of the compensation process

| | **Mass fidelity*** | | |
|---|---|---|---|
| **Test cycle dataset** | $NO_x$ | THC | CO |
| $NEDC_a$ | 0.985/0.985 | 1.002/0.997 | 1.011/1.017 |
| $NEDC_b$ | 0.974/0.974 | 0.980/0.978 | 1.029/1.027 |
| $CADC_a$ | 0.985/0.982 | 0.988/0.988 | 1.011/1.008 |
| $CADC_b$ | 0.996/0.999 | 0.989/0.990 | 0.954/0.957 |
| $ERMES_a$ | 1.003/1.003 | 1.004/1.005 | 1.013/1.014 |
| $ERMES_b$ | 0.982/0.980 | 1.003/1.002 | 1.035/1.035 |

**Ratio of overall signal masses (aligned to original / aligned+sharpened to original)*

[19] It is easy to see that time-shifting has no effect on overall mass, but this is not so evident for the sharpening process. Overall mass conservation after sharpening will be ensured as long as the elements of the sharpening filter kernel add up to unity (see section 5.4.4.1 on page 117).

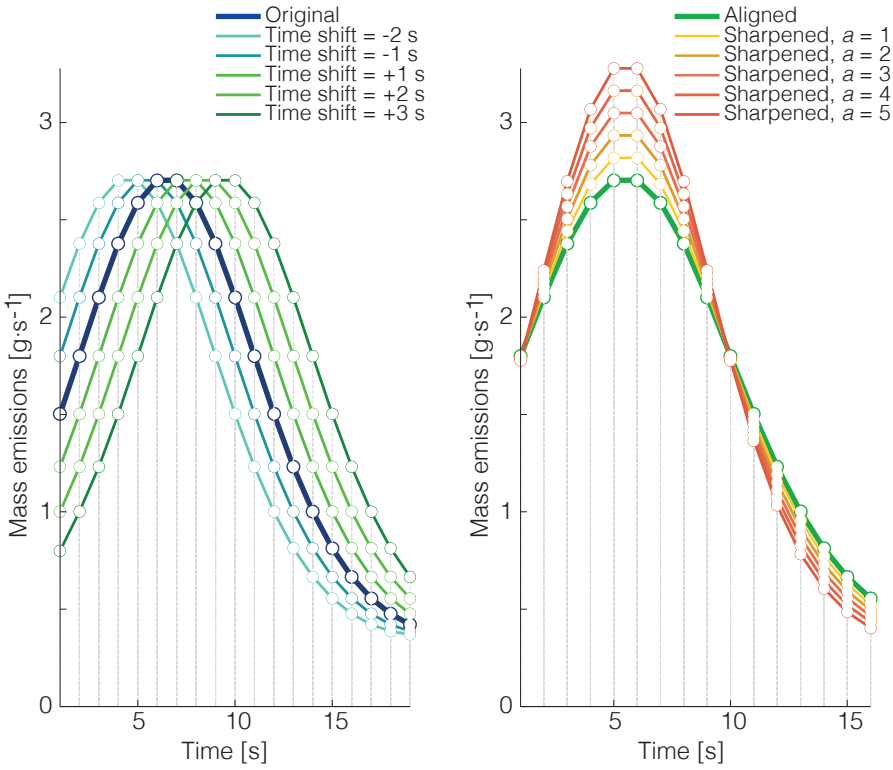


**Figure 6.11:** Illustration of the effect of time-shifting and sharpening upon mass conservation (several time shifts and sharpening filters are applied to the same small section of a mass emission signal)

#### 6.2.2.3 *Inspection of the compensation process*

Figure 6.10 is a very simple visualisation of what the compensation method does to the original mass signals. Looking at it one may wonder what would happen if, instead of a single peak of emissions, we had 'real' signals comprising long successions of features (peaks and valleys)? How would the repeated binning and reconstruction of the signals affect the results of the compensation? A weakness of the $CO_2$ tracer method in its initial stages of development was its lack of transparency: given a reference and a diluted signal for $CO_2$, the algorithm would compute the optimal delay for each data bin of the signal and for each repetition of the alignment process, and it would do the same for the sharpening level $a$ and the sharpening process. The resulting compensation parameters—*i.e.*, the vector of optimal delays for each bin and iteration alignment process, and the vector of optimal sharpening levels—could be inspected, but they were difficult to interpret because the optimal delays and degrees of sharpening are attributed to data bins rather than individual data points of the original signal.[20]

To make up for these shortcomings, the concept of *alignment* and *sharpening inspectors* was implemented. These 'inspectors' are visualisations of the level of local delay and sharpening that is introduced by the compensation process *at each data point of the original signal*. They are calculated by separately applying the local alignment and the local sharpening process to *known input signals*. The output of this process may then be used to evaluate the compensation process:

- To obtain an *inspector or the alignment process*, one simply needs to generate a *ramp* signal where the signal value at position $n$ equals $n$, and input this signal to the blind alignment process to obtain an 'aligned ramp'. If we subtract the original ramp from the aligned ramp, we obtain a estimation of the local time shifts introduced by the alignment process (see top of figure 6.12). The time shifts calculated by the alignment inspector may be positive or negative. Negative time shifts indicate that the emissions corresponding to the data point travelled faster than the average transport time for the cycle, and were thus shifted towards the *past*. Likewise, positive shifts correspond to 'slow' signal sections that were shifted towards the *future* (see section 5.4.2 on page 106).

[20] The computation of the inspectors is built into the signal compensation routine, and is automatically run by the esto tool. To our knowledge, this makes the $CO_2$ tracer method the first vehicle emission signal compensation methodology to produce comprehensive, easily interpretable reports of its own operation.

- To compute an *inspector of the sharpening process*, we can reconstruct a signal from bins whose value at each point is equal to the sharpening level *a* assigned to the bin during the compensation process (*cf.* section 5.4.4.1). This provides an estimation of the degree of sharpening that is being applied *at each point*, which is calculated as a mean of the level of sharpening *a* of the optimal 'sharpened' bins (see bottom of figure 6.12).

Both the alignment and the sharpening inspectors were computed for all the datasets of the experimental campaign. These signals are graphically represented in figures 6.13 and 6.14.

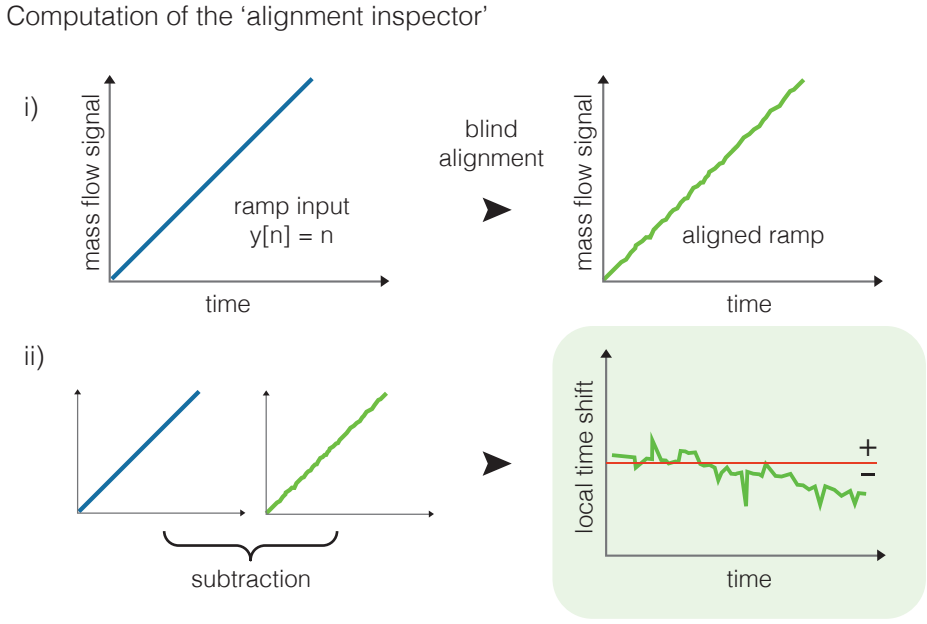


**Figure 6.12:** Computation of the inspectors of the compensation process

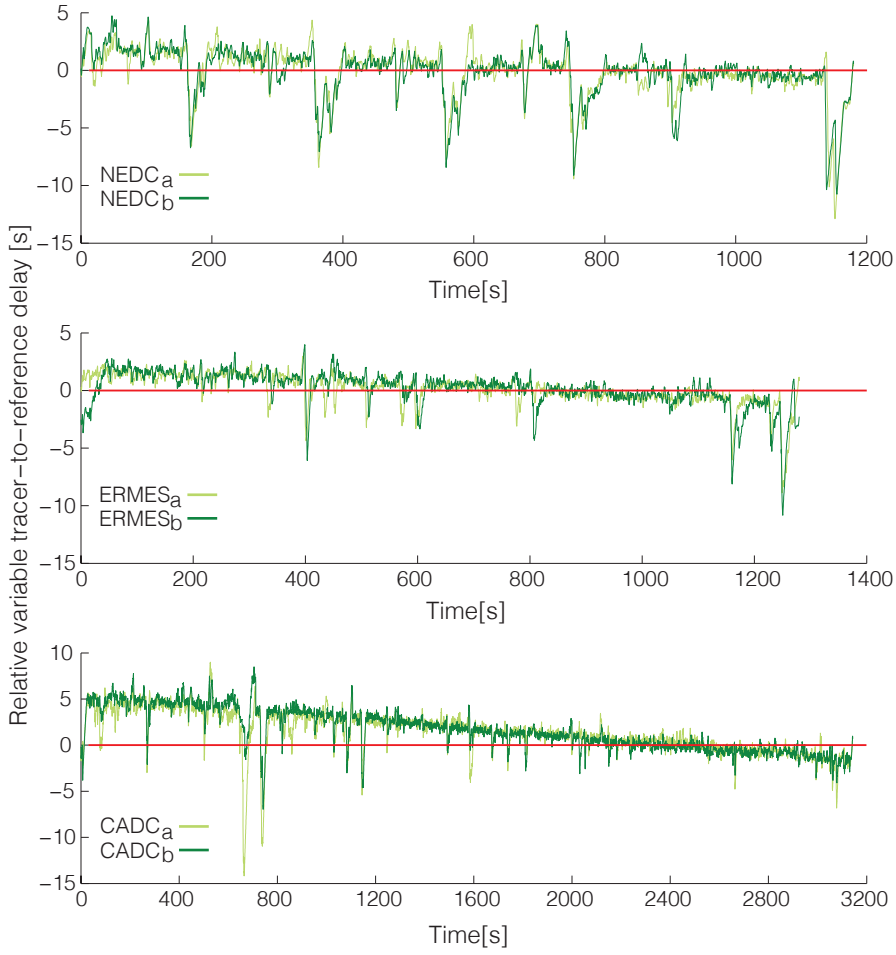


**Figure 6.13:** Inspectors of the alignment process (by test cycle)

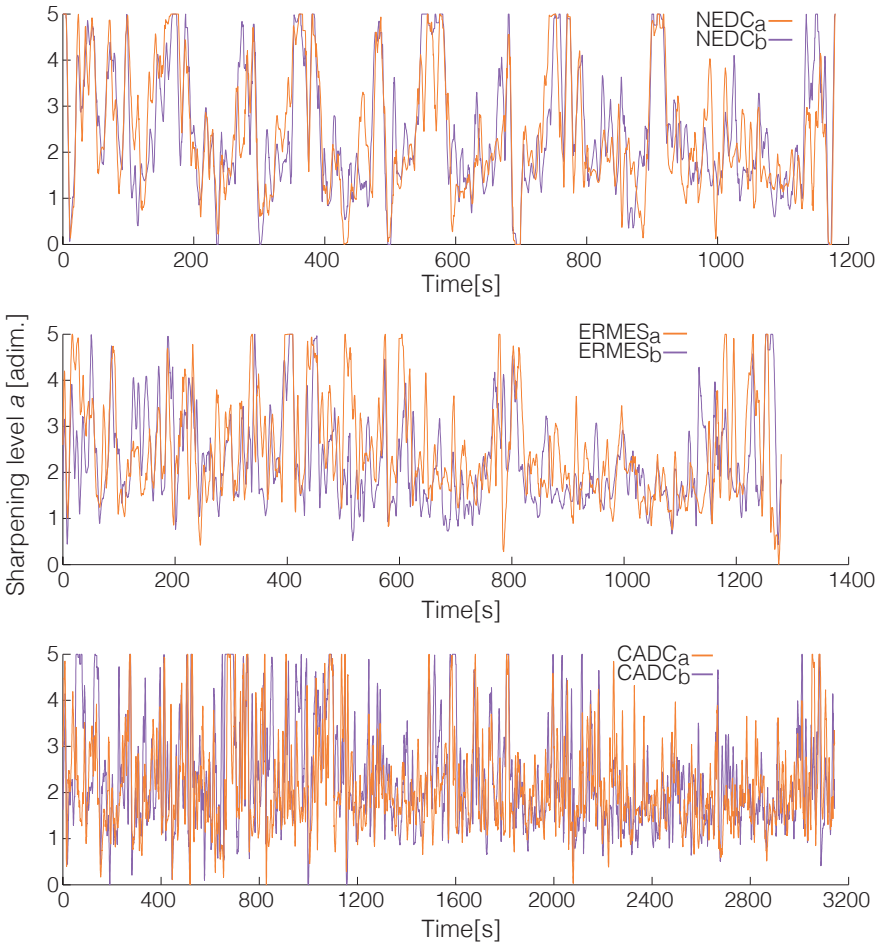


**Figure 6.14:** Inspectors of the sharpening process (by test cycle)

The alignment and sharpening inspectors provide interesting insights into the way in which the compensation process is taking place, and ultimately validate the $CO_2$ tracer method by producing further evidence of its correct operation:

- First of all, both the alignment and the sharpening inspectors show that the local level of time-shifting and signal sharpening being applied is repeatable for both instances of each test cycle used in the experimental campaign. Moreover, the time-shifting pattern is repeated for the first section of NEDC, which consists of four repetitions of the same sub-cycle. We also observe that the sharp drops in the relative delay estimated by the alignment inspector correspond with the location of fuel cut-off points that occur just before a section of smooth deceleration. These cut-off points are easily observable for the NEDC cycle (see figure 6.15). This drop in the relative delay is consistent with our expectations, considering that after these points the exhaust flow is very low and stops 'pushing' the exhaust gas through the measurement setup, thus producing a rapid increase in transport time (*i.e.*, a negative delay) for the emissions produced right afterwards.

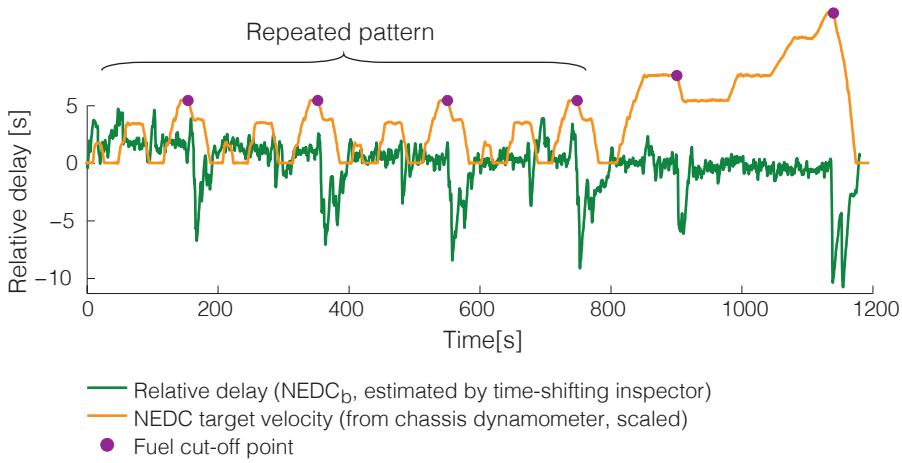


**Figure 6.15:** Fuel cut-off events identified by the alignment inspector during NEDC testing

- Secondly, we observe that the alignment inspectors feature a noticeable *slope*: the initial (urban driving, low exhaust flow) sections of the cycles have positive relative delays, whereas the final ones (highway driving, high exhaust flow) have negative relative delays. This is contrary to expectations and inconsistent with the behaviour we observed at the fuel cut-off points. We find an explanation for this anomaly if we look at figure 6.16, which shows that the volume flow at the dilution tunnel is not constant as assumed, but is instead decreased slightly by the test bench control system during the high exhaust flow sections of the test cycles. This drift is likely a temperature effect—exhaust gas is substantially hotter during highway driving—that creates the slope in the alignment inspectors, but does not prevent the $CO_2$ tracer method from correctly compensating the signals.[21]

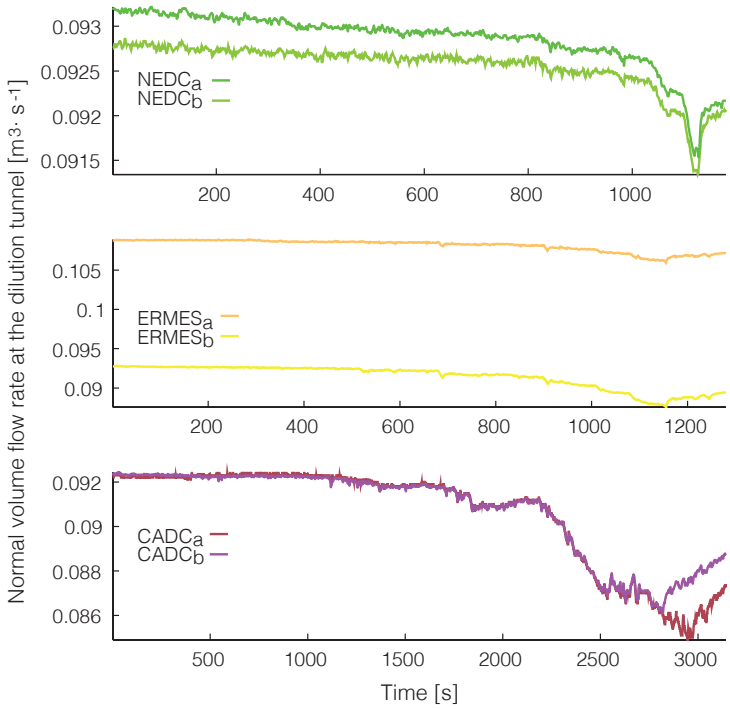


**Figure 6.16:** Volume flow rates at the dilution tunnel reported by the test bench (all datasets)

[21] This is further proof of the self-adaptive nature of the methodology, which corrects for the flow rate variations at the dilution tunnel without requiring the dilution tunnel flow signal as input.

- Third, we observe that the repeatability of the alignment process is better than that of the sharpening process. This is consistent with the fact that the alignment process compensates large deviations (delays of up to several seconds), whereas the sharpening process takes care of finer distortions (minor corrections of peak heights). In signal processing terms, the *signal-to-noise ratio* is higher for the alignment than it is for the sharpening process, and so it is less affected by the noise present in the measured signals.
- Fourth, the estimated time shifts are consistent with the expectations: on the one hand, their range of variation (between −12 and 5 seconds) is in agreement with the values reported in the literature (see figure 3.4 on page 61).[22] On the other hand, the variability of the time shifts is, as expected, higher during low-flow sections (see, again, figure 3.4). This can be observed by plotting the scatter plot of the time shifts against exhaust flow or a signal that is proportional to flow, as is done in figure 6.17.[23]

[22] The inspector only covers the variable delays introduced by the vehicle exhaust system and the raw gas line—as well as the temperature effects—and not the fixed delays introduced by the constant flow sub-systems (see table 3.3 on page 56), which are removed from the compensation after the global alignment of the reference and the tracer signals (see section 5.4.2 on page 106).

[23] The scatter plot of figure 6.17 cannot be expected to be a clear-cut hyperbola such as the one in figure 3.4 on page 61: one should bear in mind that, while the latter is a representation of the variation of transport time observed for several steady-state testing points, the former is derived from transient cycles in which the transport time of an exhaust gas bin is not solely determined by the flow or engine load with which it was produced, but also by the (variable) flow of the bins that were produced after it, and hence the increased scatter of the points.

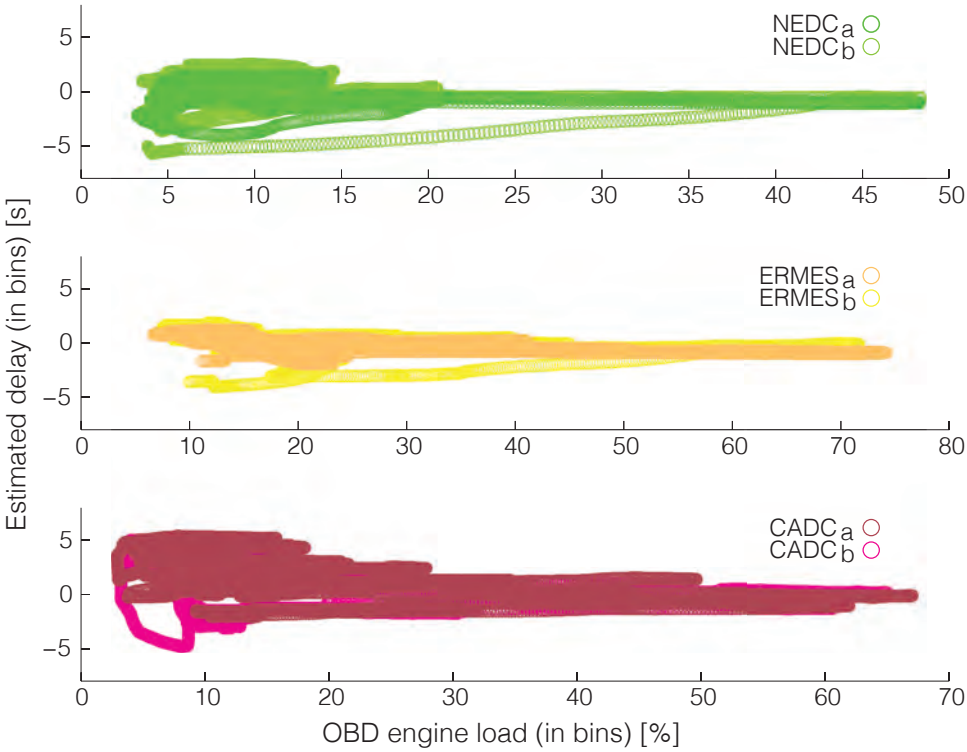


**Figure 6.17:** Scatterplots of estimated relative delays *vs* OBD engine load (all datasets)

# Chapter 7

# Conclusions

In the first chapter of this dissertation we hypothesised that vehicle emissions modelling is shifting from using aggregate data (*i.e.*, emission values averaged over several seconds or minutes) towards approaches that make use of instantaneous emission signals (*i.e.*, with resolutions of 1 Hz or more) output by current instrumentation. This was confirmed by a thorough review of the experimental techniques used to measure road vehicle emissions for modelling purposes, which we performed in chapter 2.

On the other hand, we also conjectured that instantaneous vehicle emission signals reported by conventional vehicle emissions measurement instrumentation are affected by a number of *distorting effects* that compromise their accuracy, and that these effects could be compensated through a combination of *physical modelling* and *data post-processing*. This was confirmed in chapter 3, where we also showed that, even though the presence of these distorting effects is well known to vehicle emission test bench operators, they usually have a minor impact upon aggregated emission values (*i.e.*, overall driving cycle or sub-cycle results) and thus they have often been dealt with using simple, non-systematic correction approaches such as performing the time alignment of signals through a visual match of the initial signal peaks. However, as vehicle emission models evolve towards finer time resolutions (and also as current-technology vehicles concentrate a significant portion of their emissions during a small number of short emission events), the instantaneous accuracy of emissions reported by standard vehicle emission measurement equipment needs to be further

investigated, and the implementation of more sophisticated signal compensation approaches is increasingly justified. This is especially true for laboratories that produce datasets for emission modelling purposes, and particularly for those that contribute to databases used in regulatory and research contexts such as the ERMES database of vehicle emissions.

The first objective of this dissertation was to assess the distorting effects that compromise the accuracy of instantaneous vehicle emissions signals used for vehicle emissions modelling, and to develop a methodological framework for the compensation of these signals. In chapter 3, we showed that a high temporal resolution and good aggregate accuracy of measured signals do not imply a high instantaneous accuracy (understood as a good *local* agreement of the measured signals with the corresponding 'true' mass emissions at the tailpipe or catalyst-out point). This is due to distortion effects mostly associated with the variable transport times and mixing of the exhaust gas as it travels from the point of emission to the point of measurement. In a chassis dynamometer laboratory equipped with a dilution tunnel (the most typical configuration of vehicle emission measurement setups), these two points lie up to several metres apart. This is because these facilities were not designed to support instantaneous emissions modelling, but rather to accurately measure aggregated emissions for purposes such as vehicle type-approval or conformity checks. Therefore, we conclude that emission modellers should handle the instantaneous emissions data signals reported by the measurement equipment with caution, especially when trying to allocate instantaneous mass emissions to recorded engine states in order to produce *engine emission maps* or similar high-resolution emission factors. In such cases, the implementation of an instantaneous signal compensation method will be required to achieve acceptable levels of accuracy.

In chapter 4 we proposed a *methodological framework* for the design of such a compensation method. Said methodological framework identifies the common aspects of any signal compensation method (a reference signal, a simplified model of the distorting phenomena, a compensation algorithm and appropriate signal metrics to evaluate the goodness of the compensation process), as well as the relationships among them. From the literature review of existing signal compensation methodologies, we also concluded that any signal compensation method will be based on a combination of signal post-processing and physical modelling, and thus it will require additional computation (in a suitable environment such as MATLAB®) and experimental efforts (to set up, run and periodically calibrate the compensation

method). Individual implementations will necessarily vary according to factors such as the general configuration of the measurement setup, the availability and dynamic characteristics of reference instruments and auxiliary signals, the flow measurement method or the data sampling rates.

The second objective of this dissertation was to develop a comprehensive, flexible methodology for the compensation of the distorting effects, and disseminate it among the stakeholders of the ERMES group. This is the $CO_2$ tracer method (described in chapter 5 and experimentally validated in chapter 6), which makes several original contributions to instantaneous vehicle emissions data post-processing. Among these is the operation on pollutant *mass* emission signals rather than pollutant concentration signals—which simplifies the derivation of *engine emission maps*—and the use of a 'rolling' data binning strategy—which makes an efficient use of available data to produce local estimations of the optimal compensation parameters—. The main benefits of this methodology are its low burden of experimental work (it does not require the generation of special input signals, or the measurement of exhaust temperature) and its flexibility (it adjusts automatically to changes in the measurement setup such as the modification of a pipe length; it does not require periodic calibration and it produces automatic, easy-to-interpret reports of its own performance). Furthermore, it has been fully implemented in the esto software tool, which can perform the compensation of emission signals with minimal user intervention and speed up the creation of engine emission maps. These features make the $CO_2$ tracer method a suitable approach to be adopted by emission measurement laboratories of the ERMES group, and thus it is made freely available to them.

# Bibliography


[1] Abu-Allaban, M., Rogers, C. F. and Gertler, A. W. "A quantitative description of vehicle exhaust particle size distributions in a highway tunnel". *Journal of the Air & Waste Management Association* 54.3 (2004), pp. 360–366 (cited on p. 36).

[2] Adam, T. W., Chirico, R., Clairotte, M., Elsasser, M., Manfredi, U., Martini, G., Sklorz, M., Streibel, T., Heringa, M. F., DeCarlo, P. F., Baltensperger, U., De Santi, G., Krasenbrink, A., Zimmermann, R., Prévôt, A. S. H. and Astorga, C. "Application of Modern Online Instrumentation for Chemical Analysis of Gas and Particulate Phases of Exhaust at the European Commission Heavy-Duty Vehicle Emission Laboratory". *Analytical Chemistry* 83.1 (2011), pp. 67–76 (cited on p. 24).

[3] Ajtay, D. and Weilenmann, M. "Compensation of the Exhaust Gas Transport Dynamics for Accurate Instantaneous Emission Measurements". *Environmental Science & Technology* 38.19 (2004), pp. 5141–5148 (cited on pp. 23, 50, 87, 88).

[4] Allen, J. O., Mayo, P. R., Hughes, L. S., Salmon, L. G. and Cass, G. R. "Emissions of Size-Segregated Aerosols from On-Road Vehicles in the Caldecott Tunnel". *Environmental Science & Technology* 35.21 (2001), pp. 4189–4197 (cited on p. 36).

[5] André, M. "The ARTEMIS European driving cycles for measuring car pollutant emissions". *Science of the Total Environment* 334-335 (2004), pp. 73–84 (cited on pp. 19, 127).

[6] André, M. and Rapone, M. "Analysis and modelling of the pollutant emissions from European cars regarding the driving characteristics and test cycles". *Atmospheric Environment* 43.5 (2009), pp. 986–995 (cited on p. 18).

[7] André, M., Joumard, R., Vidon, R., Tassel, P. and Perret, P. "Real-world European driving cycles, for measuring pollutant emissions from high- and low-powered cars". *Atmospheric Environment* 40.31 (2006), pp. 5944–5953 (cited on p. 18).

[8] Artelt, S., Kock, H., König, H., Levsen, K. and Rosner, G. "Engine dynamometer experiments: platinum emissions from differently aged three-way catalytic converters". *Atmospheric Environment* 33.21 (1999), pp. 3559–3567 (cited on pp. 17, 18).

[9] Aslam, M. U., Masjuki, H. H., Kalam, M. A., Abdesselam, H., Mahlia, T. M. I. and Amalina, M. A. "An experimental investigation of CNG as an alternative fuel for a retrofitted gasoline vehicle". *Fuel* 85.5-6 (2006), pp. 717–724 (cited on p. 25).

[10] Ban-Weiss, G. A., McLaughlin, J. P., Harley, R. A., Lunden, M. M., Kirchstetter, T. W., Kean, A. J., Strawa, A. W., Stevenson, E. D. and Kendall, G. R. "Long-term changes in emissions of nitrogen oxides and particulate matter from on-road gasoline and diesel vehicles". *Atmospheric Environment* 42.2 (2008), pp. 220–232 (cited on p. 36).

[11] Bannister, C. D., Wallace, F., Hawley, J. G. and Brace, C. J. "Predicting instantaneous exhaust flowrates in a constant volume sampling system". *Proceedings of the Institution of Mechanical Engineers, Part D: Journal of Automobile Engineering* 221.12 (2007), pp. 1585–1598 (cited on p. 85).

[12] Barlow, T. J., Latham, S., McCrae, I. S. and Boulter, P. G. *A reference book of driving cycles for use in the measurement of road vehicle emissions. Published Project Report PPR354*. Tech. rep. TRL Limited. Crowthorne House, Nine Mile Ride, Wokingham, Berkshire, RG40 3GA, United Kingdom, 2009 (cited on p. 18).

[13] Bergmann, M., Kirchner, U., Vogt, R. and Benter, T. "On-road and laboratory investigation of low-level PM emissions of a modern diesel particulate filter equipped diesel passenger car". *Atmospheric Environment* 43.11 (2009), pp. 1908–1916 (cited on p. 24).

[14] Bishop, G. A. and Stedman, D. H. "Measuring the emissions of passing cars". *Accounts of Chemical Research* 29 (1996), pp. 489–495 (cited on pp. 28, 29).

[15] Bishop, G. A., Starkey, J. R., Ihlenfeldt, A., Williams, W. J. and Stedman, D. H. "IR long-path photometry: a remote sensing tool for automobile emissions". *Analytical Chemistry* 61.10 (1989), 671–677A (cited on p. 28).

[16] Bishop, G. A., Morris, J. A., Stedman, D. H., Cohen, L. H., Countess, R. J., Countess, S. J., Maly, P. and Scherer, S. "The Effects of Altitude on Heavy-Duty Diesel Truck On-Road Emissions". *Environmental Science & Technology* 35.8 (2001), pp. 1574–1578 (cited on p. 31).

[17] Biswas, S., Verma, V., Schauer, J. J. and Sioutas, C. "Chemical speciation of PM emissions from heavy-duty diesel vehicles equipped with diesel particulate filter (DPF) and selective catalytic reduction (SCR) retrofits". *Atmospheric Environment* 43.11 (2009), pp. 1917–1925 (cited on p. 24).

[18] Biswas, S., Hu, S., Verma, V., Herner, J. D., Robertson, W. H., Ayala, A. and Sioutas, C. "Physical properties of particulate matter (PM) from late model heavy-duty diesel vehicles operating with advanced PM and $NO_x$ emission control technologies". *Atmospheric Environment* 42.22 (2008), pp. 5622–5634 (cited on p. 24).

[19] Borken-Kleefeld, J., Kupiainen, K., Chen, Y., Hausberger, S., Rexeis, M., Sjödin, Å., Jerksjö, M. and Tate, J. "High-emitting vehicles in laboratory and on-road measurements". *19th International Transport and Air Pollution Conference, Thessaloniki, Greece*. 2012 (cited on p. 28).

[20] Boulter, P. and McCrae, I. *ARTEMIS: Assessment and reliability of transport emission models and inventory systems. Workpackage 1300: Final Report and Dissemination. DG TREN Contract No. 1999-RD.10429. Deliverable No. 15*. Tech. rep. TRL Limited. Crowthorne House, Nine Mile Ride, Wokingham, Berkshire, RG40 3GA, United Kingdom, 2007 (cited on pp. 21, 46).

[21] Burgard, D. A., Bishop, G. A., Stedman, D. H., Gessner, V. H. and Daeschlein, C. "Remote Sensing of In-Use Heavy-Duty Diesel Trucks". *Environmental Science & Technology* 40.22 (2006), pp. 6938–6942 (cited on p. 31).

[22] Cadle, S. H. and Stevens, R. D. "Remote sensing of vehicle exhaust emissions". *Environmental Science & Technology* 28.6 (1994), 258A–265A (cited on p. 30).

[23] Canagaratna, M. R., Jayne, J. T., Ghertner, D. A., Herndon, S., Shi, Q., Jiménez, J. L., Silva, P. J., Williams, P., Lanni, T., Drewnick, F., Demerjian, K. L., Kolb, C. E. and Worsnop, D. R. "Chase Studies of Particulate Emissions from in-use New York City Vehicles". *Aerosol Science and Technology* 38.6 (2004), pp. 555–573 (cited on p. 33).

[24] Carslaw, D. C., Beevers, S. D., Tate, J. E., Westmoreland, E. J. and Williams, M. L. "Recent evidence concerning higher $NO_x$ emissions from passenger cars and light duty vehicles". *Atmospheric Environment* 45.39 (2011), pp. 7053–7063 (cited on p. 32).

[25] Chan, T. L. and Ning, Z. "On-road remote sensing of diesel vehicle emissions measurement and emission factors estimation in Hong Kong". *Atmospheric Environment* 39.36 (2005), pp. 6843–6856 (cited on p. 31).

[26] Chan, T. L., Ning, Z., Leung, C. W., Cheung, C. S., Hung, W. T. and Dong, G. "On-road remote sensing of petrol vehicle emissions measurement and emission factors estimation in Hong Kong". *Atmospheric Environment* 38.14 (2004), pp. 2055–2066 (cited on pp. 28, 31).

[27] Chang, S., Lin, T. and Lee, C. "On-road emission factors from light-duty vehicles measured in Hsuehshan Tunnel (12.9 km), the longest tunnel in Asia". *Environmental Monitoring and Assessment* 153.1 (2009), pp. 187–200 (cited on p. 36).

[28] Chao, H., Lin, T., Chao, M., Chang, F., Huang, C. and Chen, C. "Effect of methanol-containing additive on the emission of carbonyl compounds from a heavy-duty diesel engine". *Journal of Hazardous Materials* 73.1 (2000), pp. 39–54 (cited on p. 25).

[29] Chen, C., Huang, C., Jing, Q., Wang, H., Pan, H., Li, L., Zhao, J., Dai, Y., Huang, H. and Schipper, L. "On-road emission characteristics of heavy-duty diesel vehicles in Shanghai". *Atmospheric Environment* 41.26 (2007), pp. 5334–5344 (cited on p. 41).

[30] Cheng, Y., Lee, S. C., Ho, K. F. and Louie, P. K. K. "On-road particulate matter ($PM_{2.5}$) and gaseous emissions in the Shing Mun Tunnel, Hong Kong". *Atmospheric Environment* 40.23 (2006), pp. 4235–4245 (cited on p. 36).

[31] Chiang, H., Tsai, J., Yao, Y. and Ho, W. "Deterioration of gasoline vehicle emissions and effectiveness of tune-up for high-polluted vehicles". *Transportation Research Part D: Transport and Environment* 13.1 (2008), pp. 47–53 (cited on p. 23).

[32] Choi, H.-W. and Frey, H. C. "Estimating Diesel Vehicle Emission Factors at Constant and High Speeds for Short Road Segments". *Transportation Research Record: Journal of the Transportation Research Board* 2158 (2010), pp. 19–27 (cited on p. 21).

[33] Choi, H.-W. and Frey, H. C. "Light duty gasoline vehicle emission factors at high transient and constant speeds for short road segments". *Transportation Research Part D* 14.8 (2009), pp. 610–614 (cited on p. 21).

[34] Cicero-Fernández, P., Long, J. R. and Winer, A. M. "Effects of grades and other loads on on-road emissions of hydrocarbons and carbon monoxide". *Journal of the Air & Waste Management Association* 47.8 (1997), pp. 898–904 (cited on p. 38).

[35] Clark, N., Tehranian, A., Jarrett, R. P. and Nine, R. D. "Translation of distance-specific emissions rates between different heavy-duty vehicle chassis test schedules". *SAE Technical Paper Series paper number 2002-01-1754* (2002) (cited on p. 23).

[36] Cocker III, D. R., Shah, S. D., Johnson, K., Miller, J. W. and Norbeck, J. M. "Development and Application of a Mobile Laboratory for Measuring Emissions from Diesel Engines. 1. Regulated Gaseous Emissions". *Environmental Science & Technology* 38.7 (2004), pp. 2182–2189 (cited on p. 42).

[37] Cocker III, D. R., Shah, S. D., Johnson, K. C., Zhu, X., Miller, J. W. and Norbeck, J. M. "Development and Application of a Mobile Laboratory for Measuring Emissions from Diesel Engines. 2. Sampling for Toxics and Particulate Matter". *Environmental Science & Technology* 38.24 (2004), pp. 6809–6816 (cited on p. 42).

[38] Colberg, C. A., Tona, B., Stahel, W. A., Meier, M. and Staehelin, J. "Comparison of a road traffic emission model (HBEFA) with emissions derived from measurements in the Gubrist road tunnel, Switzerland". *Atmospheric Environment* 39.26 (2005), pp. 4703–4714 (cited on p. 36).

[39] Colberg, C. A., Tona, B., Catone, G., Sangiorgio, C., Stahel, W. A., Sturm, P. and Staehelin, J. "Statistical analysis of the vehicle pollutant emissions derived from several European road tunnel studies". *Atmospheric Environment* 39.13 (2005), pp. 2499–2511 (cited on p. 36).

[40] CONCAWE, *Motor vehicle emission regulations and fuel specifications. Part 1: 2004/2005 update*. Tech. rep. Conservation of Clean Air and Water in Europe (CONCAWE). Boulevard du Souverain 165, 1160 Brussels, Belgium, 2006 (cited on p. 18).

[41] CONCAWE, *Motor vehicle emission regulations and fuel specifications. Part 2: historic review (1996-2005)*. Tech. rep. Conservation of Clean Air and Water in Europe (CONCAWE). Boulevard du Souverain 165, 1160 Brussels, Belgium, 2006 (cited on p. 18).

[42] Corsmeier, U., Imhof, D., Kohler, M., Kühlwein, J., Kurtenbach, R., Petrea, M., Rosenbohm, E., Vogel, B. and Vogt, U. "Comparison of measured and model-calculated real-world traffic emissions". *Atmospheric Environment* 39.31 (2005), pp. 5760–5775 (cited on p. 35).

[43] Daham, B., Andrews, G. E., Li, H., Ballesteros, R., Bell, M. C., Tate, J. and Ropkins, K. "Application of a portable FTIR for measuring on-road emissions". *SAE Technical Paper Series paper number 2005-01-0676* (2005) (cited on p. 41).

[44] De Petris, C., Diana, S., Police, V. and Giglio, V. "Some problems in the improvement of measurement of transient emissions". *SAE Technical Paper Series paper number 941949 (originally presented at the International Fuels & Lubricants Meeting Exposition, October 17, 1994, Baltimore, Maryland, USA)* (1994) (cited on p. 86).

[45] Dearth, M. A., Butler, J. W., Colvin, A., Gierczak, C., Kaberline, S. and Korniski, T. "SemtechD: The chassis roll evaluation of a commercial portable emission measurement system (PEMS)". *SAE Technical Paper Series paper number 2005-04-11* (2005) (cited on p. 41).

[46] de Haan, P. and Keller, M. "Modelling fuel consumption and pollutant emissions based on real-world driving patterns: the HBEFA approach". *International Journal of Environment and Pollution* 22.3 (2004), pp. 240–258 (cited on p. 14).

[47] Durbin, T. D., Wilson, R., Norbeck, J., Miller, J., Huai, T. and Rhee, S. "Estimates of the emission rates of ammonia from light-duty vehicles using standard chassis dynamometer test cycles". *Atmospheric Environment* 36.9 (2002), pp. 1475–1482 (cited on p. 24).

[48] Durbin, T. D., Johnson, K., Miller, J. W., Maldonado, H. and Chernich, D. "Emissions from heavy-duty vehicles under actual on-road driving conditions". *Atmospheric Environment* 42.20 (2008), pp. 4812–4821 (cited on p. 43).

[49] Durbin, T. D., Johnson, K., Cocker III, D. R., Miller, J., Maldonado, H., Shah, A., Ensfield, C., Weaver, C., Akard, M. and Harvey, N. "Evaluation and comparison of portable emissions measurement systems and federal reference methods for emissions from a back-up generator and a diesel truck operated on a chassis dynamometer". *Environmental Science & Technology* 41.17 (2007), pp. 6199–6204 (cited on p. 41).

[50] EC, Commission Regulation (EU) No. 582/2011 of 25 May 2011 implementing and amending Regulation (EC) No. 595/2009 of the European Parliament and of the Council with respect to emissions from heavy duty vehicles (Euro VI) and amending Annexes I and III to Directive 2007/46/EC of the European Parliament and of the Council. Brussels, Belgium, 2011 (cited on p. 39).

[51] EC, Commission Regulation (EU) No. 64/2012 of 23 January 2012 amending Regulation (EU) No. 582/2011 implementing and amending Regulation (EC) No. 595/2009 of the European Parliament and of the Council with respect to emissions from heavy duty vehicles (Euro VI). Brussels, Belgium, 2012 (cited on p. 39).

[52] EC, European Commission White Paper. Road to a Single European Transport Area—Towards a competitive and resource efficient transport system. Brussels, Belgium, 2011 (cited on p. 11).

[53] Ekström, M., Sjödin, Å. and Andreasson, K. "Evaluation of the COPERT III emission model with on-road optical remote sensing measurements". *Atmospheric Environment* 38.38 (2004), pp. 6631–6641 (cited on p. 31).

[54] El-Fadel, M. and Hashisho, Z. "Vehicular emissions and air quality assessment in roadway tunnels: The Salim Slam tunnel". *Transportation Research Part D: Transport and Environment* 5.5 (2000), pp. 355–372 (cited on p. 34).

[55] El-Fadel, M. and Hashisho, Z. "Vehicular emissions in roadway tunnels: a critical review." *Critical Reviews in Environmental Science and Technology* 31.2 (2001), pp. 125–174 (cited on p. 35).

[56] Esteves-Booth, A., Muneer, T., Kirby, H., Kubie, J. and Hunter, J. "The measurement of vehicular driving cycle within the city of Edinburgh". *Transportation Research Part D: Transport and Environment* 6.3 (2001), pp. 209–220 (cited on p. 19).

[57] Faiz, A., Weaver, C. S. and Walsh, M. P. *Air pollution from motor vehicles. Standards and technologies for controlling emissions*. The World Bank. Washington DC, USA, 1996 (cited on p. 12).

[58] Fanick, E. R. and Williamson, I. "Comparison of emission and fuel economy characteristics of ethanol and Diesel blends in a heavy-duty Diesel engine". *International Symposium on Alcohol Fuels XIV*. Phuket, Thailand, 2002 (cited on p. 25).

[59] Fontaras, G., Pistikopoulos, P. and Samaras, Z. "Experimental evaluation of hybrid vehicle fuel economy and pollutant emissions over real-world simulation driving cycles". *Atmospheric Environment* 42.18 (2008), pp. 4023–4035 (cited on p. 23).

[60] Fontaras, G., Martini, G., Manfredi, U., Marotta, A., Krasenbrink, A., Maffioletti, F., Terenghi, R. and Colombo, M. "Assessment of on-road emissions of four Euro V diesel and CNG waste collection trucks for supporting air-quality improvement initiatives in the city of Milan". *Science of the Total Environment* 426.2012 (2012), pp. 65–72 (cited on p. 25).

[61] Fontaras, G., Franco, V., Dilara, P., Martini, G. and Manfredi, U. "Development and review of Euro 5 passenger car emission factors based on experimental results over various driving cycles". *Science of the Total Environment* 468-469.C (2013), pp. 1034–1042 (cited on p. 24).

[62] Fontaras, G., Kouridis, H., Samaras, Z., Elst, D. and Gense, R. "Use of a vehicle-modelling tool for predicting $CO_2$ emissions in the framework of European regulations for light goods vehicles". *Atmospheric Environment* 41.14 (2007), pp. 3009–3021 (cited on pp. 23, 25).

[63] Franco, V., Fontaras, G. and Dilara, P. "Towards Improved Vehicle Emissions Estimation in Europe". *Procedia—Social and Behavioral Sciences* 48.0 (2012), pp. 1304–1313 (cited on p. 14).

[64] Franco, V., Fontaras, G., Geivanidis, S., Weilenmann, M. and Dilara, P. *Compensation of measurement dynamics of instantaneous signals for vehicle emission factor modelling. European Commission Joint Research Centre Technical Report*. Unpublished manuscript, 2014 (cited on pp. 80, 124).

[65] Franco, V., Kousoulidou, M., Muntean, M., Ntziachristos, L., Hausberger, S. and Dilara, P. "Road vehicle emission factors development: A review". *Atmospheric Environment* 70.C (2013), pp. 84–97 (cited on p. 8).

[66] Frey, H. C. and Eichenberger, D. A. *Remote Sensing of Mobile Source Air Pollutant Emissions: Variability and Uncertainty in On-road Emissions Estimates of Carbon Monoxide and Hydrocarbons for School and Transit Buses. Report No. FHWY/NC/97-005*. Tech. rep. prepared by the Center for Transportation Engineering Studies, Department of Civil Engineering, North Carolina State University, Raleigh (NC) 27695-7908, USA for Division of Highways, North Carolina Department of Transportation, P.O. Box 25201, Raleigh (NC) 27611-5201, USA, 1997 (cited on p. 28).

[67] Frey, H. C. and Kangwookk, K. "In-use measurement of the activity, fuel use, and emissions of eight cement mixer trucks operated on each of petroleum diesel and soy-based B20 biodiesel". *Transportation Research Part D* 14.8 (2009), pp. 585–592 (cited on p. 42).

[68] Frey, H. C. and Kim, K. "Comparison of real-world fuel use and emissions for dump trucks fueled with B20 biodiesel versus petroleum diesel". *Transportation Research Record: Journal of the Transportation Research Board* 1987 (2006), pp. 110–117 (cited on p. 42).

[69] Frey, H. C., Zhang, K. and Rouphail, N. M. "Fuel use and emissions comparisons for alternative routes, time of day, road grade, and vehicles based on in-use measurements". *Environmental Science & Technology* 42.7 (2008), pp. 2483–2489 (cited on p. 41).

[70] Frey, H. C., Zhang, K. and Rouphail, N. M. "Vehicle-Specific Emissions Modeling Based upon on-Road Measurements". *Environmental Science & Technology* 44.9 (2010), pp. 3594–3600 (cited on p. 30).

[71] Frey, H. C., Rouphail, N. M., Zhai, H., Farias, T. L. and Gonçalves, G. A. "Comparing real-world fuel consumption for diesel- and hydrogen-fueled transit buses and implication for emissions". *Transportation Research Part D: Transport and Environment* 12.4 (2007), pp. 281–291 (cited on p. 42).

[72] Frey, H. C., Unal, A., Rouphail, N. M. and Colyar, J. D. "On-Road Measurement of Vehicle Tailpipe Emissions Using a Portable Instrument". *Journal of the Air & Waste Management Association* 53.8 (2003), pp. 992–1002 (cited on p. 37).

[73] Geivanidis, S. and Samaras, Z. "Development of a dynamic model for the reconstruction of tailpipe emissions from measurements on a constant volume sampling dilution system". *Measurement Science and Technology* 19 (2008), pp. 15404–15414 (cited on pp. 23, 53, 57, 84, 87, 88).

[74] Geller, M. D., Sardar, S. B., Phuleria, H., Fine, P. M. and Sioutas, C. "Measurements of particle number and mass concentrations and size distributions in a tunnel environment". *Environmental Science & Technology* 39.22 (2005), pp. 8653–8663 (cited on p. 35).

[75] Gierczak, C. A., Korniski, T. J., Wallington, T. J. and Butler, J. W. "Laboratory Evaluation of the SEMTECH-G® Portable Emissions Measurement System (PEMS) For Gasoline Fueled Vehicles". *SAE Technical Paper Series paper number 2006-01-1081* (2006) (cited on p. 41).

[76] Gkatzoflias, D., Kouridis, C., Ntziachristos, L. and Samaras, Z. *COPERT IV. Computer programme to calculate emissions from road transport. User manual (version 5.0)*. 2007 (cited on p. 14).

[77] Graver, B. M., Frey, H. C. and Choi, H.-W. "In-Use Measurement of Activity, Energy Use, and Emissions of a Plug-in Hybrid Electric Vehicle". *Environmental Science & Technology* 45.20 (2011), pp. 9044–9051 (cited on p. 42).

[78] Grieshop, A. P., Lipsky, E. M., Pekney, N. J., Takahama, S. and Robinson, A. L. "Fine particle emission factors from vehicles in a highway tunnel: Effects of fleet composition and season". *Atmospheric Environment* 40 (2006), pp. 287–298 (cited on p. 36).

[79] Guo, H., Zhang, Q. and Shi, Y. "Evaluation of the International Vehicle Emission (IVE) model with on-road remote sensing measurements". *Journal of Environmental Sciences* 19.7 (2007), pp. 818–826 (cited on p. 31).

[80] Guo, H., Zhang, Q., Shi, Y. and Wang, D. "On-road remote sensing measurements and fuel-based motor vehicle emission inventory in Hangzhou, China". *Atmospheric Environment* 41.14 (2007), pp. 3095–3107 (cited on p. 31).

[81] Hausberger, S., Rexeis, M., Zallinger, M. and Luz, R. *Emission Factors from the Model PHEM for the HBEFA Version 3. Report Nr. I-20a/2009 Haus-Em 33a/08/679*. Tech. rep. Graz University of Technology. Institute for internal combustion engines and thermodynamics. Inffeldgasse 19, A-8010 Graz, Austria, 2009 (cited on p. 22).

[82] Hausberger, S., Rodler, J., Sturm, P. and Rexeis, M. "Emission factors for heavy-duty vehicles and validation by tunnel measurements". *Atmospheric Environment* 37.37 (2003), pp. 5237–5245 (cited on p. 36).

[83] Hausberger, S., Kies, A., Laine, P., Rexeis, M., Samaras, Z., Sandström-Dahl, C., Schulte, L.-E., Silberholz, G., Steven, H. and Verbeek, R. *Reduction and Testing of Greenhouse Gas Emissions from Heavy Duty Vehicles—LOT 2. Development and testing of a certification procedure for $CO_2$ emissions and fuel consumption of HDV. Final Report*. Tech. rep. University of Technology Graz. Institute for internal combustion engines and thermodynamics. Inffeldgasse 19, A-8010 Graz, Austria, 2012 (cited on p. 26).

[84] Hawirko, J. D. and Checkel, M. D. "Quantifying Vehicle Emission Factors for Various Ambient Conditions Using An On-Road, Real-Time Emissions

System". *SAE Technical Paper Series paper number 2003-01-0301* (2003) (cited on p. 41).

[85] Hawirko, J. D. and Checkel, M. D. "Real-Time, On-Road Measurement of Driving Behavior, Engine Parameters and Exhaust Emissions". *SAE Technical Paper Series paper number 2002-01-1714* (2002) (cited on p. 40).

[86] Hawley, J. G., Brace, C. J., Cox, A., Ketcher, D. and Stark, R. "Calculation of Mass Emissions on a Chassis Dynamometer". *SAE Technical Paper Series paper number 2003-01-0395* (2003) (cited on p. 85).

[87] Hawley, J. G., Bannister, C. D., Brace, C. J., Cox, A., Ketcher, D. and Stark, R. "Further Investigations on Time-Alignment". *SAE Technical Paper Series paper number 2004-01-1441* (2004) (cited on p. 85).

[88] Heeb, N. V., Saxer, C. J., Forss, A.-M. and Brühlmann, S. "Correlation of hydrogen, ammonia and nitrogen monoxide (nitric oxide) emissions of gasoline-fueled Euro-3 passenger cars at transient driving". *Atmospheric Environment* 40.20 (2006), pp. 3750–3763 (cited on p. 24).

[89] Heeb, N. V., Forss, A.-M., Saxer, C. J. and Wilhelm, P. "Methane, benzene and alkyl benzene cold start emission data of gasoline-driven passenger cars representing the vehicle technology of the last two decades". *Atmospheric Environment* 37.37 (2003), pp. 5185–5195 (cited on p. 24).

[90] Heeb, N. V., Forss, A.-M., Brühlmann, S., Lüscher, R., Saxer, C. J. and Hug, P. "Three-way catalyst-induced formation of ammonia- velocity- and acceleration-dependent emission factors". *Atmospheric Environment* 40.31 (2006), pp. 5986–5997 (cited on p. 24).

[91] Herndon, S. C., Shorter, J. H., Zahniser, M. S., Wormhoudt, J., Nelson, D. D., Demerjian, K. L. and Kolb, C. E. "Real-Time Measurements of $SO_2$, $H_2CO$, and $CH_4$ Emissions from In-Use Curbside Passenger Buses in New York City Using a Chase Vehicle". *Environmental Science & Technology* 39.20 (2005), pp. 7984–7990 (cited on p. 33).

[92] Heywood, J. B. *Internal Combustion Engine Fundamentals*. McGraw-Hill, New York, 1988 (cited on p. 29).

[93] Ho, K.-f., Ho, S. S. H., Lee, S. C., Cheng, Y., Chow, J. C., Watson, J. G., Louie, P. K. K. and Tian, L. "Emissions of gas- and particle-phase polycyclic aromatic hydrocarbons (PAHs) in the Shing Mun Tunnel, Hong Kong". *Atmospheric Environment* 43.40 (2009), pp. 6343–6351 (cited on p. 36).

[94] Hsu, Y.-C., Tsai, J.-H., Chen, H.-W. and Lin, W.-Y. "Tunnel study of on-road vehicle emissions and the photochemical potential in Taiwan". *Chemosphere* 42.3 (2001), pp. 227–234 (cited on p. 36).

[95] Huai, T., Durbin, T. D., Miller, J. W. and Norbeck, J. M. "Estimates of the emission rates of nitrous oxide from light-duty vehicles using different chassis dynamometer test cycles". *Atmospheric Environment* 38.38 (2004), pp. 6621–6629 (cited on p. 24).

[96] Hueglin, C., Buchmann, B. and Weber, R. O. "Long-term observation of real-world road traffic emission factors on a motorway in Switzerland". *Atmospheric Environment* 40.20 (2006), pp. 3696–3709 (cited on pp. 31, 34).

[97] ICCT, *Certification procedures for advanced technology heavy-duty vehicles. Evaluating test methods and opportunities for global alignment. White Paper No. 16*. Tech. rep. The International Council on Clean Transportation. 1225 I Street NW Suite 900. Washington DC, USA, 2012 (cited on p. 26).

[98] Ingalls, M. N., Smith, L. R. and Kirksey, R. E. *Measurements of on-road vehicle emission factors in the California South Coast Air Basin—Volume 1: Regulated emissions. Report No. SwRI-1604; NTIS document PB8922095*. Tech. rep. prepared by the Southwest Research Institute, San Antonio (TX), USA for the Coordinating Research Council, Inc., Atlanta (GA), USA, 1989 (cited on p. 35).

[99] IPCC, World Meteorological Organization/United Nations Environment Programme National Greenhouse Gas Inventories Programme. Revised Terms Of Reference of the Emission Factors Database Editorial Board. Geneva, Switzerland, 2003 (cited on p. 20).

[100] Jamriska, M., Morawska, L., Thomas, S. and He, C. "Diesel Bus Emissions Measured in a Tunnel Study". *Environmental Science & Technology* 38.24 (2004), pp. 6701–6709 (cited on p. 34).

[101] Jiménez, J. L. "Understanding and quantifying motor vehicle emissions with vehicle specific power and TILDAS remote sensing". PhD thesis. Massachussets Institute of Technology (USA). Dept. of Mechanical Engineering, 1999 (cited on p. 29).

[102] Jiménez, J. L., McManus, J. B., Shorter, J. H., Nelson, D. D., Zahniser, M., Koplow, M., McRae, G. J. and Kolb, C. E. "Cross road and mobile tunable infrared laser measurements of nitrous oxide emissions from motor

vehicles". *Chemosphere - Global Change Science* 2.3-4 (2000), pp. 397–412 (cited on pp. 28, 29).

[103] Johnson, K. C., Durbin, T. D., Jung, H., Chaudhary, A., Cocker III, D. R., Herner, J. D., Robertson, W. H., Huai, T., Ayala, A. and Kittelson, D. "Evaluation of the European PMP Methodologies during On-Road and Chassis Dynamometer Testing for DPF Equipped Heavy-Duty Diesel Vehicles". *Aerosol Science and Technology* 43.10 (2009), pp. 962–969 (cited on p. 41).

[104] Johnson, K. C., Durbin, T. D., Cocker III, D. R., Miller, W. J., Bishnu, D. K., Maldonado, H., Moynahan, N., Ensfield, C. and Laroo, C. A. "On-road comparison of a portable emission measurement system with a mobile reference laboratory for a heavy-duty diesel vehicle". *Atmospheric Environment* 43.18 (2009), pp. 2877–2883 (cited on p. 41).

[105] Kågeson, P. *Cycle-beating and the EU Test Cycle for Cars. Report T&E 98/3*. Tech. rep. T&E European Federation for Transport and Environment. Boulevard de Waterloo 34, Brussels, Belgium, 1998 (cited on p. 18).

[106] Kamarianakis, Y. and Gao, H. O. "Accounting for Exhaust Gas Transport Dynamics in Instantaneous Emission Models via Smooth Transition Regression". *Environmental Science & Technology* 44.4 (2010), pp. 1320–1326 (cited on p. 86).

[107] Kean, A., Sawyer, R., Harley, R. and Kendall, G. "Trends in Exhaust Emissions from In-Use California Light-Duty Vehicles, 1994-2001". *SAE Technical Paper Series paper number 2002-01-1713* (2002) (cited on p. 36).

[108] Kean, A. J., Harley, R. A. and Kendall, G. R. "Effects of Vehicle Speed and Engine Load on Motor Vehicle Emissions". *Environmental Science & Technology* 37.17 (2003), pp. 3739–3746 (cited on pp. 35, 36).

[109] Kean, A. J., Littlejohn, D., Ban-Weiss, G. A., Harley, R. A., Kirchstetter, T. W. and Lunden, M. M. "Trends in on-road vehicle emissions of ammonia". *Atmospheric Environment* 43.8 (2009), pp. 1565–1570 (cited on p. 36).

[110] Kear, T. and Niemeier, D. A. "On-Road Heavy-Duty Diesel Particulate Matter Emissions Modeled Using Chassis Dynamometer Data". *Environmental Science & Technology* 40.24 (2006), pp. 7828–7833 (cited on p. 25).

[111] Keller, M. and Kljun, N. *Assessment and reliability of transport emission models and inventory systems (ARTEMIS). Road emission model—Model Description. DG TREN Contract No. 1999-RD.10429. Deliverable No. 13*. Tech. rep.

INFRAS. Muehlemattstrasse 45, CH-3007 Bern, Switzerland, 2007 (cited on p. 15).

[112] Kirchstetter, T. W., Harley, R. A., Kreisberg, N. M., Stolzenburg, M. R. and Hering, S. V. "On-road measurement of fine particle and nitrogen oxide emissions from light- and heavy-duty motor vehicles". *Atmospheric Environment* 33.18 (1999), pp. 2955–2968 (cited on p. 35).

[113] Kittelson, D. B., Watts, W. F., Johnson, J. P., Schauer, J. J. and Lawson, D. R. "On-road and laboratory evaluation of combustion aerosols – Part 2: Summary of Spark Ignition Engine Results". *Journal of Aerosol Science* 37.8 (2006), pp. 931–949 (cited on p. 33).

[114] Knorr, W., Hausberger, S. and Helms, H. *Weiterentwicklung der Emissionsfaktoren für das Handbuch für Emissionsfaktoren (HBEFA)*. Tech. rep. Institut für Energie- und Umweltforschung Heidelberg GmbH (ifeu, Institute for Energy and Environmental Research). Wilckensstraße 3, D-69120 Heidelberg, Germany, 2011 (cited on p. 19).

[115] Ko, Y.-W. and Cho, C.-H. "Characterization of large fleets of vehicle exhaust emissions in middle Taiwan by remote sensing". *Science of the Total Environment* 354.1 (2005), pp. 75–82 (cited on p. 28).

[116] Kousoulidou, M. "Experimental and theoretical investigation of European road transport emissions evolution with the use of conventional fuels and biofuels". PhD thesis. Aristotle University of Thessaloniki (Greece). Dept. of Mechanical Engineering, 2011 (cited on pp. 22, 42).

[117] Kousoulidou, M., Ntziachristos, L., Gkeivanidis, S., Samaras, Z., Franco, V. and Dilara, P. " Validation of the COPERT road emission inventory model with real-use data". *US EPA 19th Annual International Emission Inventory Conference. Emissions Inventories—Informing Emerging Issues*. San Antonio (TX), USA, 2010 (cited on p. 40).

[118] Kousoulidou, M., Fontaras, G., Ntziachristos, L. and Samaras, Z. "Biodiesel blend effects on common-rail diesel combustion and emissions". *Fuel* 89.11 (2010), pp. 3442–3449 (cited on p. 25).

[119] Kousoulidou, M., Ntziachristos, L., Fontaras, G., Martini, G., Dilara, P. and Samaras, Z. "Impact of biodiesel application at various blending ratios on passenger cars of different fueling technologies". *Fuel* 98.2012 (2012), pp. 88–94 (cited on p. 25).

[120] Kousoulidou, M., Ntziachristos, L., Franco, V., Gkeivanidis, S., Samaras, Z. and Dilara, P. "Use of Portable Emissions Measurement System (PEMS) for

Validation and Development of Passenger Car Emission Factors". *Transport and Air Pollution 18th International Symposium*. Dübendorf (Zürich), Switzerland, 2010 (cited on p. 40).

[121] Kousoulidou, M., Ntziachristos, L., Hausberger, S. and Rexeis, M. *Validation and Improvement of CORINAIR's Emission Factors for Road Transport using Real-World Emissions Measurements. LAT Report number 10.RE.0031.V1.* Tech. rep. Laboratory of Applied Thermodynamics. Aristotle University of Thessaloniki. P.O. Box 458 GR-54124, Thessaloniki, Greece, 2010 (cited on pp. 12, 22).

[122] Kwakernaak, H. and Sivan, R. *Modern Signals and Systems*. Prentice Hall, Englewood Cliffs, NJ (USA), 1991 (cited on p. 80).

[123] Le Anh, T., Hausberger, S. and Zallinger, M. "Correction for accurate instantaneous emission measurements of passenger cars". *Air Pollution XIV. WIT Transactions on Ecology and the Environment, Vol. 86*. 2006 (cited on pp. 77, 88).

[124] Lee, W. "A cost- and time-effective hardware-in-the-loop simulation platform for automotive engine control systems". *Proceedings of the Institution of Mechanical Engineers, Part D: Journal of Automobile Engineering*. 2003, pp. 41–52 (cited on p. 17).

[125] Lenaers, G. and Van Poppel, M. "A Tunable Diode Laser Measurement Technique for the On-Board Evaluation of Tail Pipe Ammonia Emissions". *SAE Technical Paper Series paper number 2005-24-018* (2005) (cited on p. 41).

[126] Lenaers, G. and Van Poppel, M. "Mobile Emission Measurements for Assessing Low Emitting Vehicles Exemplified on a CRT-Equipped Bus". *International Journal of Energy for a Clean Environment* 6.1 (2005), pp. 55–69 (cited on p. 42).

[127] Lenaers, G. and Van Poppel, M. "On-board Emission and Odour Measurements on Euro 2 Buses Retrofitted with Different Combinations of PM Traps and SCR". *SAE Technical Paper Series paper number 2007-24-0109* (2007) (cited on p. 42).

[128] Levenspiel, O. *Tracer Technology. Modeling the Flow of Fluids*. Springer, 2012 (cited on p. 96).

[129] Levenspiel, O. and Smith, W. K. "Notes on the diffusion-type model for the longitudinal mixing of fluids in flow". *Chemical Engineering Science* 50.24 (1957), pp. 3891–3896 (cited on p. 91).

[130] Liu, H., Barth, M., Scora, G., Davis, N. and Lents, J. "Using Portable Emission Measurement Systems for Transportation Emissions Studies". *Transportation Research Record: Journal of the Transportation Research Board* 2158.-1 (2010), pp. 54–60 (cited on p. 41).

[131] Livingston, C., Rieger, P. and Winer, A. "Ammonia emissions from a representative in-use fleet of light and medium-duty vehicles in the California South Coast Air Basin". *Atmospheric Environment* 43.21 (2009), pp. 3326–3333 (cited on p. 24).

[132] Madireddy, M. R. "Methods for Reconstruction of Transient Emissions from Heavy-Duty Vehicles". PhD thesis. West Virginia University (USA). College of Engineering and Mineral Resources, 2008 (cited on p. 86).

[133] Madireddy, M. R. and Clark, N. N. "Attempts to enhance the differential coefficients method for reconstruction of transient emissions from heavy-duty vehicles". *International Journal of Engine Research* 10.1 (2008), pp. 65–70 (cited on p. 86).

[134] Madireddy, M. R. and Clark, N. N. "Sequential inversion technique and differential coefficient approach for accurate instantaneous emissions measurement". *International Journal of Engine Research* 7.6 (2006), pp. 437–446 (cited on p. 86).

[135] Mamakos, A., Carriero, M., Bonnel, P., Demircioglu, H., Douglas, K., Alessandrini, S., Forni, F., Montigny, F. and Lesueur, D. *EU-PEMS PM evaluation program—third report—further study on post-DPF PM/PN emissions. European Commission Joint Research Centre Technical Report EUR 24883 EN*. Publications Office of the European Union. 2 rue Mercier, L-2985 Luxembourg, Luxembourg, 2011 (cited on p. 37).

[136] Maricq, M. M., Podsiadlik, D. H. and Chase, R. E. "Examination of the Size-Resolved and Transient Nature of Motor Vehicle Particle Emissions". *Environmental Science & Technology* 33.10 (1999), pp. 1618–1626 (cited on p. 33).

[137] Maykut, N. N., Lewtas, J., Kim, E. and Larson, T. V. "Source Apportionment of $PM_{2.5}$ at an Urban IMPROVE Site in Seattle, Washington". *Environmental Science & Technology* 37.22 (2003), pp. 5135–5142 (cited on p. 11).

[138] Mellios, G., Hausberger, S., Keller, M., Samaras, Z. and Ntziachristos, L. *Parameterisation of fuel consumption and $CO_2$ emissions of passenger cars and light commercial vehicles for modelling purposes. European Commission Joint*

*Research Centre Technical Report EUR 24927 EN*. Publications Office of the European Union. 2 rue Mercier, L-2985 Luxembourg, Luxembourg, 2011 (cited on pp. 16, 18).

[139] Miguel, A. H., Kirchstetter, T. W., Harley, R. A. and Hering, S. V. "On-road Emissions of Particulate Polycyclic Aromatic Hydrocarbons and Black Carbon from Gasoline and Diesel Vehicles". *Environmental Science & Technology* 32.4 (1998), pp. 450–455 (cited on p. 35).

[140] Miyazaki, T., Takada, Y. and Iida, N. "Development of On-Board System to Measure Running Condition and Actual $NO_x$ Emissions From Freight Vehicle". *SAE Technical Paper Series paper number 2002-01-0613* (2002) (cited on p. 40).

[141] Mohr, M., Forss, A.-M. and Steffen, D. "Particulate emissions of gasoline vehicles and influence of the sampling procedure". *SAE Technical Paper Series paper number 2000-01-1137* (2000) (cited on p. 24).

[142] Morawska, L., Ristovski, Z., Johnson, G., Jayaratne, R. and Mengersen, K. "Novel Method for On-Road Emission Factor Measurements Using a Plume Capture Trailer". *Environmental Science & Technology* 41.2 (2007), pp. 574–579 (cited on p. 33).

[143] Morawska, L., Bofinger, N. D., Kosic, L. and Nwankwoala, A. "Submicron and supermicron particles from diesel vehicle emissions". *Environmental Science & Technology* 32 (1998), pp. 2033–2042 (cited on p. 23).

[144] Nam, E. K., Gierczak, C. A. and Butler, J. W. "A comparison of real-world and modelled emissions under conditions of variable driver aggressiveness". *82nd Annual Meeting of the Transportation Research board Transportation Research Board 500 Fifth St NW, Washington DC, USA* (2003) (cited on p. 41).

[145] Nelson, P., Tibbett, A. and Day, S. "Effects of vehicle type and fuel quality on real world toxic emissions from Diesel vehicles". *Atmospheric Environment* 42.21 (2008), pp. 5291–5303 (cited on p. 25).

[146] Nine, R. D., Clark, N. N., Daley, J. J. and Atkinson, C. M. "Development of a heavy-duty chassis dynamometer driving route". *Proceedings of the Institution of Mechanical Engineers, Part D: Journal of Automobile Engineering*. 1999, pp. 561–574 (cited on p. 15).

[147] Ntziachristos, L. and Samaras, Z. "Speed-dependent representative emission factors for catalyst passenger cars and influencing parameters". *Atmospheric Environment* 34.27 (2000), pp. 4611–4619 (cited on p. 18).

[148] Ogata, K. *Modern control engineering*. Fourth edition. Prentice Hall. Pearson Education International, 2002 (cited on pp. 48, 80, 95).

[149] Oh, S. H. and Cavendish, J. C. "Mathematical modeling of catalytic converter lightoff. Part II: Model verification by engine-dynamometer experiments". *AIChE Journal* 31.6 (1985), pp. 935–942 (cited on p. 17).

[150] Olfert, J. S., Symonds, J. and Collings, N. "The effective density and fractal dimension of particles emitted from a light-duty diesel vehicle with a diesel oxidation catalyst". *Journal of Aerosol Science* 38.1 (2007), pp. 69–82 (cited on p. 24).

[151] Oprešnik, S. R., Seljak, T., Bizjan, F. and Katrašnik, T. "Exhaust emissions and fuel consumption of a triple-fuel spark-ignition engine powered passenger car". *Transportation Research Part D: Transport and Environment* 17.3 (2012), pp. 221–227 (cited on p. 38).

[152] Pelkmans, L. and Debal, P. "Comparison of on-road emissions with emissions measured on chassis dynamometer test cycles". *Transportation Research Part D: Transport and Environment* 11.4 (2006), pp. 233–241 (cited on pp. 23, 25, 41).

[153] Peng, C.-Y., Yang, H.-H., Lan, C.-H. and Chien, S.-M. "Effects of the biodiesel blend fuel on aldehyde emissions from diesel engine exhaust". *Atmospheric Environment* 42.5 (2008), pp. 906–915 (cited on p. 25).

[154] Pierson, W. R. and Brachaczek, W. W. "Particulate matter associated with vehicles on the road. II". *Aerosol Science and Technology* 2 (1983), pp. 1–40 (cited on p. 35).

[155] Pierson, W. R., Gertler, A. W. and Robinson, N. F. "Real-world automotive emissions–Summary of studies in the Fort McHenry and Tuscarora mountain tunnels". *Atmospheric Environment* 30.12 (1996), pp. 2233–2256 (cited on p. 35).

[156] Pirjola, L., Parviainen, H., Hussein, T., Valli, A., Hämeri, K., Aalto, P., Virtanen, A., Keskinen, J., Pakkanen, T. A., Mäkelä, T. and Hillamo, R. E. "'Sniffer'–a novel tool for chasing vehicles and measuring traffic pollutants". *Atmospheric Environment* 38.22 (2004), pp. 3625–3635 (cited on p. 33).

[157] Querol, X., Viana, M., Alastuey, A., Amato, F., Moreno, T., Castillo, S., Pey, J., de la Rosa, J., Sánchez de la Campa, A., Artíñano, B., Salvador, P., García Dos Santos, S., Fernández-Patier, R., Moreno-Grau, S., Negral, L., Minguillón, M. C., Monfort, E., Gil, J. I., Inza, A., Ortega, L. A., Santamaría, J. M. and Zabalza, J. "Source origin of trace elements in PM

from regional background, urban and industrial sites of Spain". *Atmospheric Environment* 41.34 (2007), pp. 7219–7231 (cited on p. 11).

[158] Ramamurthy, R. and Clark, N. N. "Atmospheric Emissions Inventory Data for Heavy-Duty Vehicles". *Environmental Science & Technology* 33.1 (1999), pp. 55–62 (cited on p. 23).

[159] Ramamurthy, R., Clark, N. N., Atkinson, C. M. and Lyons, D. W. "Models for Predicting Transient Heavy Duty Vehicle Emissions". *SAE Technical Paper Series paper number 982652* (1998), pp. 1–16 (cited on p. 86).

[160] Rapone, M., Della Ragione, L., Prati, M. V. and Violetti, N. "Driving Behavior and Emission Results for a Small Size Gasoline Car in Urban Operation". *SAE Technical Paper Series paper number 2000-01-2960* (2000) (cited on p. 19).

[161] Ristovski, Z., Jayaratne, E. R., Morawska, L., Ayoko, G. A. and Lim, M. "Particle and carbon dioxide emissions from passenger vehicles operating on unleaded petrol and LPG fuel". *Science of the Total Environment* 345.1-3 (2005), pp. 93–98 (cited on p. 25).

[162] Rogak, S. N., Pott, U., Dann, T. and Wang, D. "Gaseous emissions from vehicles in a traffic tunnel in Vancouver, British Columbia". *Journal of the Air & Waste Management Association* 48.7 (1998), pp. 604–615 (cited on p. 35).

[163] Rubino, L., Bonnel, P., Hummel, R., Krasenbrink, A., Manfredi, U., De Santi, G., Perotti, M. and Bomba, G. "PEMS Light Duty Vehicles Application: Experiences in downtown Milan". *SAE Technical Paper Series paper number 2007-24-0113* (2007) (cited on p. 39).

[164] Rubino, L., Bonnel, P., Carriero, M. and Krasenbrink, A. "Portable Emission Measurement System (PEMS) For Heavy Duty Diesel Vehicle PM Measurement: The European PM PEMS Program". *SAE International Journal of Engines* 2.2 (2010), pp. 660–673 (cited on p. 41).

[165] Sadler, L., Jenkins, N., Legassick, W. and Sokhi, R. S. "Remote sensing of vehicle emissions on British urban roads". *Science of the Total Environment* 189-190 (1996), pp. 155–160 (cited on p. 28).

[166] SAE, Constant Volume Sampler System for Exhaust Emissions Measurement. SAE standard J1094. 2011 (cited on p. 52).

[167] Sánchez-Ccoyllo, O., Ynoue, R., Martins, L., Astolfo, R., Miranda, R., Freitas, E., Borges, A., Fornaro, A., Freitas, H. and Moreira, A. "Vehicular particulate matter emissions in road tunnels in São Paulo, Brazil".

*Environmental Monitoring and Assessment* 149.1 (2009), pp. 241–249 (cited on p. 36).

[168] Schifter, I., Díaz, L., Múgica, V. and López-Salinas, E. "Fuel-based motor vehicle emission inventory for the metropolitan area of Mexico city". *Atmospheric Environment* 39.5 (2005), pp. 931–940 (cited on p. 31).

[169] Schifter, I., Díaz, L., Rodríguez, R., Durán, J. and Chávez, O. "Trends in exhaust emissions from in-use Mexico City vehicles, 2000–2006. A remote sensing study". *Environmental Monitoring and Assessment* 137.1-3 (2007), pp. 459–470 (cited on p. 32).

[170] Shah, S. D., Cocker III, D. R., Miller, J. W. and Norbeck, J. M. "Emission Rates of Particulate Matter and Elemental and Organic Carbon from In-Use Diesel Engines". *Environmental Science & Technology* 38.9 (2004), pp. 2544–2550 (cited on p. 42).

[171] Shah, S. D., Johnson, K. C., Wayne Miller, J. and Cocker III, D. R. "Emission rates of regulated pollutants from on-road heavy-duty diesel vehicles". *Atmospheric Environment* 40.1 (2006), pp. 147–153 (cited on p. 42).

[172] Shorter, J. H., Herndon, S., Zahniser, M. S., Nelson, D. D., Wormhoudt, J., Demerjian, K. L. and Kolb, C. E. "Real-Time Measurements of Nitrogen Oxide Emissions from In-Use New York City Transit Buses Using a Chase Vehicle". *Environmental Science & Technology* 39.20 (2005), pp. 7991–8000 (cited on pp. 32, 33).

[173] Silva, C. M., Farias, T. L., Frey, H. C. and Rouphail, N. M. "Evaluation of numerical models for simulation of real-world hot-stabilized fuel consumption and emissions of gasoline light-duty vehicles". *Transportation Research Part D: Transport and Environment* 11.5 (2006), pp. 377–385 (cited on p. 42).

[174] Silva, C., Ross, M. and Farias, T. "Evaluation of energy consumption, emissions and cost of plug-in hybrid vehicles". *Energy Conversion and Management* 50.7 (2009), pp. 1635–1643 (cited on p. 26).

[175] Singer, B. C. and Harley, R. A. "Fuel-based motor vehicle emission inventory". *Journal of the Air & Waste Management Association* 46.6 (1996), pp. 581–593 (cited on pp. 29, 30).

[176] Singh, R. B. and Sloan, J. J. "A high-resolution $NO_x$ emission factor model for North American motor vehicles". *Atmospheric Environment* 40.27 (2006), pp. 5214–5223 (cited on p. 36).

[177] Sjödin, Å. and Lenner, M. "On-road measurements of single vehicle pollutant emissions, speed and acceleration for large fleets of vehicles in different traffic environments". *Science of the Total Environment* 169.1-3 (1995), pp. 157–165 (cited on pp. 28, 35).

[178] Sjödin, Å., Persson, K., Andreasson, K., Arlander, B. and Galle, B. "On-road emission factors derived from measurements in a traffic tunnel". *International Journal of Vehicle Design* 20.1-4 (1998), pp. 147–158 (cited on p. 35).

[179] Smit, R., Ntziachristos, L. and Boulter, P. "Validation of road vehicle and traffic emission models—A review and meta-analysis". *Atmospheric Environment* 44.25 (2010), pp. 2943–2953 (cited on p. 12).

[180] Smith, D. E. and Hodgson, J. W. "Application of signal reconstruction to on-road emissions testing". *SAE Technical Paper Series paper number 1999-01-1462* (1999) (cited on p. 86).

[181] Smith, S. W. *The Scientist and Engineer's Guide to Digital Signal Processing. 1st Edition. ISBN-13: 978-0966017632*. 1997 (cited on p. 98).

[182] Soltic, P. and Weilenmann, M. "$NO_2$/NO emissions of gasoline passenger cars and light-duty trucks with Euro-2 emission standard". *Atmospheric Environment* 37.37 (2003), pp. 5207–5216 (cited on p. 24).

[183] Staehelin, J., Schläpfer, K., Bürgin, T., Steinemann, U., Schneider, S., Brunner, D., Bäumle, M., Meier, M., Zahner, C. and Keiser, S. "Emission factors from road traffic from a tunnel study (Gubrist tunnel, Switzerland). Part I: concept and first results". *Science of the Total Environment* 169.1-3 (1995), pp. 141–147 (cited on p. 35).

[184] Staehelin, J., Keller, C., Stahel, W. A., Schläpfer, K., Steinemann, U., Bürgin, T. and Schneider, S. "Modelling emission factors of road traffic from a tunnel study". *Environmetrics* 8.3 (1997), pp. 219–239 (cited on p. 35).

[185] Stedman, D. H. and Bishop, G. A. "On-road evaluation of an automobile emission test program". *Environmental Science & Technology* 31.3 (1997), pp. 927–931 (cited on p. 31).

[186] Stemmler, K., Bugmann, S., Buchmann, B., Reimann, S. and Staehelin, J. "Large decrease of VOC emissions of Switzerland's car fleet during the past decade: results from a highway tunnel study". *Atmospheric Environment* 39.6 (2005), pp. 1009–1018 (cited on p. 36).

[187] Steven, H. *Development of a Worldwide Harmonised Heavy-duty Engine Emissions Test Cycle. Final Report. TRANS/WP29/GRPE/2001/2 Informal*

*document No. 2. GRPE 42nd session*. Tech. rep. United Nations Economic Commission for Europe (UNECE). Palais des Nations, CH-1211 Geneva 10, Switzerland, 2001 (cited on p. 20).

[188] Sturm, P. J. and Hausberger, S. *Energy and fuel consumption from heavy duty vehicles. COST 346—Final Report*. Tech. rep. Graz University of Technology. Institute for Internal Combustion Engines and Thermodynamics. Inffeldgasse 19, A-8010 Graz, Austria, 2005 (cited on p. 15).

[189] Sturm, P. J., Baltensperger, U., Bacher, M., Lechner, B., Hausberger, S., Heiden, B., Imhof, D., Weingartner, E., Prévôt, A. S. H., Kurtenbach, R. and Wiesen, P. "Roadside measurements of particulate matter size distribution". *Atmospheric Environment* 37.37 (2003), pp. 5273–5281 (cited on p. 35).

[190] Traver, M. L., Tennant, C. J., McDaniel, T. I., McConnell, S. S., Bailey, B. K. and Maldonado, H. "Interlaboratory Cross-Check of Heavy-Duty Vehicle Chassis Dynamometers". *SAE Technical Paper Series paper number 2002-01-2879* (2002) (cited on p. 16).

[191] Tzirakis, E., Karavalakis, G., Schinas, P. and Korres, D. "Diesel-water Emulsion Emissions and Performance Evaluation in Public Buses in Attica Basin". *SAE Technical Paper Series paper number 2006-01-3398* (2006) (cited on p. 42).

[192] Unal, A., Frey, H. C. and Rouphail, N. M. "Quantification of Highway Vehicle Emissions Hot Spots Based upon On-Board Measurements". *Journal of the Air & Waste Management Association* 54.2 (2004), pp. 130–140 (cited on p. 41).

[193] Unal, A., Rouphail, N. M. and Frey, H. C. "Effect of Arterial Signalization and Level of Service on Measured Vehicle Emissions". *Transportation Research Record: Journal of the Transportation Research Board* 1842 (2003), pp. 47–56 (cited on p. 41).

[194] UNECE, World Forum for Harmonization of Vehicle Regulations. Regulation No. 101 revision 2. Uniform provisions concerning the approval of passenger cars powered by an internal combustion engine only, or powered by a hybrid electric power train with regard to the measurement of the emission of carbon dioxide and fuel consumption and/or the measurement of electric energy consumption and electric range, and of categories M1 and N1 vehicles powered by an electric power train only with regard to the measurement of electric energy consumption and electric range uniform

provisions concerning the approval of passenger cars powered by an internal combustion engine only, or powered by a hybrid electric power train with regard to the measurement of the emission of carbon dioxide and fuel consumption and/or the measurement of electric energy consumption and electric range, and of categories M1 and N1 vehicles powered by an electric power train only with regard to the measurement of electric energy consumption and electric range. 2005 (cited on p. 26).

[195] USEPA, *A Comprehensive Analysis of Biodiesel Impacts on Exhaust Emissions. Draft Technical Report EPA420-P-02-001*. Tech. rep. U.S. Environmental Protection Agency. Office of Transportation and Air Quality. Assessment and Standards Division. 2000 Traverwood Drive, Ann Arbor (MI) 48105, USA, 2002 (cited on p. 25).

[196] USEPA, Engine-Testing Procedures, Title 40 Code of Federal Regulations 1065, subpart J. 2005 (cited on p. 39).

[197] USEPA, *Motor Vehicle Emission Simulator (MOVES). User Guide for MOVES2010b. Report EPA-420-B-12-001b*. Tech. rep. U.S. Environmental Protection Agency. Office of Transportation and Air Quality. Assessment and Standards Division. 2000 Traverwood Drive, Ann Arbor (MI) 48105, USA, 2012 (cited on p. 19).

[198] Vojtíšek-Lom, M. and Cobb, J. T. "Vehicle Mass Emissions Measurement Using a Portable 5-Gas Exhaust Analyzer and Engine Computer Data". *Proceedings of Emission Inventory: Planning for the Future Conference Air & Waste Management Association Pittsburgh, PA (USA) pp. 656-669*. 1997 (cited on pp. 37, 40).

[199] Vollmer, M. K., Juergens, N., Steinbacher, M., Reimann, S., Weilenmann, M. and Buchmann, B. "Road vehicle emissions of molecular hydrogen ($H_2$) from a tunnel study". *Atmospheric Environment* 41.37 (2007), pp. 8355–8369 (cited on p. 36).

[200] Wang, W., Clark, N., Lyons, D., Yang, R., Gautam, M., Bata, R. and Loth, J. "Emissions comparisons from alternative fuel buses and diesel buses with a chassis dynamometer testing facility". *Environmental Science & Technology* 31.11 (1997), pp. 3132–3137 (cited on pp. 15, 23).

[201] Wang, W., Lyons, D. W., Clark, N. N., Gautam, M. and Norton, P. "Emissions from Nine Heavy Trucks Fueled by Diesel and Biodiesel Blend without Engine Modification". *Environmental Science & Technology* 34.6 (2000), pp. 933–939 (cited on p. 25).

[202] Wehner, B., Uhrner, U., Lowis, S. von, Zallinger, M. and Wiedensohler, A. "Aerosol number size distributions within the exhaust plume of a diesel and a gasoline passenger car under on-road conditions and determination of emission factors". *Atmospheric Environment* 43.6 (2009), pp. 1235–1245 (cited on p. 31).

[203] Weilenmann, M., Bach, C. and Rüdy, C. "Aspects of instantaneous emission measurement ". *International Journal of Vehicle Design* 27 (2001), pp. 94–104 (cited on p. 87).

[204] Weilenmann, M., Soltic, P. and Ajtay, D. "Describing and compensating gas transport dynamics for accurate instantaneous emission measurement". *Atmospheric Environment* 37.37 (2003), pp. 5137–5145 (cited on pp. 23, 61, 74, 87, 88).

[205] Weilenmann, M., Soltic, P., Saxer, C., Forss, A.-M. and Heeb, N. "Regulated and nonregulated diesel and gasoline cold start emissions at different temperatures". *Atmospheric Environment* 39.13 (2005), pp. 2433–2441 (cited on p. 24).

[206] Weiss, M., Bonnel, P., Hummel, R. and Steininger, N. *A complementary emissions test for light-duty vehicles: Assessing the technical feasibility of candidate procedures. European Commission Joint Research Centre Technical Report EUR 25572 EN*. Publications Office of the European Union. 2 rue Mercier, L-2985 Luxembourg, Luxembourg, 2013 (cited on p. 39).

[207] Weiss, M., Bonnel, P., Hummel, R., Manfredi, U., Colombo, R., Lanappe, G., Lelijour, P. and Sculati, M. *Analyzing on-road emissions of light-duty vehicles with Portable Emission Measurement Systems (PEMS). European Commission Joint Research Centre Technical Report EUR 24697 EN*. Publications Office of the European Union. 2 rue Mercier, L-2985 Luxembourg, Luxembourg, 2011 (cited on pp. 18, 39).

[208] Weiss, M., Bonnel, P., Hummel, R., Provenza, A. and Manfredi, U. "On-Road Emissions of Light-Duty Vehicles in Europe". *Environmental Science & Technology* 45.19 (2011), pp. 8575–8581 (cited on p. 39).

[209] Westerdahl, D., Wang, X., Pan, X. and Zhang, K. M. "Characterization of on-road vehicle emission factors and microenvironmental air quality in Beijing, China". *Atmospheric Environment* 43.3 (2009), pp. 697–705 (cited on p. 31).

[210] Whitfield, J. C. and Harris, D. B. "Comparison of heavy-duty diesel emissions from engine and chassis dynamometers and on-road testing".

*Eighth Coordinating Research Council On-road Vehicle Emissions Workshop. San Diego, CA (USA)*. Coordinating Research Council. 3650 Mansell Road. Suite 140 Alpharetta, GA 30022, USA., 1998 (cited on p. 23).

[211] WHO, Fact sheet No. 313. Air quality and health (updated March 2014). 2014. URL: http://www.who.int/mediacentre/factsheets/fs313/en/index.html (cited on p. 11).

[212] Xie, S., Bluett, J. G., Fisher, G., Kuschel, G. I. and Stedman, D. H. "On-road remote sensing of vehicle exhaust emissions in Auckland, New Zealand". *Clean Air and Environmental Quality* 39.4 (2005), pp. 37–42 (cited on p. 32).

[213] Yanowitz, J., McCormick, R. L. and Graboski, M. S. "In-Use Emissions from Heavy-Duty Diesel Vehicles". *Environmental Science & Technology* 34.5 (2000), pp. 729–740 (cited on p. 15).

[214] Yanowitz, J., Graboski, M. S., Ryan, L. B. A., Alleman, T. L. and McCormick, R. L. "Chassis Dynamometer Study of Emissions from 21 In-Use Heavy-Duty Diesel Vehicles". *Environmental Science & Technology* 33.2 (1999), pp. 209–216 (cited on p. 23).

[215] Yu, L. "Remote Vehicle Exhaust Emission Sensing for Traffic Simulation and Optimization Models". *Transportation Research Part D: Transport and Environment* 3.5 (1998), pp. 337–347 (cited on p. 30).

[216] Zallinger, M. "Mikroskopische Simulation der Emissionen von Personenkraftfahrzeugen". PhD thesis. Technical University of Graz (Austria). Institut für Verbrennungskraftmaschinen und Thermodynamik, 2010 (cited on p. 21).

[217] Zhang, K. and Frey, C. "Evaluation of Response Time of a Portable System for In-Use Vehicle Tailpipe Emissions Measurement". *Environmental Science & Technology* 42.1 (2008), pp. 221–227 (cited on p. 41).

# Index

Cover art: Lena R-F